STUDY OF ANIMAL SIGNALS AND NEURAL PROCESSING, WITH APPLICATIONS TO ADVANCED SONAR SYSTEMS

Richard A. Altes

ESL Incorporated

Prepared for:

Naval Undersea Center

10 August 1973

STUDY OF ANIMAL SIGNALS AND NEURAL PROCESSING, WITH APPLICATIONS TO ADVANCED SONAR SYSTEMS

by Richard A. Altes, Ph. D.

Prepared for the Biosystem Research Department of the Naval Undersea Center under Contract No. N00123-73-C-1144

ESL INCORPORATED

ELECTROMAGNETIC SYSTEMS LABORATORIES
495 JAVA DRIVE • SUNNYVALE • CALIFORNIA

ESL-PR115
Copy No. 16

ESL INCORPORATED
Electromagnetic Syetems Laboratories
Sunnyvale, California

Progress Report
No. ESL-PR115
10 August 1973

STUDY OF ANIMAL SIGNALS AND NEURAL PROCESSING, WITH APPLICATIONS TO ADVANCED SONAR SYSTEMS

by Richard A. Altes, Ph. D.

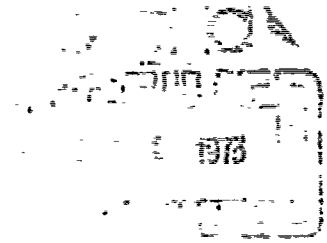

Prepared for the Biosystem Research Department of the Naval Undersea Center under Contract No. N00123-73-C-1144

This Document Consists of 221 Pages

Copy No. 16 of 100 Copies

CONTENTS

CONTENTS -- Continued

CONTENTS -- Continued

CONTENTS -- Addendum

ILLUSTRATIONS

ILLUSTRATIONS -- Continued

ILLUSTRATIONS -- Continued

ILLUSTRATIONS -- Continued

ILLUSTRATIONS -- Continued

TABLES

Typing for this report was done by Janice Reed.

STUDY OF ANIMAL SIGNALS AND NEURAL PROCESSING, WITH APPLICATIONS TO ADVANCED SONAR SYSTEMS

1. INTRODUCTION.

This progress report summarizes the work done under contract No. N00123-73-C-1144. The report extends the results obtained under two previous contracts.[2, 3] All three contracts were performed under the auspices of the Biosystem Research Department of the Naval Undersea Center, San Diego, California.*

The report begins with a summary of past results, along with some remarks that pertain to newer discoveries. An important new approach to the analysis of animal echolocation behavior is presented in Section 3. This approach is exciting because it relates the sonar signals used by bats and cetaceans to well-accepted models of the mammalian auditory processor. It is analogous to approaching the problem from "away around on the far side",[1] a vantage point from which animal echolocation behavior and the theory that has been used to explain it became much more obvious and easily accepted.

The fourth and fifth sections consider likelihood ratio testing and signal to interference maximization as applied to our model of the animal sonar system. It is demonstrated that wideband signals constitute a more practical set of basis functions than sinusoids, when the receiver is completely linear.

*The advice, encouragement, and criticism of W. E. Evans and C. S. Johnson (both of NUC) has been especially helpful.

1. --Continued.

The sixth section describes some new results concerning bat signals. It was previously thought[3] that bat signals are used to convey amplitude modulation (AM) information. More recent results indicate that bat signals, like those of cetaceans, can be explained in terms of linear filter characterization. This finding, however, does not negate the AM hypothesis. For certain carrier signals, it happens that AM can be described as a linear filtering operation.

The seventh section describes an experiment that is presently being undertaken as a practical test of the theory.

The eighth section describes two alternative models of the auditory system. Both models involve a set of constant-Q filters, but the model suggested by the author incorporates filters with narrower bandwidths, which are viewed as the basic components from which the constant-Q filters are constructed.

The ninth section deals with the problem of minimizing the volume under the wideband ambiguity function. Volume minimization is of only incidental importance for animal echolocation, but is of interest to designers of conventional sonars when planar targets are assumed.

It has been mentioned that, for certain carrier signals, AM can be described as a linear filtering operation. This set of carrier signals is composed of all waveforms that can be expressed as finite order polynomials over a bounded frequency interval $[0, W]$. The advantages of these waveforms for characterization of time varying linear systems and for communication are discussed in Section 10. Taylor series

1. --Continued.

characterization of signal spectra provides a viewpoint from which one can easily discern the quantitative equivalence between time varying filters (or targets, or channels) and time invariant ones.

The mathematical processes involved in animal echolocation are intimately related to the processing of speech by the human auditory system. This relation is pursued in Section II, where a new method of extracting information from speech is suggested. The method can be interpreted as a speech decoding algorithm. Such an algorithm can be applied to data reduction for transmission of speech, to computer understanding of speech, and to phoneme synthesis.

The Appendix includes some mathematical properties of the signals that have been derived to explain animal echolocation behavior.

1.1 Raisons d' Etre ; Motivations.

Although the preceding paragraphs preview the contents of this report, they may not provide sufficient reason to proceed unless a particular subject has caught the reader's eye. It is advisable, then, to consider the report from the viewpoint of motivation.

The U. S. Navy has spent more than a few dollars to support this research, and the author has spent more than a few hours to carry it out. To what ends have this time and money been spent? The report gives some results, but what were the questions and concerns that motivated the research? Some of the questions are well defined; others are somewhat nebulous. The questions seem to fit three major categories:

I. Sonar Systems.

A. Specific Questions.

How should a sonar system deal with the commonly observed situation in which a target echo only faintly resembles a wideband transmitted signal? Is there a general mathematical description for such a phenomenon? Can the phenomenon be exploited for target recognition or clutter suppression? Can it be circumvented so that matched filtering can be applied to wideband sonar echoes? What signals and filters are optimum for (a) exploiting or (b) circumventing the phenomenon?

B. Nebulous Questions.

Can an <u>automatic</u> man made sonar system duplicate (or better) the target recognition and clutter suppression capability of cetaceans and bats? How would such a system work?

1.1 --Continued.

II. Animal Echolocation.

A. Specific Questions.

Is there a restricted set of signals that encompasses most animal echolocation waveforms? Is there a general theory that is applicable to both porpoise and bat sonar? What is the meaning of existing neurophysiological and psychoacoustic data, in terms of a mathematical model of the animals' receivers?

B. Nebulous Questions.

If animal echolocation behavior is mathematically explained, what then? Will neurophysiologists and psychoacousticians be given a new set of interesting experiments to perform, in order to discover how the theory is implemented? Can neurophysiological data reveal new processing implementations that would be useful to the engineer? Does an understanding of animal echolocation lead to an understanding of other auditory processes, such as speech recognition?

III. Communication Theory, Medicine, and Other Applications.

A. Specific Questions.

How do the answers to the above questions directly benefit the analysis and synthesis of man made communication systems, as well as sonar systems? Are there some straightforward applications to medicine, e.g., to diagnostic ultrasound?

1.1 --Continued.

B. Nebulous Questions.

How can other branches of engineering or science benefit from an understanding of animal echolocation systems?

Most of the above questions are answered, with varying degrees of confidence and completeness, in this report. It is the author's hope that the report not only answers some past questions, but generates insights for interesting and useful future work. It is also hoped that the reader now has sufficient motivation to investigate this report, as well as related research, in further detail.

"The prospects of using animal echolocation are inexhaustible in the area of technology, engineering development and in all those problems which have been raised by bionics. Numerous articles and books have been written on this, and diverse judgments have been offered at special conferences and symposia. But up to now they have reflected usually hypotheses, searches, desires, and dreams rather than specific results. We might recall here the wise words of the professor at Leningrad University, A. A. Ukhtomskiy: 'Man is a very powerful being: if he begins to dream seriously, then this means that sooner or later the dream will come true'."[31]

2. REVIEW OF PREVIOUS RESULTS.

2.1 A Signal Processing Model.

The cetacean sonar signal processor is modelled as shown in Figure 2-1. Auditory threshold data (Figure 2-2) seems to imply the existence of the whitening filter shown in the Figure 2-1. For a constant internal threshold T_I, the externally measured threshold of hearing $T_E(\omega)$ should satisfy the equation

$$T_E(\omega)\ W(\omega) = T_I \qquad (2\text{-}1)$$

where $W(\omega)$ is the transfer function of the whitening filter. Given the shape of $W(\omega)$ from Figure 2-2 and Equation (2-1), one would expect $W(\omega)$ to vary inversely with $S_N(\omega)$, the ambient noise power spectral density. Figure 2-3 indicates that $W(\omega)$ indeed behaves as a whitening filter.

2.2 Description of Objects; Target Transfer Function.

Many engineers have suggested that radar/sonar echoes can be described as linear transformations of transmitted waveforms.[4-9] This description implies that the Fourier transform of the echo, $E(\omega)$, can be expressed as the product of the target transfer function, $T(\omega)$, and the Fourier transform of the transmitted signal, $U(\omega)$;

$$E(\omega) = T(\omega)\ U(\omega)\ . \qquad (2\text{-}2)$$

Simple geometrical forms (spheres, cylinders, cones, etc.) have radar or sonar cross sections, $|T(\omega)|^2$, that can generally be represented by only a few

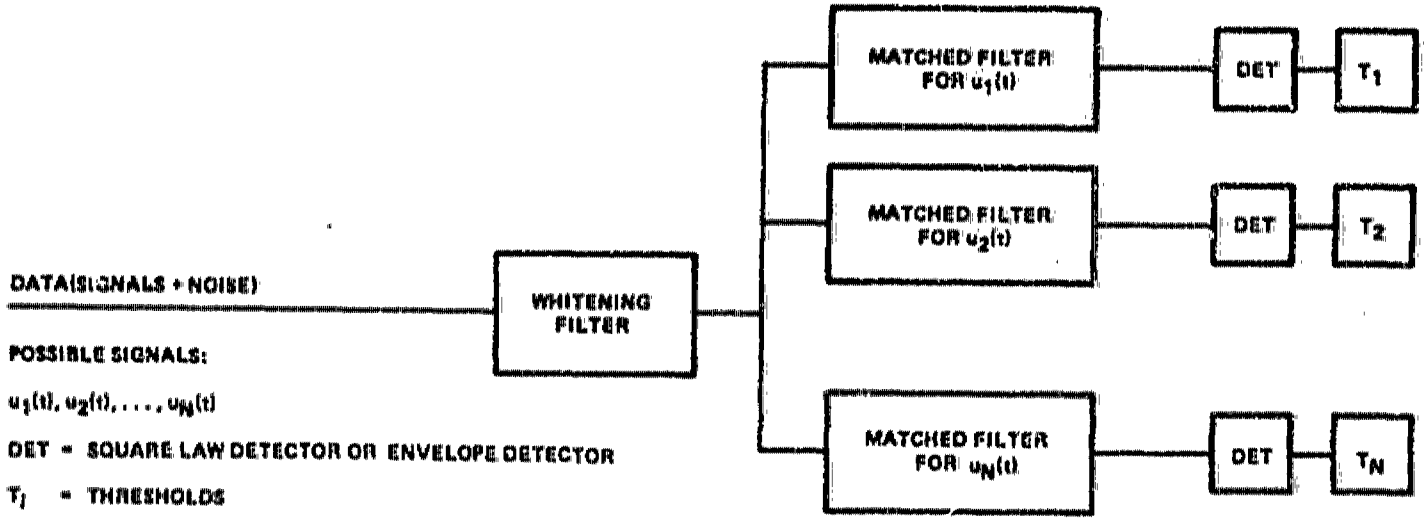

Figure 2-1. The Optimum Linear Receiver for uncorrelated signals, $u_1(t)$, $u_2(t)$, ..., $u_N(t)$.

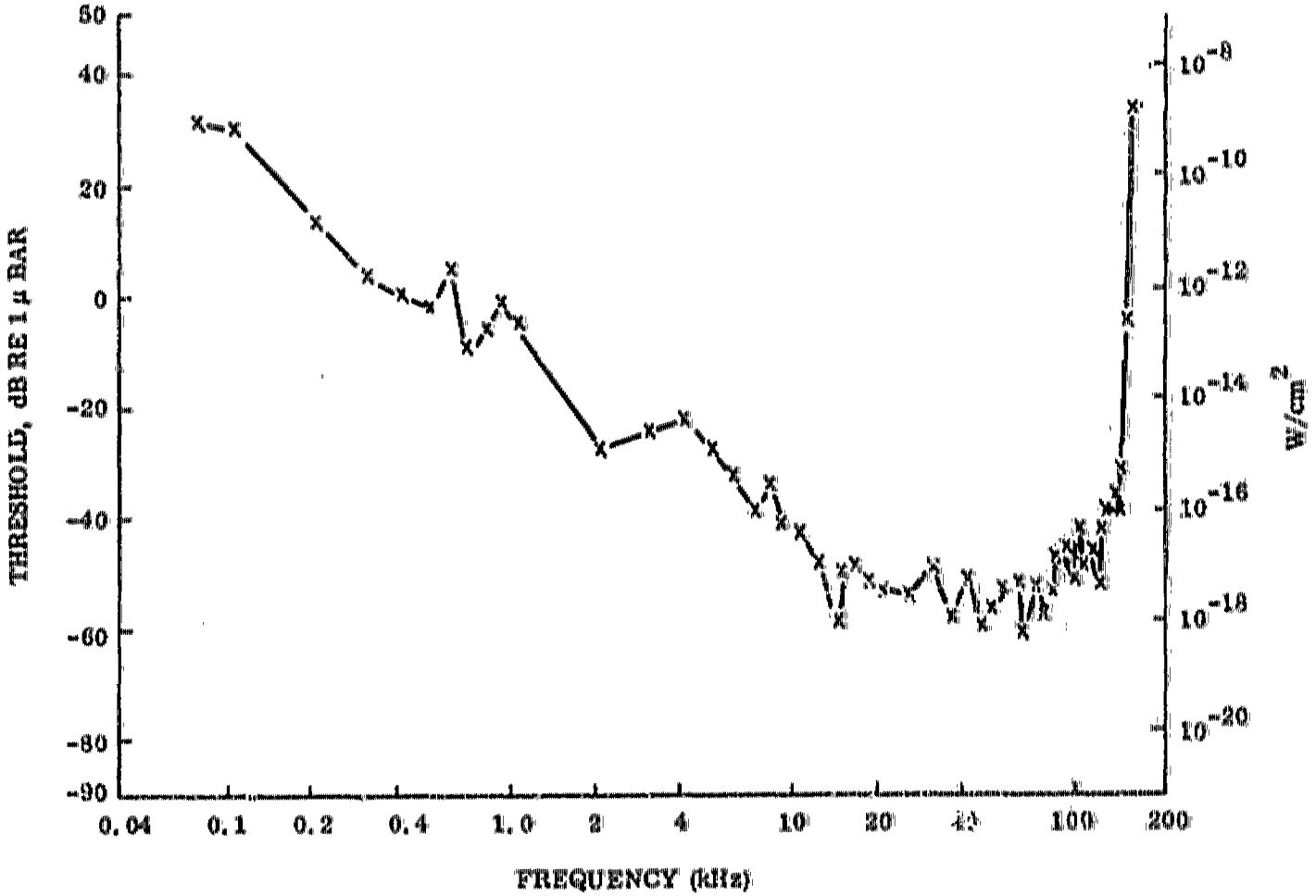

Figure 2-2. Porpoise Audiogram

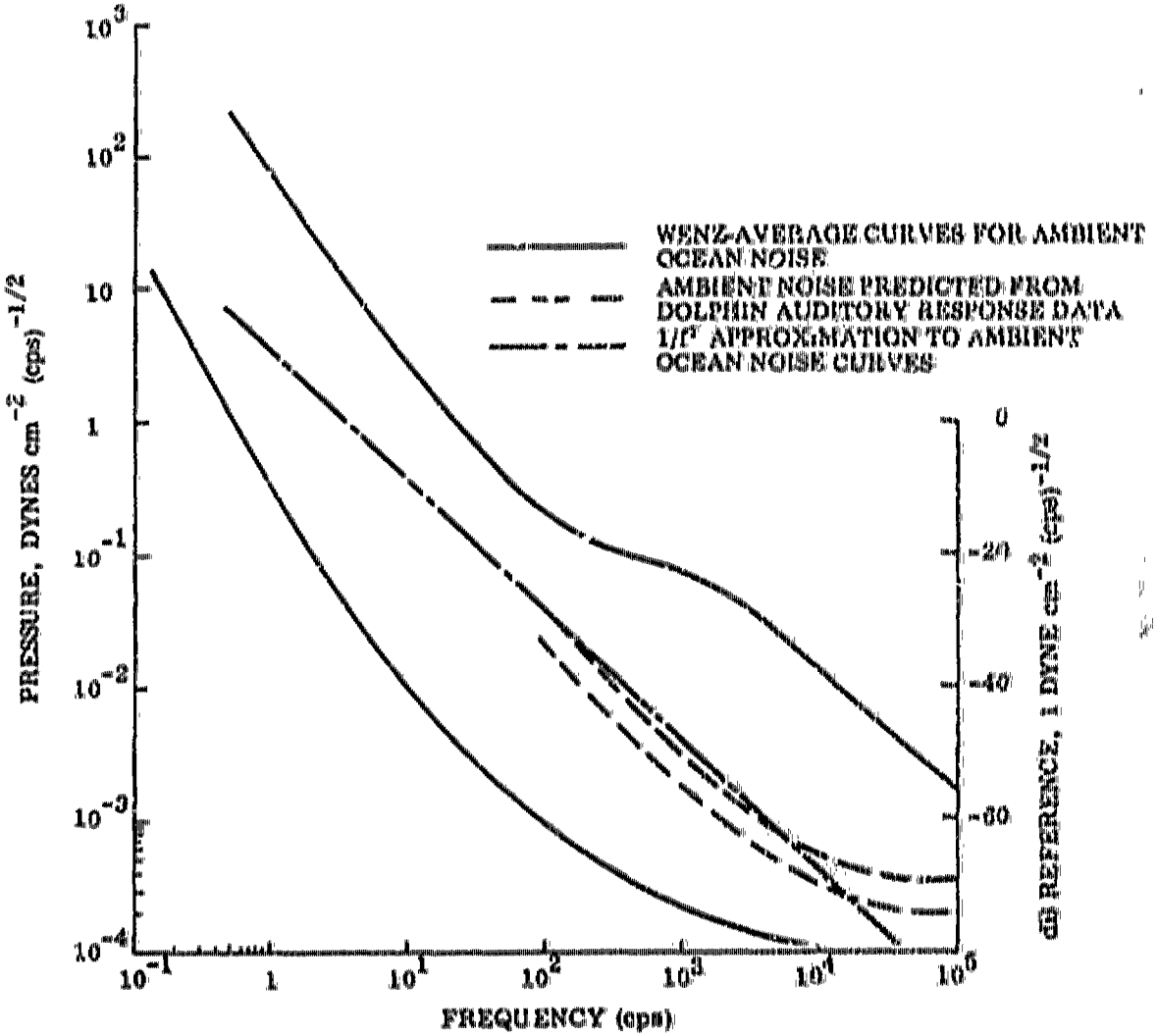

Figure 2-3. Ambient Ocean Noise as a Function of Frequency. Predicted Curves Assume That the Dolphin is Equipped With a Whitening Filter

2.2 --Continued.

terms of a Taylor series.[10, 11] A Taylor series or polynomial representation should therefore be an efficient way to characterize T (ω) with a minimum number of parameters*.

Suppose that each filter in Figure 1 could isolate a different coefficient of the polynomial

$$T(\omega) = a_0 + a_1 \omega + a_2 \omega^2 + \ldots . \qquad (2\text{-}3)$$

A large number of filters would generally not be required. Substituting (2-3) into (2-2),

$$E(\omega) = a_0 U(\omega) + a_1 \omega U(\omega) + a_2 \omega^2 U(\omega) + \ldots . \qquad (2\text{-}4)$$

Characterization of a target in terms of the a_i's is only possible if the components of the series (2-4) can be separated. To accomplish this separation the signal should have the property that $\omega^m U(\omega)$ and $\omega^n U(\omega)$ are uncorrelated, for $m \neq n$. A filter matched to $\omega^n U(\omega)$ should respond strongly to a signal with transform $\omega^m U(\omega)$ only if $m = n$. This requirement is illustrated in Figure 2-4. If the requirement is satisfied then there will be no confusion due to cross correlation effects.

The situation shown in Figure 2-4 will apply to signals that 1) have the property that

---

* A pleasing aspect of a series representation of target transfer function is that the simplest target, a flat plane, has the simplest series expansion, viz., $T(\omega) = a_0$.

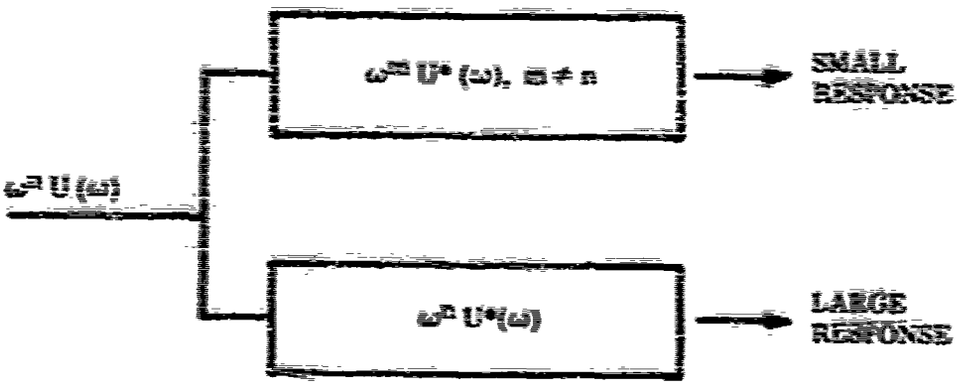

Figure 2-4. Illustration of the Decorrelation Requirement

2.2 —Continued.

$$\omega^{n} U(\omega) = C_n U(\omega/k^n) \qquad (2\text{-}6)$$

and $\frac{n}{2}$ are sufficiently sensitive to scale mismatch;

$$\max_{\tau} | C_n C_m \chi_{nm}(\tau, k^{n-m}) |^2 << | C_m^2 \chi_{mm}(\tau, 1) |^2, \qquad (2\text{-}6)$$

where $\chi_{nm}(\tau, s)$ is the wideband ambiguity function

$$\chi_{nm}(\tau, s) = \frac{1}{2\pi s^{1/2}} \int_{-\infty}^{\infty} U(\omega) U^*(\omega/s) e^{-j\omega\tau} d\omega. \qquad (2\text{-}7)$$

Equation (2-5) is satisfied by Analytic signals with Fourier transform*

$$U(\omega) = \omega^{\nu} e^{-(\log \omega)^2 / 2 \log k} G(\log \omega / \log k) \qquad (2\text{-}8)$$

where ν is any number and $G(\cdot)$ is any function such that $G(x + n) = G(x)$, where n is an integer (e.g., $G(x) = \sin 2\pi x$).

Signals described by (2-8) that are sufficiently sensitive to scale mismatch in the sense of (2-6) provide a means of target characterization via the Taylor series coefficients of a reflector's transfer function. Target description can thus be accomplished by signals that lie in the intersection of two sets, as shown in Figure 2-5.

* A derivation of (2-8) is given in the Appendix.

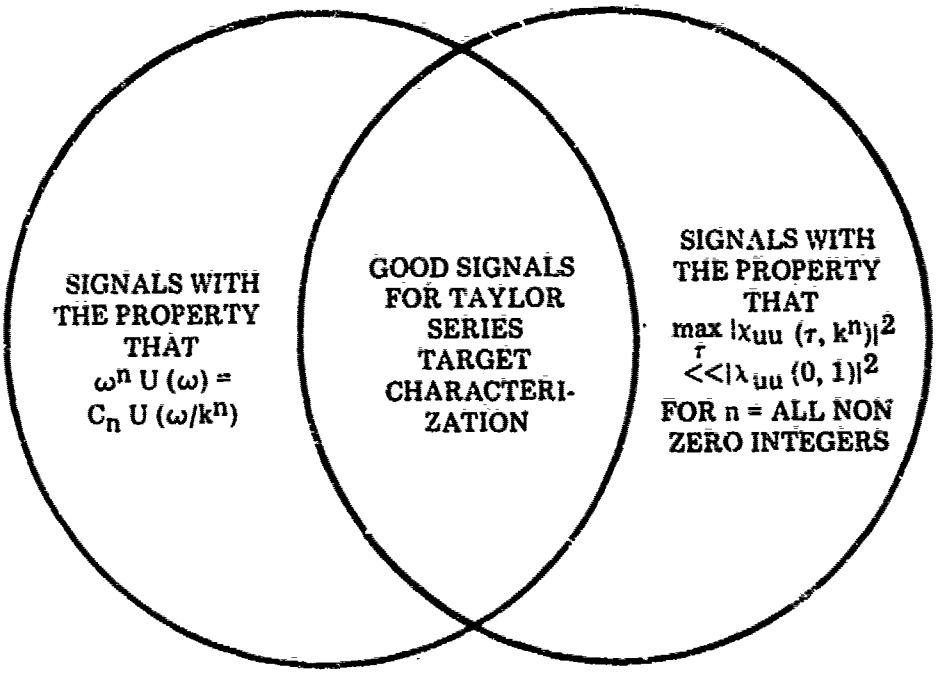

Figure 2-5. An Illustration of a Signal Design Method to Achieve the Decorrelation Requirement Shown in Figure 2-4.

2.2 --Continued.

The first set consists of all signals that satisfy condition (2-5). The second set consists of signals that are sensitive to scale mismatches of order k, k^2, k^3, etc.

It can be shown[3] that the whitening filter in Figure 2-1 has no effect upon target characterization with the signals (2-8), provided

$$W(\omega) \approx \omega^2 \qquad (2\text{-}9)$$

as shown in Figure 2-3. Each filter in Figure 1 is then matched to a differently scaled version of the transmitted signal, and the output of each filter estimates the value of a different target coefficient in Equation (2-3).

Tursiops Echolocation Signals

The measured waveforms * in Figure 2-6 were recorded while a Tursiops, vision occluded by opaque rubber cups, was discriminating between two acoustically different targets.[12]

The theoretical signals in Figure 2-6 correspond to different versions of (2-8), as listed in Table 2-1. The animal whose signals are shown in Figure 2-6 was born wild, and demonstrated a well developed ability to discriminate between targets

* All porpoise signals shown in this report were measured by W. E. Evans of NUC.

Table 2-1. Mathematical Expressions for the Theoretical Signals in Figure 2-6.

1. $$U(\omega) = -\omega^{-1.30} e^{-(\log \omega)^2} [1 + (.15j) e^{-j 8\pi \log \omega}] \cdot [1 - (.08j) e^{-j 4\pi \log \omega}] e^{j(-2\pi \log \omega + \pi/8)}$$

2. $$U(\omega) = \omega^{-0.9} e^{-(\log \omega)^2} [1 - (0.2j) e^{-j(8\pi \log \omega - \pi/4)}] \cdot e^{-j 2\pi \log \omega}$$

3. $$U(\omega) = \omega^{-11.2} e^{-4(\log \omega)^2} e^{-j 4\pi \log \omega} \cdot e^{-0.2 \sin(8\pi \log \omega)}$$

4. $$U(\omega) = \omega^{-5.4} e^{-2(\log \omega)^2} e^{-j 6\pi \log \omega} \cdot e^{-0.1 \cos(4\pi \log \omega) - j\pi/2}$$

5. $$U(\omega) = \omega^{-11.2} e^{-4(\log \omega)^2} e^{-j 4\pi \log \omega} \cdot e^{-0.2 \sin(8\pi \log \omega) - j\pi/2}$$

Table 2-1. -- Continued.

6. $$U(\omega) = \omega^{-5.4}\, e^{-2(\log \omega)^2}\, e^{-j\, 2\pi \log \omega}$$

$$\cdot\, e^{0.3 \sin (4\pi \log \omega + \pi/4) + j(0.15)\pi}$$

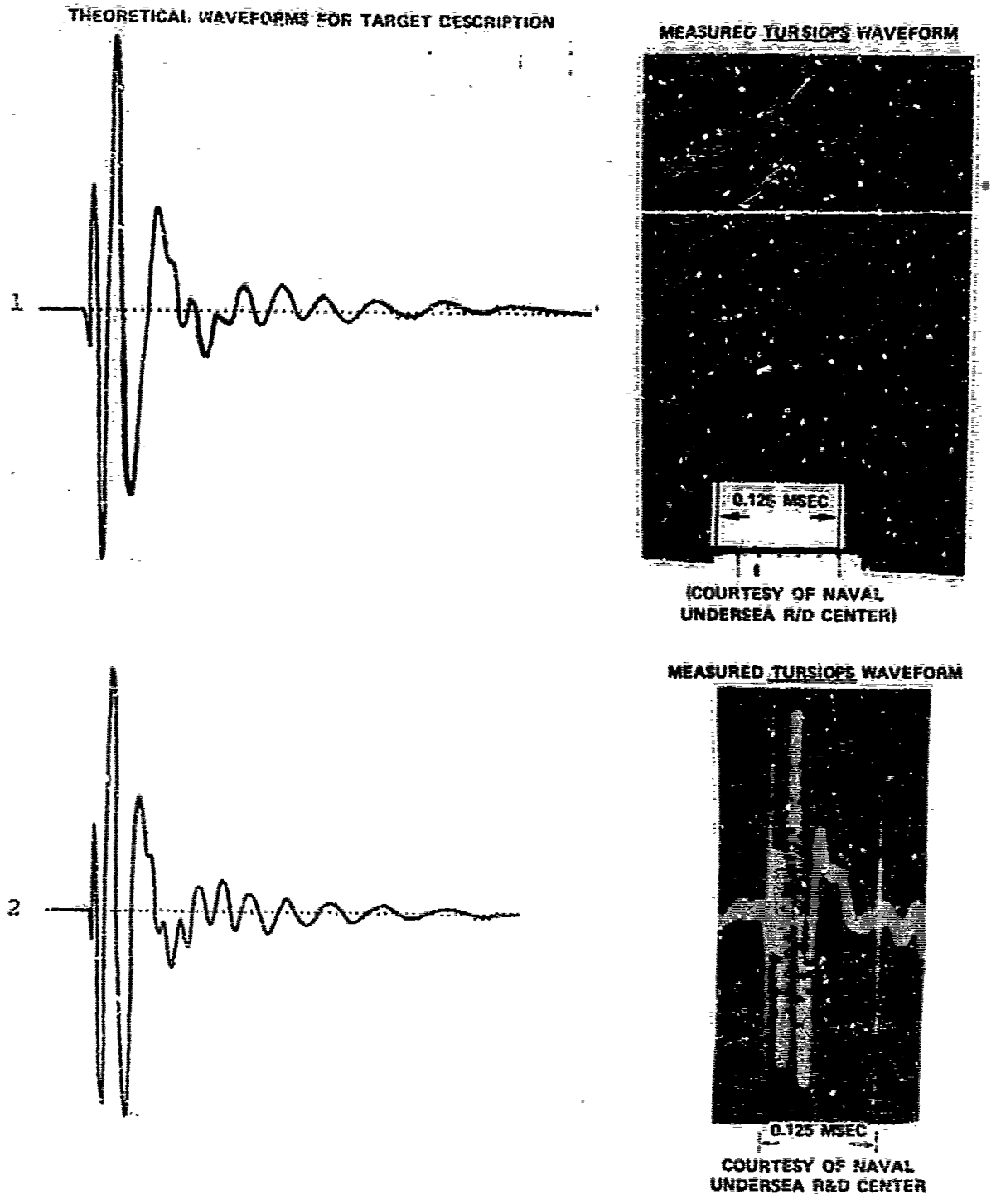

Figure 2-6. Theoretical and Measured Tursiops Sonar Signals (Experienced Animal Born Wild)

Figure 2-6. -- Continued

MEASURED TURSIOPS WAVEFORMS

3

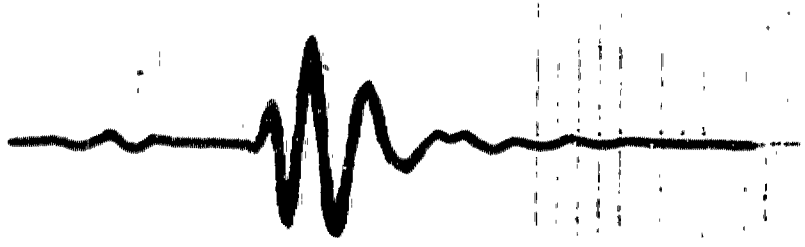

(COURTESY OF NAVAL
UNDERSEA R&D CENTER)

0.1 msec

0.125 msec

4

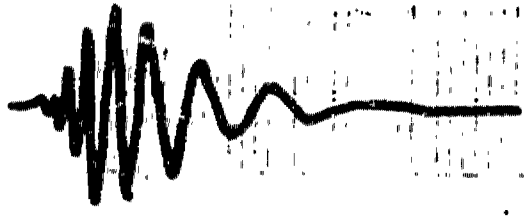

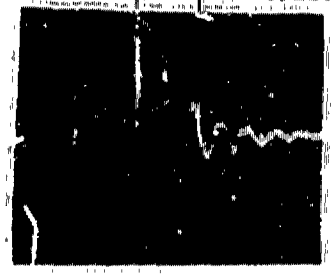

5

0.125
msec

Figure 2-6. -- Continued

2. _____--Continued.

by means of echolocation. At the time the signals were recorded this ability had become perfected even further, so that comparatively few pulses were used to perform the discrimination.

The measured waveforms in Figure 2-7 were recorded when a dolphin was performing range discrimination between two identical targets. The animal in this case was a Tursiops that had been born and raised in captivity. When this inexperienced animal was first induced to accept the rubber cups that occlude vision, he avoided large objects but was very cautious about getting too close to them. The animal could not initially find or recognize dead fish and exhibited an obviously startled reaction when he happened to bump into one. The dolphin learned quickly, however, and could soon recognize a fish or a hand in the water. It was interesting that a fish held in a hand constituted a new recognition problem, even though fish and hand could be recognized separately.

Even after developing the ability to discriminate between targets, the inexperienced animal's signals were occasionally unorthodox, as shown in Figure 2-7. Although the two measured signals in Figure 2-7 do not appear similar to those in Figure 2-6, the theoretical waveforms can still be expressed in terms of the functions (2-8). The parameters of the theoretical signals are given in Table 2-2.

The theoretical waveforms in Figures 2-6 and 2-7 are very similar to those used by Tursiops. This similarity suggests that the porpoise signals are "good waveforms for target description," as depicted in Figure 2-5. The theoretical waveforms that coincide with Tursiops signals can be further analyzed to determine their

Table 2-2. Mathematical Expressions for the Theoretical Signals in Figure 2-7.

1. $$U(\omega) = \omega^{-1.7}\, e^{-.94\,(\log \omega)^2}\, [\,1 + 1.6\, e^{-j\,[\,4\pi\,(.94)\log\omega - 3\pi/8\,]}\,]$$
$$\cdot\ [\,1 - .325\, e^{-j\,[\,2\pi\,(.94)\log\omega + \pi/4\,]}\,]$$
$$\cdot\ e^{-j\,[\,\pi\,(.94)\log\omega + .4\pi\,]}$$

2. $$U(\omega) = \omega^{-1.7}\, e^{-.94\,(\log \omega)^2}\, [\,1 + 2.0\, e^{-j\,[\,4\pi\,(.94)\log\omega - 3\pi/8\,]}\,]$$
$$\cdot\ [\,1 - .325\, e^{-j\,[\,2\pi\,(.94)\log\omega + \pi/4\,]}\,]$$
$$\cdot\ e^{-j\,[\,\pi\,(.94)\log\omega + .4\pi\,]}$$

Theoretical Signals

Measured Tursiops Waveforms

1

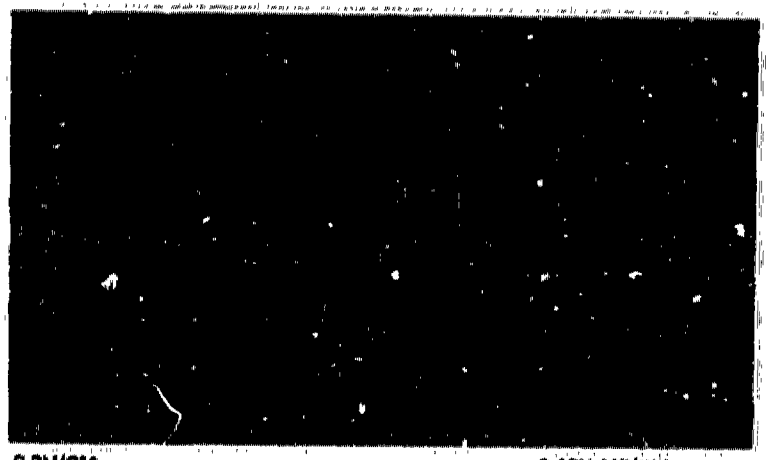

2

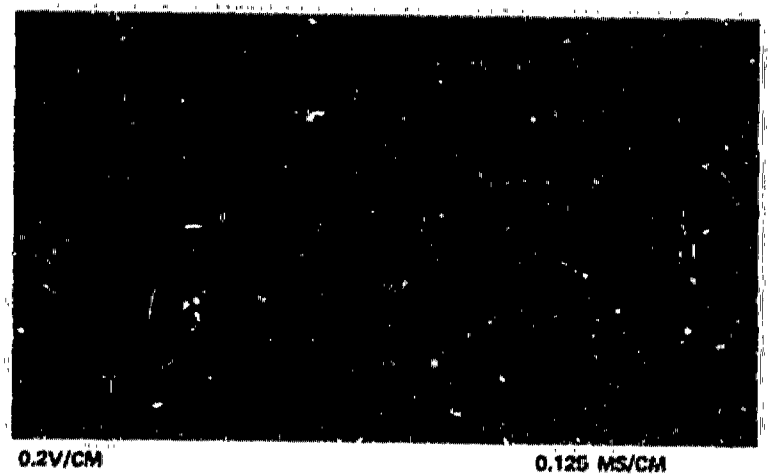

Figure 2-7. Theoretical and Measured Tursiops Sonar Signals (Inexperienced Animal Born in Captivity)

2.2 --Continued.

efficacy for target description and clutter suppression, as well as their resistance to confusion when objects are moving.

The wideband ambiguity function of the first theoretical signal in Figure 2-6 is shown in Figure 2-8. Figure 2-8 shows the region of the stretch axis where typical target velocities (±20 knots) would appear. The response of the filter $U^*(\omega)$ to energy normalized echoes of the form $k^{-n/2} U(\omega/k^n)$ for $n = 1$ and $n = 2$ correspond to profiles drawn along the dotted lines in the figure.

The ambiguity function can be interpreted as the response of the filter $U^*(\omega)$, matched to the transmitted signal, to energy normalized echoes that are scaled versions of the transmitted signal. With this interpretation it is evident that the signal will work well for detecting large planar objects surrounded by small Rayleigh scatterers. The sonar cross section, $|T(\omega)|^2$, of a Rayleigh scatterer [13] varies as ω^4. Since such a scatterer is small in comparison with a wavelength, $T(\omega)$ will have negligible phase variation as a function of frequency. Therefore $T(\omega)$ is proportional to ω^2. The filter's response to a planar target is at $s = 1$ in Figure 2-8, while the response to a Rayleigh scatterer is at $s = k^2$.

The ambiguity function can also be interpreted as the response of the filter $k^{-n/2} U^*(\omega/k^n)$ to other scaled, energy normalized versions of $U(\omega)$. If one is looking for a small scatterer against a large, flat reflecting surface, the filter function is $k^{-\frac{1}{2}} U^*(\omega/k^2)$ and the clutter is the unscaled signal with transform $U(\omega)$. The response of this filter to an energy normalized echo from the flat reflector is

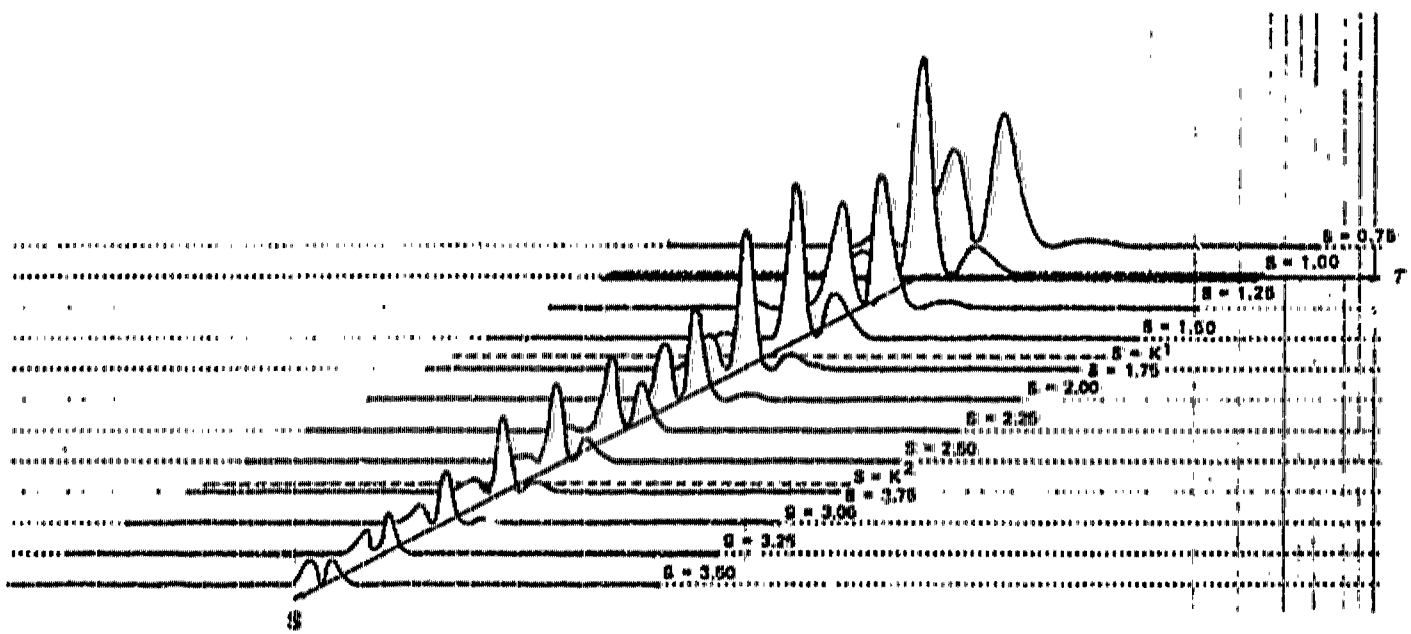

Figure 2-8. The Wideband Ambiguity Function of the First Theoretical Waveform in Figure 2-6 and Table 2-1. Shaded Region Shows the Range of s-Values Associated with Target Motion. Positions of k^1 and k^2 Profiles are Shown by Dotted Lines.

2.2 --Continued.

then given by the $s = k^{-2}$ profile * in Figure 2-8, while the response to the small scatterer is given by the $s = 1$ profile.

The ambiguity function of the theoretical Tursiops signal indicates that the waveform should work well for detecting a small object amid planar clutter. Indeed, Tursiops appear capable of locating and identifying a small target that is positioned against a highly reflective surface, e.g., fish floating at air/water interface, fish in contact with a rock, or fish on a flat bottom.

The shaded region of the ambiguity plane in Figure 2-8 illustrates that little confusion is introduced by moving targets, since the scale factor associated with motion is much less than that associated with reflection from complex objects. The signal is sufficiently scale sensitive for target description, but lacks the time-bandwidth product[14] to be truly doppler resolvent.

* Although the $s = k^{-2}$ profile is not illustrated in Figure 2-8, it can be shown that the maximum height of the k^{-2} profile is the same as that of the k^{2} profile.

2.2 --Continued.

It can be shown that many Tursiops echolocation signals resemble optimally scale sensitive waveforms when signal bandwidth is rigidly constrained.[2,15] These similarities have caused some confusion because (1) bandwidth and duration are so rigidly constrained that the signals are not sufficiently resolvent to measure velocity induced (doppler) stretch and (2) the signals are generally used to investigate fixed, immobile targets. The theory of target description summarized in Figure 5 provides an explanation for both of these phenomena.

2.3 Signal - Filter Design for Shape Discrimination between Different Targets.

A fundamental assumption was used to explain dolphin signals, i.e., that sonar echoes can be conceived as linear transformations of transmitted waveforms. Echoes can then be described as a simple convolution of target impulse response and transmitted signal. In the frequency domain,

$$E_T(\omega) = T(\omega)\ U(\omega) \qquad (2\text{-}10)$$

where $E_T(\omega)$ is the Fourier transform of the echo, $T(\omega)$ is the target transfer function, and $U(\omega)$ is the Fourier transform of the transmitted signal.

Standard procedures for radar/sonar clutter suppression generally exploit range and velocity differences to discriminate against spurious targets.[16,17,18,19,20] It would seem, however, that little attention has been given to the possibility of clutter suppression by impulse response characterization. If target and clutter transfer

2.3 --Continued.

functions are reasonably well known (or if they can be measured) then it should be possible to discriminate against interfering reflectors even when the reflectors have range and velocity identical to those of the target.

Let $V^*(\omega)$ be the transfer function of the filter that is used to process received echoes, and let

$$E_C(\omega) = C(\omega)\ U(\omega) \tag{2-11}$$

be the echo from a typical clutter reflector. If $v(t)$ is the inverse Fourier transform of $V(\omega)$, then the response of the filter to a given clutter echo is

$$R(\tau) = \int_{-\infty}^{\infty} v(t)\ e_c^*(t+\tau)\ dt \tag{2-12}$$

where $e_c(t)$ is the inverse Fourier transform of $E_c(\omega)$. In terms of spectra,

$$R(\tau) = (1/2\pi) \int_{-\infty}^{\infty} V(\omega)\ E_c^*(\omega)\ e^{-j\omega\tau}\ d\omega$$

$$= (1/2\pi) \int_{-\infty}^{\infty} V(\omega)\ U^*(\omega)\ C^*(\omega)\ e^{-j\omega\tau}\ d\omega\ . \tag{2-13}$$

2.3 --Continued.

Let $p(\tau)$ be a probability density function that describes the range distribution of clutter reflectors, where τ is measured relative to the target. The expected output power (clutter response) of the filter is then

$$\text{clutter response} = E_c \int_{-\infty}^{\infty} p(\tau) \mid R(\tau) \mid^2 d\tau \qquad (2\text{-}14)$$

where E_c is the total energy of clutter returns. Since τ is measured relative to the target, $\tau = 0$ corresponds to the arrival time of the target echo. The response of the filter to the target echo is

$$\text{target response} = E_s \mid (1/2\pi) \int_{-\infty}^{\infty} T(\omega)\ U(\omega)\ V^*(\omega)\ e^{j\omega\tau}\, d\omega \mid^2, \qquad (2\text{-}15)$$

where E_s is the signal energy.

Since the maximum response is assumed to occur at $\tau = 0$,

$$\text{maximum target response} = E_s \mid (1/2\pi) \int_{-\infty}^{\infty} T(\omega)\, U(\omega)\, V^*(\omega)\, d\omega \mid^2. \qquad (2\text{-}16)$$

Assuming that the noise is approximately white over the receiver's bandwidth, the expected noise response of the filter is

2.3 --Continued.

$$\text{noise response} = (N_o/2) \cdot (1/2\pi) \int_{-\infty}^{\infty} |V(\omega)|^2 \, d\omega \qquad (2\text{-}17)$$

where $N_o/2$ is the noise power spectral density.

Interference is the sum of the noise response and the clutter response. The signal-to-interference ratio is then

$$SIR = \frac{E_s \left| \frac{1}{2\pi} \int_{-\infty}^{\infty} T(\omega)\, U(\omega)\, V^*(\omega)\, d\omega \right|^2}{\frac{N_o}{2} \cdot \frac{1}{2\pi} \int_{-\infty}^{\infty} |V(\omega)|^2 d\omega + E_c \int_{-\infty}^{\infty} p(\tau) |R(\tau)|^2 d\tau}$$

$$= \frac{\frac{2\mu}{N_o} \int_{-\infty}^{\infty} T(\omega)\, U(\omega)\, V^*(\omega)\, d\omega}{\int_{-\infty}^{\infty} |V(\omega)|^2 d\omega + \frac{2E_c}{2\pi N_o} \int_{-\infty}^{\infty} \int_{-\infty}^{\infty} V(x)\, H(\omega, x) V^*(\omega)\, dx\, d\omega} \qquad (2\text{-}18)$$

where

$$\mu = \frac{E_s}{2\pi} \left[\int_{-\infty}^{\infty} T(\omega)\, U(\omega)\, V^*(\omega)\, d\omega \right]^* \qquad (2\text{-}19)$$

2.3 --Continued.

and

$$H(\omega, x) = \int_{-\infty}^{\infty} p(\tau)\ U(\omega)\ C(\omega)\ U^*(x)\ C^*(x)\ e^{-\frac{i}{2}(x-\omega)\tau}\, d\tau\ . \qquad (2\text{-}20)$$

The filter function $V(\omega)$ that maximizes SIR will maximize the numerator of (2-18) while constraining the denominator to be small. For energy normalized filter functions, this approach leads to a constrained version of the Schwarz inequality.[21] The solution is

$$V(\omega) = (2\mu/N_o)\ T(\omega)\ U(\omega) - (2E_c/2\pi N_o) \int_{-\infty}^{\infty} V(x)\ H(\omega, x)\ dx. \qquad (2\text{-}21)$$

If clutter is assumed to be uniformly distributed in range, then

$$H(\omega, x) = 2\pi p(0)\ U(\omega)\ C(\omega)\ U^*(x)\ C^*(x)\ \delta(x-\omega) \qquad (2\text{-}22)$$

and

$$V^*(\omega) = \frac{\mu\ T^*(\omega)\ U^*(\omega)}{\frac{N_o}{2} + E_c p(0)\ |\ U(\omega)\ C(\omega)\ |^2}\ . \qquad (2\text{-}23)$$

Using (2-10) and (2-11), the maximum SIR receiver for white noise can be written

2.3 --Continued.

$$F(\omega) = \frac{E_T^*(\omega)}{k + |E_c(\omega)|^2} \quad . \tag{2-24}$$

Equations (2-23) and (2-24) give the best filter function for a given signal. The next step is to find the best signal for a given filter.

Since we are working with unit energy functions,

$$\int_{-\infty}^{\infty} |V(\omega)|^2 \, d\omega = \int_{-\infty}^{\infty} |U(\omega)|^2 \, d\omega = 2\pi E_u = 2\pi . \tag{2-25}$$

Equation (2-18) can then be rewritten

$$SIR = \frac{\frac{2\mu}{N_o} \int_{-\infty}^{\infty} T(\omega) \, V^*(\omega) \, U(\omega) \, d\omega}{\int_{-\infty}^{\infty} |U(\omega)|^2 d\omega + \frac{2E_c}{2\pi N_o} \int_{-\infty}^{\infty} \int_{-\infty}^{\infty} U^*(x) \, G(\omega, x) \, U(\omega) \, dx d\omega} \tag{2-26}$$

where

$$G(\omega, x) = \int_{-\infty}^{\infty} p(\tau) \, V^*(\omega) \, C(\omega) \, V(x) \, C^*(x) \, e^{-j(x-\omega)\tau} \, d\tau \quad . \tag{2-27}$$

2.3 --Continued.

Comparison of Equations (2-26, 2-27) with Equations (2-16, 2-20) reveals that when

$$V(\omega) \text{ is replaced by } U^*(\omega) \tag{2-28}$$

and

$$U(\omega) \text{ is replaced by } V^*(\omega) \tag{2-29}$$

the SIR is unchanged. The substitutions (2-28, 2-29) can then be applied to Equation (2-23), yielding

$$U(\omega) = \frac{\mu T^*(\omega) V(\omega)}{\frac{N_o}{2} + E_c p(0) \left| V(\omega) C(\omega) \right|^2} . \tag{2-30}$$

Indeed, the expression (2-26) is maximized when

$$U^*(\omega) = (2\mu/N_o) T(\omega) V^*(\omega) - (2E_c/2\pi N_o) \int_{-\infty}^{\infty} U^*(x) G(\omega, x) dx, \tag{2-31}$$

and when $p(\tau)$ is uniformly distributed in range, Equation (2-31) becomes identical with Equation (2-30).

2.3 --Continued.

Given an initial signal with Fourier transform $U_1(\omega)$, the best filter function $V_1^*(\omega)$ is given by Equation (2-23). The best signal $U_2(\omega)$ corresponding to $V_1(\omega)$ is then given by Equation (2-30). One can thus find the optimum signal-filter pair by iterative substitution into Equations (2-23) and (2-30). The optimum combination will result in negligible change when additional iterations are applied in an attempt to obtain better signal and filter functions.

The above procedure gives an optimum signal-filter pair for clutter suppression on the basis of reflector shapes, for a white noise background. The usual background encountered in the open ocean and in harbors is generally colored, however, as shown in Figure 2-3. For a noise spectrum $S_N(\omega)$ that has a colored component $S_c(\omega)$, the optimum filter function changes. Let

$$S_N(\omega) = N_o/2 + S_c(\omega), \qquad (2\text{-}32)$$

so that the noise response in (2-17) becomes

$$\text{noise response} = (N_o/2) \cdot (1/2\pi) \int_{-\infty}^{\infty} |V(\omega)|^2 \, d\omega$$

$$+ (1/2\pi) \int_{-\infty}^{\infty} S_c(\omega) |V(\omega)|^2 \, d\omega \, . \qquad (2\text{-}33)$$

2.3 ____ --Continued.

When the extra term in (2-33) is included in the denominator of the SIR in Equation (2-18), the filter function that maximizes SIR must satisfy the equation

$$V(\omega) = \frac{2\mu}{N_o} T(\omega) U(\omega) - \frac{2E_c}{2\pi N_o} \int_{-\infty}^{\infty} V(x) H(\omega, x)\, dx$$

$$- (2/N_o)\, S_c(\omega)\, V(\omega), \qquad (2\text{-}34)$$

i.e., an extra term is added to the right hand side of Equation (2-21).

Again assuming that clutter is uniformly distributed in range, the optimum filter function becomes

$$V^*(\omega) = \frac{\mu T^*(\omega) U^*(\omega)}{\frac{N_o}{2} + S_c(\omega) + E_c p(0) |U(\omega) C(\omega)|^2} . \qquad (2\text{-}35)$$

Since the colored noise term in (2-33) is independent of the signal, the expression (2-30) for the optimum signal is unchanged. Nevertheless, a simultaneous solution of Equations (2-30) and (2-35) for an optimum signal-filter pair will generally result in a different signal function when colored noise is introduced.

As in the clutter-free situation, it appears that the optimum filter is matched to the signal when noise is white, but a mismatched filter is optimum when

2.3 --Continued.

noise is not white. This observation is justified by assuming that V (ω) and U (ω) are identical. Under this assumption, both (2-30) and (2-23) become

$$\frac{N_o}{2} + E_c\, p(0) \mid V(\omega)\, C(\omega) \mid^2 = \mu\, T^*(\omega) \quad . \tag{2-36}$$

Taking the magnitude of both sides,

$$\mid V(\omega) \mid^2 = \mid U(\omega) \mid^2 = \frac{\mu \mid T(\omega) \mid - N_o/2}{E_c\, p(0) \mid C(\omega) \mid^2} \quad . \tag{2-37}$$

In frequency intervals where $N_o/2 > \mu \mid T(\omega) \mid$, no useful information can be obtained for making a decision about the presence or absence of a target. Therefore,

$$\mid V(\omega) \mid^2 = \mid U(\omega) \mid^2 = \frac{\max\left[\mu \mid T(\omega) \mid - N_o/2,\ 0\right]}{E_c\, p(0) \mid C(\omega) \mid^2} \quad . \tag{2-38}$$

If V (ω) and U (ω) are assumed to be identical for the colored noise situation, the above procedure leads to a contradiction; (2-30) and(2-35) give

$$\mu \mid T(\omega) \mid = \frac{N_o}{2} + S_c(\omega) + E_c\, p(0) \mid V(\omega)\, C(\omega) \mid^2$$

$$= \frac{N_o}{2} + E_c\, p(0) \mid V(\omega)\, C(\omega) \mid^2 \quad . \tag{2-39}$$

2.3 --Continued.

The two quantities on the right hand side of (2-39) cannot be equal unless $S_c(\omega) = 0$. A matched filter is only optimum when the additive noise has constant power spectral density. For colored noise, a mismatched filter results in a larger signal to interference ratio.

3. LINEAR FILTERS FOR TAYLOR SERIES SIGNAL ANALYSIS, WITH APPLICATIONS TO THEORIES OF HEARING AND ANIMAL ECHO-LOCATION.

How does one determine the Taylor series spectral coefficients of any given time function? The method that first springs to mind is to evaluate the derivatives of the function's Fourier transform at $\omega = 0$. This method, however, has certain disadvantages which will be discussed.

A better scheme would be to find a linear filtering operation such that each coefficient is determined by measuring a maximum filter response. Such an operation can indeed be constructed. The resulting processor is a bank of constant Q filters.

The importance of this filtering technique is that the resulting processor corresponds closely to psychoacoustic models of the mammalian auditory spectrum analyzer. The correspondence implies that the sound processors of porpoises, bats, and people are all designed for Taylor series spectral analysis. The efficient utilization of these processors as sonar receivers involves the transmission of a particular set of echolocation signals. This signal set is the same as the one described in Section 2.

In summary, one can start from the premise that signals are to be analyzed in terms of their Taylor series spectral coefficients. With this premise, one can derive both the signals and the sonar processors that are employed for animal echolocation.

3.1 Taylor Series Signal Analysis.

Suppose a received signal f (t) is to be described in terms of the complex power series coefficients of its Fourier transform F (ω), i.e., in terms of f_0, f_1, ..., f_n, ..., where

$$F(\omega) = \sum_{n=0}^{\infty} f_n \omega^n \quad . \tag{3-1}$$

A straightforward way to obtain the Taylor coefficients $n! f_n$ is to multiply f (t) by $(j t)^n$ and measure the d. c. level of the resulting function, i.e., to evaluate

$$\frac{d^m}{d\omega^m} F(\omega) \Bigg|_{\omega = 0} = m! f_m \quad . \tag{3-2}$$

Such a procedure is disadvantageous because it involves a nonlinear operation in the time domain and because it assumes that the time of arrival of f (t) is known. It is also only reasonable if f (t) has a known duration T, so that (3-2) can be determined by the operation

$$\int_0^T (j t)^m f(t)\, dt = m! f_m \quad . \tag{3-3}$$

3.1 --Continued.

The interval [0, T] over which f (t) is not identically zero must be well defined a priori, unless there is no extraneous noise.

When white noise is added, the ratio of signal power to noise power at the output of the processor (3-3) is

$$\frac{|\, m\,!\, f_m \,|^2}{\frac{N_o}{2}\int_o^T t^{2m}\, dt} = \frac{(2m+1)\,|\, m\,!\, f_m \,|^2}{\left(\frac{N_o}{2}\right) T^{2m+1}} \qquad (3\text{-}4)$$

where $N_o/2$ is the power spectral density of the added noise. For T = 1, (3-4) indicates that the signal to noise ratio increases with m, so that the higher order components are more accurately estimated than the lower order ones. The lower order terms, however, are generally more important than the higher coefficients if F (ω) is to be approximated over a bounded frequency interval with a finite number of coefficients. The dependence of signal to noise ratio on the order of the estimated coefficients must be listed as a disadvantage of the method described by (3-3).

The above disadvantages will be overcome if we can find a set of uncorrelated, unit energy functions $\phi_n(\omega)$ with the property that

$$\omega^n\, \phi_o(\omega) = C(n)\, \phi_n(\omega) \ . \qquad (3\text{-}5)$$

3.1 --Continued.

To say that the unit energy functions $\phi_n(\omega)$ are uncorrelated is to say that

$$\max_t \left| \frac{1}{2\pi} \int_0^\infty \phi_n(\omega)\ \phi_m^*(\omega)\, e^{j\omega t}\, d\omega \right|^2 << 1 \ . \qquad (3\text{-}6)$$

Condition (3-6) is somewhat stronger than the usual quasi-orthogonality condition,

$$\frac{1}{2\pi} \int_0^\infty \phi_n(\omega)\ \phi_m^*(\omega)\, d\omega = \begin{cases} 1 \ , & m = n \\ \text{a number} << 1 \ , & m \neq n \ . \end{cases} \qquad (3\text{-}7)$$

The integrals in (3-6) and (3-7) are taken over a semi-infinite interval because the $\phi_n(\omega)$ are assumed to be Analytic.[22, 23]

Functions with the properties (3-5) and (3-6) can be used to determine the Taylor coefficients of a given signal. The method is simply to substitute (3-5) into (3-1), so that

$$F(\omega) = \sum_{n=0}^{\infty} f_n\ C(n)\ \phi_n(\omega) / \phi_o(\omega) \ . \qquad (3\text{-}8)$$

Both sides of (3-8) can be multiplied by $C(m)^{-1}\, \phi_o(\omega)\, \phi_m^*(\omega)$, yielding

3.1 --Continued.

$$C(m)^{-1} \left[F(\omega)\ \phi_o(\omega)\ \phi_m^*(\omega) \right] = \sum_{n=0}^{\infty} \frac{C(n)}{C(m)} f_n \left[\phi_n(\omega)\ \phi_m^*(\omega) \right]. \tag{3-9}$$

Taking the Fourier transform of both sides and utilizing property (3-6),

$$\frac{C(m)^{-1}}{2\pi} \int_o^{\infty} F(\omega)\ \phi_o(\omega)\ \phi_{in}^*(\omega)\ e^{j\omega t}\, d\omega \approx f_m\ R_{\phi_m}(t) \tag{3-10}$$

where

$$R_{\phi_m}(t) = \frac{1}{2\pi} \int_o^{\infty} |\ \phi_m(\omega)\ |^2\ e^{j\omega t}\, d\omega \tag{3-11}$$

is the autocorrelation function of the time signal $\phi_m(t)$ whose Fourier transform is $\phi_m(\omega)$. Since

$$\max_t R_{\phi_m}(t) = \frac{1}{2\pi} \int_o^{\infty} |\ \phi_m(\omega)\ |^2\, d\omega \triangleq 1,$$

we have

$$\max_t \left[\frac{C(m)^{-1}}{2\pi} \int_o^{\infty} F(\omega)\ \phi_o(\omega)\ \phi_m^*(\omega)\ e^{j\omega t}\, d\omega \right] \approx f_m. \tag{3-12}$$

3.1 --Continued.

The approximation in (3-12) depends upon the extent to which the inequality (3-6) holds true. It will be shown in Section 4, however, that the f_n's can be accurately determined even if the "much less than" sign in (3-6) is replaced by a simple "less than" sign.

A set of functions that satisfy (3-5) and (3-6) has already been derived. The signals are given by

$$\phi_n(\omega) = U(\omega / k^n) \; / \; E_n^{1/2} \tag{3-13}$$

where $U(\omega)$ is given by Equation (2-8) and E_n is the energy of the function $U(\omega/k^n)$. Writing the left hand side of (3-9) in terms of $U(\omega)$,

$$C(m)^{-1} \; F(\omega) \; U(\omega) \; U^*(\omega / k^m) \; / \; (E_o E_m)^{1/2}$$

$$= \frac{C(m)^{-1} \; F(\omega)}{(E_o E_m)^{1/2}} \left[U(\omega) \quad C(m)^{-1} \; \omega^m \; U(\omega) \right]^*$$

$$= \frac{|C(m)|^{-2} \; F(\omega)}{(E_o E_m)^{1/2}} \left[\omega^{m/2} \; U(\omega) \right] \left[\omega^{m/2} \; U(\omega) \right]^*$$

$$= \frac{|C(m)|^{-2} \; F(\omega)}{(E_o E_m)^{1/2}} \; |C(m/2)|^2 \; |U(\omega / k^{m/2})|^2 \; . \tag{3-14}$$

3.1 --Continued.

To find f_m , pass f (t) through a filter with transfer function proportional to $| U (\omega / k^{m/2}) |^2$.

The filter transfer functions $| U (\omega / k^{m/2}) |^2$, m = 0, 1, 2, ..., N constitute a bank of constant-Q filters, since each transfer function is a stretched version of the preceding transfer function. More exactly, the ratio of center frequency, ω_o, to centralized mean square bandwidth, $D_\omega - \omega_o$, is constant. The constant-Q property is easily demonstrated by defining

$$\omega_o = \int_0^\infty \omega \, | U (\omega) |^2 \, d\omega \; / \; \int_0^\infty | U (\omega) |^2 \, d\omega$$

$$D_\omega = \left[\int_0^\infty \omega^2 \, | U (\omega) |^2 \, d\omega \; / \; \int_0^\infty | U (\omega) |^2 \, d\omega \right]^{1/2}. \quad (3\text{-}15)$$

By changing variables in the integrals, it is easily shown that when $U (\omega) \longrightarrow U (\omega / k^{m/2})$,

$$\omega_o \longrightarrow k^{m/2} \omega_o$$

$$D_\omega \longrightarrow k^{m/2} D_\omega$$

and $Q = \omega_o / (D_\omega - \omega_o)$ remains unchanged.

3.1 ---Continued.

The above mathematical manipulations can be summarized as follows:

In order to measure the spectral coefficient f_m of a given time function f (t), process f (t) with a filter whose transfer function is $| U (\omega / k^{m/2}) |^2$, where U ($\omega$) is given by Equation (2-8). The maximum filter response is proportional to f_m, provided the parameter k is sufficiently large.

To measure all the coefficients $f_o, f_1, \ldots, f_N$, use a bank of filters with transfer functions $| U (\omega / k^{n/2}) |^2$, n = 0, 1, 2, ... , N. This bank of filters has the property that all the transfer functions have the same Q, i.e., the same center frequency to bandwidth ratio.

If one is interested in the spectral Taylor coefficients of a filter with transfer function F (ω), one can pass the signal u (t), with Fourier transform U (ω), through the filter. The resulting signal (with spectrum F (ω) U (ω))can then be processed with a bank of filters whose transfer functions are proportional to $U^* (\omega / k^n)$, n = 0, 1, 2, ... , N. This filter bank also exhibits the constant Q property.

If one were to find a constant-Q filter bank in the laboratory (or in nature), and if the filter transfer functions had the correct shape, one could conclude that the filter bank is designed for Taylor series spectral analysis. The filters could be used for characterizing linear systems if one could generate the proper signal, u (t).

3.2 The Ear as a Spectrum Analyzer.

As a consequence of masking experiments [24, 25, 26] and an analysis of cochlear dynamics[27], the human ear is commonly modeled as a spectrum analyzer composed of constant-Q filters. The exact shape of these filters seems to be dependent upon the level of the signals that are used in the masking experiments.[78] For reasonably low levels, however, the shapes of the ear's filter transfer functions are very similar to the shape of $| U(\omega) |^2$, where $U(\omega)$ is given by Equation (2-8), provided $| G(\omega) | = 1$. That is,

$$U(\omega) = \omega^{\nu} e^{-\left[(\log \omega)^2 / 2 \log k\right]} e^{j 2\pi n \log \omega / \log k}, \qquad (3\text{-}16)$$

where $n = 0, \pm 1, \pm 2, \ldots$. Consider, for example, Zwicker's excitation curve[24] for a 1 kHz signal at 40 dB. Zwicker's curve, plotted in terms of voltage level (rather than dB) vs frequency (rather than critical band units)[28], is shown in Figure 3-1. Figure 3-2 is a scaled version of the function $\exp [-32 (\log \omega)^2]$. The two curves are very nearly identical.

As a consequence of this similarity, it can be postulated that the ear analyses signals in terms of the Taylor coefficients of their Fourier transforms. This observation may be very important for the efficient analysis, synthesis, and transmission of speech.

There is one disconcerting aspect concerning the similarity between the curves in Figures 3-1 and 3-2. If

$$| U(\omega) |^2 = \exp [-32 (\log \omega)^2] \qquad (3\text{-}17)$$

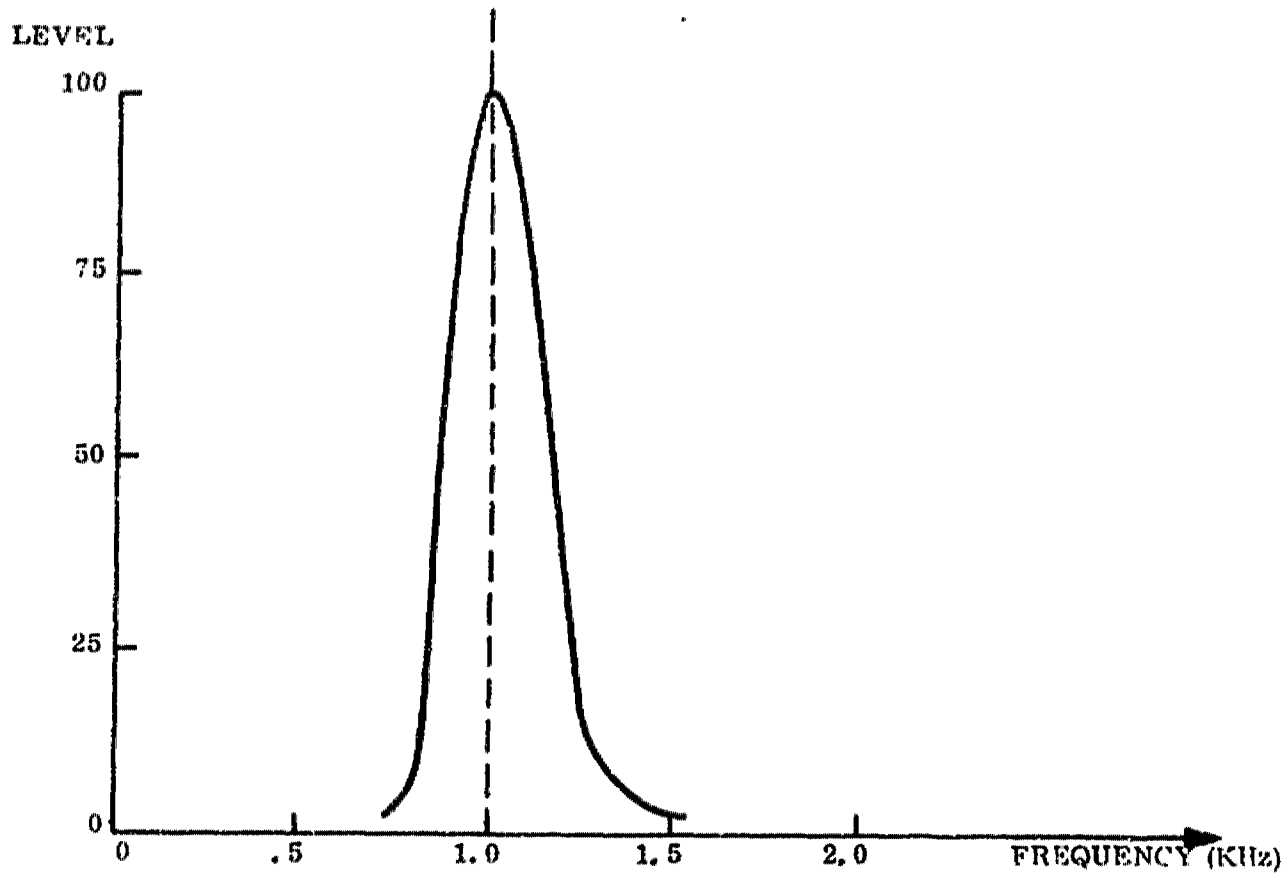

Figure 3-1. Zwicker's Excitation Curve for a Signal Frequency of 1 KHz at an Excitation Level of 40 dB. The shape of this Curve is Similar to Masking Data Measured by other Researchers. 24, 25 Note Linear Level Scale (rather than dB) and KHz frequency scale (rather than critical band units).

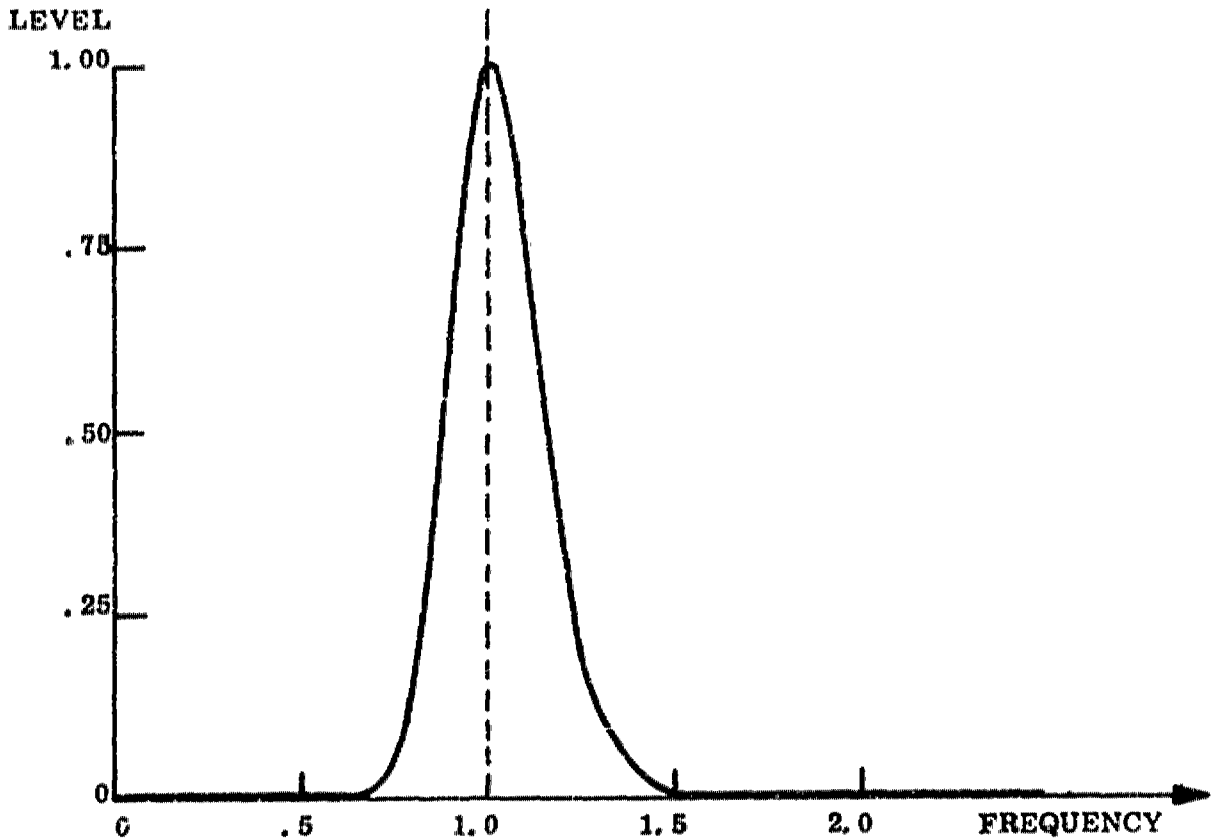

Figure 3-2. A Plot of $| U(\omega) |^2 = \exp [-32 (\log \omega)^2]$.

3.2 --Continued.

then $\log k = 1/32$, or

$$k = 1.0318 \ . \tag{3-18}$$

When $\phi_n(\omega)$ is defined as in (3-13), the left hand side of (3-6) becomes $\max_t | \chi_{uu}(t, k^{m-n}) |^2$, where $| \chi_{uu}(\tau, s) |^2$ is the wideband ambiguity function of the signal with Fourier transform (2-8). It can be shown (Appendix and Reference 3) that

$$\max_t | \chi_{uu}(t, k^{m-n}) |^2 = k^{-(m-n)^2/2} \ . \tag{3-19}$$

For $(m - n) = 1$, Equation (3-6) can only be written with a simple "less than" sign (rather than $<<$) for the value of k given by (3-18). This situation is not disastrous, however, because a linear transformation of the filter outputs can still result in determination of the individual coefficients f_m. Such a transformation arises naturally when a likelihood ratio test is applied to the filter outputs. A receiver that implements a likelihood ratio test is discussed in Section 4.

It should also be mentioned that the bandwidths of the ear's filter bank may be increased, allowing for a larger value of k.* D. M. Green[29] has found that human listeners increase their effective bandwidth to detect a wideband noise-like signal masked by additive noise. Green's data suggests that "critical bands are not fixed in width but are adjustable so as to match the particular detection situation."

* It is shown in the Appendix that the centralized bandwidth is proportional to the square root of $k^{3/2}(k^{1/2} - 1)$. A larger value of k thus implies a larger centralized bandwidth, and conversely.

3.3 Animal Echolocation.

The foregoing results provide an extremely simple and elegant approach to our previous observations about animal echolocation signals (Section 2). Suppose that a given receiver analyzes auditory signals in terms of the Taylor series coefficients of their Fourier transforms. If such a receiver incorporates a constant Q (or critical bandwidth) filter bank, it effectively performs the operation shown in Equation 3-14. According to the left hand side of 3-14, incoming data is multiplied by U (ω), where U (ω) is given by (2-8). The resulting product is then multiplied by $U^*(\omega/k^m)$, $m = 0, 1, 2, \ldots$.

Consider the utilization of such a receiver in a sonar system. As before, it is assumed that targets can be characterized in terms of their transfer functions. Letting F (ω) represent the target transfer function, a target can be characterized by transmitting a signal U (ω), as in Equation (2-8). The echo is then the product U (ω) $\times$ F (ω). This product should be multiplied by $U^*(\omega/k^m)$, $m = 0, 1, 2, \ldots$, as in Figure 1-1, in order to determine the power series coefficients o F (ω).

Given a set of constant-Q (critical bandwidth) filters, a natural method of signal analysis is to determine the Taylor coefficients of received signal spectra. Sonar target description can then be accomplished by determining the Taylor coefficients of target transfer functions. The waveforms that should be used for such a characterization are the set of signals that have already been matched to those employed by the Atlantic Bottlenose Dolphin ! Filtered versions of the same signals are used by the bat Myotis lucifugus. This observation is further discussed in Section 6.

3.4 Discussion.

Our model of ear as a particular kind of spectrum analyzer justifies the use of a specific class of functions for animal echolocation. The fact that these functions are actually utilized by bats and dolphins adds further validity to our model of the auditory processor.

The above analysis strongly suggests that the class of functions (3-16) is suitable not only for utilization by animals, but by humans as well. Indeed, when a dolphin-like pulse is reflected from different targets and suitably scaled, people can hear the difference between the echoes.[73] This experiment, together with the foregoing analysis, suggests that the signals should be incorporated into ultrasonic guidance devices for blind people[30] and into small s. s for scuba divers.[31]

Finally, the above results suggest that a study of animal echolocation can provide important clues for analysis of speech, both of cetaceans (if their communication sounds can indeed be classified as speech) and humans. These ideas will be reconsidered in Section 11.

4. LIKELIHOOD RATIO TESTING WITH FILTERS THAT IMPLEMENT A TAYLOR SERIES SPECTRUM ANALYSIS.

4.1 Processing the Filter Responses.

The receiver in Figure 1-1 does not fully specify the processing that should be applied to the outputs of the constant Q filters. A more complete specification can be obtained by subjecting the filter outputs to a likelihood ratio test.

The filter outputs are to be processed in order (i) to detect a signal with known Fourier transform F (ω) or (ii) to estimate the Taylor coefficients of F (ω) when they are not known a priori, i.e., to perform Taylor series spectrum analysis.

When the input signal has Fourier transform F (ω) U (ω), it will be shown that the same initial operation is performed on the receiver outputs (i) to decorrelate the noise responses for maximum likelihood detection of a known spectrum F (ω), and (ii) to determine the Taylor coefficients of an unknown spectrum F (ω). It will be shown that the ideal detector implements a simple correlation process on the filter outputs, while the maximum likelihood estimator measures the mean of a transformed version of the filter responses.

In the case of sonar, U (ω) is the transmitted signal spectrum, F (ω) is the target transfer function, and U (ω) F (ω) is the echo. When F (ω) itself is the received signal, one can determine the Taylor coefficients of the spectrum H (ω), where F (ω) $\equiv$ H (ω) U (ω). Since the function U (ω) has known coefficients, the coefficients of F (ω) can be determined from the measured H (ω) coefficients. It will be shown that the F (ω) coefficients are obtained from those of H (ω) by means of a convolution operation.

4.2 The Covariance of the Filter Responses with White Noise at the Input.

Assuming that the received signal has a spectrum $F(\omega)\, U(\omega)$ or $F(\omega) \equiv H(\omega)\, U(\omega)$, we want to determine the Taylor coefficients of $F(\omega)$ or $H(\omega)$. According to (3-14), the signal can be analyzed with a bank of filters with transfer functions $U^*(\omega / k^m) / C(m) (E_o E_m)^{1/2}$, $m = 0, 1, 2, \ldots$. To determine the weighted coefficients $C(m) f_m$, the filter bank consists of unit energy transfer functions

$$Z_m(\omega) = U^*(\omega / k^m) / E_m^{1/2} \qquad (4\text{-}1)$$

where $E_o \equiv 1$.

Let

$N_m(t)$ = noise at output of filter number m

$z_m(t)$ = impulse response of filter number m

= inverse Fourier transform of $Z_m(\omega)$

$N(t)$ = noise at the input

$R_{NN}(t)$ = autocorrelation function of N (t).

The likelihood ratio test involves a computation of two covariance matrices (for noise alone and for signal plus noise) at the filter outputs. To compute the noise covariance matrix at the filter outputs, one must determine $E\{N_n(t)\, N_m^*(t)\}$.

4.2 --Continued.

where

$$N_n(t) = \int_{-\infty}^{\infty} N(t-x)\, z_n(x)\, dx$$

$$N_m(t) = \int_{-\infty}^{\infty} N(t-y)\, z_m(y)\, dy \quad . \qquad (4\text{-}2)$$

From (4-2),

$$E\{N_n(t)\, N_m^*(t)\} = \iint_{-\infty}^{\infty} E\{N(t-x)\, N^*(t-y)\}\, z_n(x)\, z_m^*(y)\, dxdy$$

$$= \iint_{-\infty}^{\infty} R_{NN}(x-y)\, z_n(x)\, z_m^*(y)\, dxdy \quad . \qquad (4\text{-}3)$$

Assuming that the input noise is white, i.e.,

$$R_{NN}(x-y) = N_o/2\, \delta(x-y), \qquad (4\text{-}4)$$

$$E\{N_n, N_m^*\} = \frac{N_o}{2} \int_{-\infty}^{\infty} z_n(x)\, z_m^*(x)\, dx$$

$$= \left(\frac{N_o}{2}\right)\left(\frac{1}{2\pi}\right) \int_0^{\infty} Z_n(\omega)\, Z_m^*(\omega)\, d\omega \quad . \qquad (4\text{-}5)$$

4.2 -- Continued.

For U (ω) given by (2-8),

$$\frac{1}{2\pi} \int_0^\infty Z_n(\omega)\, Z_m^*(\omega)\, d\omega = \chi_{uu}(0, k^{n-m}) \quad . \tag{4-6}$$

4.3 Detection of a Signal with Spectrum F (ω) U (ω).

When a signal with spectrum F (ω) U (ω) is applied to the input of the receiver, the response of the m^{th} filter (with transfer function $Z_m(\omega)$) is

$$\begin{aligned} g_m &= \max_t \left[\frac{1}{2\pi} \int_0^\infty F(\omega)\, U(\omega)\, Z_m(\omega)\, e^{j\omega t}\, d\omega \right] \\ &= \max_t \sum_{n=0}^{\infty} f_n \left[\frac{1}{2\pi} \int_0^\infty \omega^n\, U(\omega)\, Z_m(\omega)\, e^{j\omega t}\, d\omega \right] \\ &= \max_t \sum_{n=0}^{\infty} f_n\, C(n)\, E_n^{1/2} \left[\frac{1}{2\pi} \int_0^\infty Z_n^*(\omega)\, Z_m(\omega)\, e^{j\omega t}\, d\omega \right] \\ &= \sum_{n=0}^{\infty} f_n\, C(n)\, E_n^{1/2} \max_t \chi_{uu}(k^m t, k^{n-m}) \\ &= \sum_{n=0}^{\infty} f_n\, C(n)\, E_n^{1/2}\, \chi_{uu}(0, k^{n-m}) \quad . \end{aligned} \tag{4-7}$$

4.3 --Continued.

Letting

$$\hat{f}_n = f_n \, C(n) \, E_n^{1/2}, \tag{4-8}$$

and using the relation (see Appendix)

$$\chi_{uu}(0, k^{n-m}) = k^{-(n-m)^2/4}, \tag{4-9}$$

Equation (4-7) gives

$$\begin{bmatrix} g_0 \\ g_1 \\ \cdot \\ \cdot \\ \cdot \\ \cdot \\ \cdot \\ g_N \end{bmatrix} = \begin{bmatrix} k^0 & k^{-1/4} & \cdots & k^{-N^2/4} \\ k^{-1/4} & k^0 & \cdots & k^{-(N-1)^2/4} \\ \cdot & \cdot & & \\ \cdot & \cdot & & \\ \cdot & \cdot & & \\ \cdot & \cdot & & \\ \cdot & \cdot & & \\ k^{-N^2/4} & k^{-(N-1)^2/4} & \cdots & k^0 \end{bmatrix} \begin{bmatrix} \hat{f}_0 \\ \hat{f}_1 \\ \cdot \\ \cdot \\ \cdot \\ \cdot \\ \cdot \\ \hat{f}_N \end{bmatrix}. \tag{4-10}$$

4.3 --Continued.

Letting $\underline{\underline{K}}_o$ be the covariance matrix of the noise outputs, Equations (4-5), (4-6), and (4-9) imply that

$$\underline{\underline{K}}_o = \left[E \left\{ N_n , N_m^* \right\} \right] = \frac{N_o}{2} \left[k^{-(n-m)^2/4} \right] \tag{4-11}$$

or

$$\underline{g} = \frac{2}{N_o} \underline{\underline{K}}_o \hat{\underline{f}} \tag{4-12}$$

Another covariance matrix must be computed in order to apply a likelihood ratio test. This matrix is the covariance of signal plus noise at the filter outputs. For noise with zero mean, the elements of the matrix are

$$E \left\{ \left[g_n + N_n (t) \right] \left[g_m^* + N_m^* (t) \right] \right\} - E \left\{ g_n \right\} E \left\{ g_m^* \right\}$$

$$= E \left\{ N_n (t) N_m^* (t) \right\} \tag{4-13}$$

where it has been assumed that the components g_n correspond to a deterministic signal, so that $E \left\{ g_n g_m^* \right\} = E \left\{ g_n \right\} E \left\{ g_m^* \right\}$.

Letting $\underline{\underline{K}}_1$ be the covariance matrix of filter outputs when a nonrandom signal and additive noise are present at the input of the receiver, Equations (4-13) and (4-11) give

*In Equation (4-11), the symbol [f (n, m)] indicates a matrix such that the element in the n^{th} row and m^{th} column is given by f (n, m).

4.3 --Continued.

$$\underline{\underline{K}}_1 = \underline{\underline{K}}_0 = \frac{N_o}{2} \left[k^{-(n-m)^2/4} \right] . \qquad (4\text{-}14)$$

Assuming that the input noise N (t) is Gaussian, the likelihood ratio test[32] compares the quantity

$$\ell (\underline{R}) = (\underline{R}^T - \underline{M}_o^T)\, \underline{\underline{Q}}_o\, (\underline{R} - \underline{M}_o) - (\underline{R}^T - \underline{M}_1^T)\, \underline{\underline{Q}}_1\, (\underline{R} - \underline{M}_1) \qquad (4\text{-}15)$$

with a threshold. In (4-15), $\underline{R}$ is the data vector, i.e., the voltages that appear at the filter outputs at any given time. The vector $\underline{M}_o$ is the mean of the data vector when the signal is absent, and $\underline{M}_1$ is the mean of the data when signal is present. For the case under consideration, $\underline{M}_o = 0$ and $\underline{M}_1 = \underline{g}$. Finally, $\underline{\underline{Q}}_o = \underline{\underline{K}}_o^{-1}$ and $\underline{\underline{Q}}_1 = \underline{\underline{K}}_1^{-1}$.

For the case of a nonrandom signal in the presence of white, Gaussian noise, we have determined that $\underline{\underline{K}}_o = \underline{\underline{K}}_1$, in accordance with Equation (4-14). In such a case, (4-15) simplifies[32] to the expression

$$\ell (\underline{R}) = \underline{R}^T\, \underline{\underline{Q}}_o\, (\underline{M}_1 - \underline{M}_o) = \underline{R}^T\, \underline{\underline{Q}}_o\, \underline{g} . \qquad (4\text{-}16)$$

The above expression is very meaningful in terms of Equations (4-10) and (4-11), since

$$\hat{\underline{f}} = \frac{N_o}{2}\, \underline{\underline{Q}}_o\, \underline{g} . \qquad (4\text{-}17)$$

4.3 --Continued.

Substituting (4-17) into (4-16) and neglecting the constant multiple $N_o/2$ (since a constant multiple merely changes the value of the threshold),

$$\ell(R) = R^T \hat{f} = \sum_{n=0}^{N} r_n \hat{f}_n \quad . \tag{4-18}$$

Equation (4-18) describes a correlation process. The filter outputs r_n are correlated with the signal coefficients $\hat{f}_n$. The process is illustrated in Figure 4-1.

In (4-16), the receiver operates on the data vector $\underline{R}$ in such a way as to decorrelate the noise readings. The transformed data should then be correlated with the expected values of the filter outputs when the signal is present. These values, however, are related to the weighted coefficients $C(n) E_n^{1/2} f_n$ by a transformation which is the inverse of the first (decorrelation) transformation. The result is a direct correlation of filter outputs and known coefficients, with no matrix transformations at all.

4.4 The Effect of Linear Filtering on the Taylor Coefficients of a Signal's Fourier Transform.

It has been assumed that (i) the input noise is white (Equation 4-4) and (ii) that the desired coefficients are those of $F(\omega)$, where the input signal has spectrum $F(\omega) U(\omega)$. With these assumptions, a simple processing implementation has been obtained. In the interest of simplicity, it is therefore reasonable to assume (i) that a

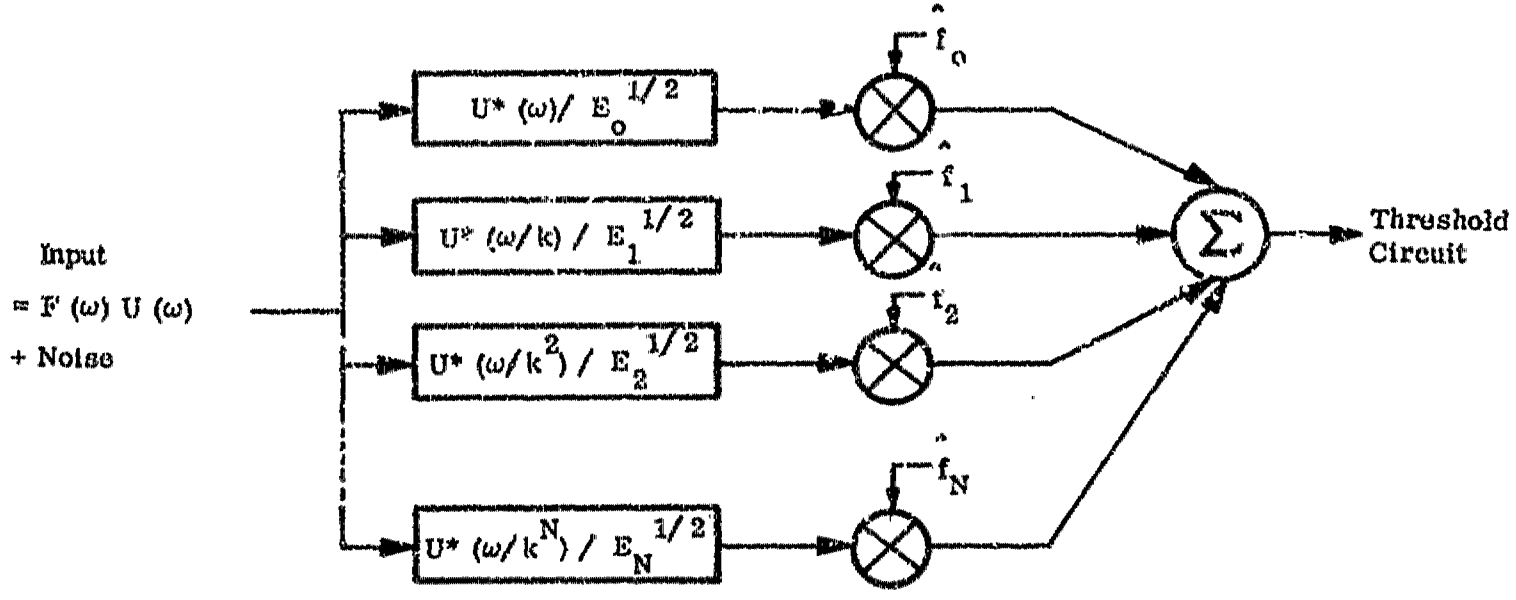

Figure 4-1. Detection of a Signal with Spectrum F (ω) U (ω) When the Taylor Series Coefficients of F (ω) are known.

4.4 --Continued.

whitening filter precedes the receiver when colored noise is present and (ii) that all input spectra can be written as the product of U (ω) with a finite order polynomial $\sum_{n=0}^{N} f_n \omega^n$. *

To discover the effect of these assumptions on the measured coefficients, it is necessary to investigate the change in a spectrum's Taylor series when the corresponding time signal is passed through a linear filter.

Consider the product A (ω) B (ω), where A (ω) can be visualized as the Fourier transform of a signal which is processed by a linear filter with transfer function B (ω). Let

$$A(\omega) = a_o + a_1 \omega + a_2 \omega^2 + \ldots + a_N \omega^N \qquad (4\text{-}19)$$

and

$$B(\omega) = b_o + b_1 \omega + b_2 \omega^2 + \ldots + b_N \omega^N \quad . \qquad (4\text{-}20)$$

---

* Notice that $\sum_{n=0}^{N} f_n \omega^n$ is neither band limited nor energy limited (square integrable) for N bounded and $0 \leq \omega \leq \infty$. For U ($\omega$) given by (2-8), however, the function $\left[\sum_{n=0}^{N} f_n \omega^n \right] U(\omega)$ is both band limited (in the mean square sense) and in $L^2(0, \infty)$.

4.4 --Continued.

Then

$$C(\omega) = A(\omega)\ B(\omega)$$

$$= c_o + c_1 \omega + c_2 \omega^2 + \ldots + c_{2N} \omega^{2N} \qquad (4\text{-}21)$$

where

$$\begin{bmatrix} c_o \\ c_1 \\ c_2 \\ \vdots \\ c_N \\ c_{N+1} \\ c_{N+2} \\ \vdots \\ c_{2N} \end{bmatrix} = \begin{bmatrix} a_o & 0 & 0 & \cdots & 0 \\ a_1 & a_o & 0 & \cdots & 0 \\ a_2 & a_1 & a_o & \cdots & 0 \\ \vdots & & & & \\ a_N & a_{N-1} & a_{N-2} & \cdots & a_o \\ 0 & a_N & a_{N-1} & \cdots & a_1 \\ 0 & 0 & a_N & \cdots & a_2 \\ \vdots & & & & \\ 0 & 0 & \cdots & & a_N \end{bmatrix} \begin{bmatrix} b_o \\ b_1 \\ b_2 \\ \vdots \\ b_N \end{bmatrix} . \qquad (4\text{-}22)$$

4.4 --Continued.

Now consider the convolution of two signals a (x) and b (x) ;

$$c(\tau) = \int_{-\infty}^{\infty} a(\tau - x)\, b(x)\, dx \equiv a(x) * b(x) \quad . \tag{4-23}$$

The convolution of the vectors $(a_o, a_1, \ldots a_N)$ and $(b_o, b_1, \ldots, b_N)$ is then obtained by reversing the a-vector and translating it with respect to the b- vector. For each translation, the convolution is the sum of the products of the corresponding elements. In matrix notation,

$$\begin{bmatrix} c_o \\ c_1 \\ c_2 \\ \vdots \\ c_N \\ c_{N+1} \\ c_{N+2} \\ \vdots \\ c_{2N} \end{bmatrix} = \begin{bmatrix} a_o & 0 & 0 & \cdots & 0 \\ a_1 & a_o & 0 & \cdots & 0 \\ a_2 & a_1 & a_o & \cdots & 0 \\ \vdots & \vdots & \vdots & & \vdots \\ a_N & a_{N-1} & a_{N-2} & \cdots & a_o \\ 0 & a_N & a_{N-1} & \cdots & a_1 \\ 0 & 0 & a_N & \cdots & a_2 \\ \vdots & \vdots & \vdots & & \vdots \\ 0 & 0 & 0 & \cdots & a_N \end{bmatrix} \begin{bmatrix} b_o \\ b_1 \\ b_2 \\ \vdots \\ b_N \end{bmatrix} . \tag{4-24}$$

4.4 --Continued.

Comparison of (4-22) and (4-24) demonstrates that the Taylor coefficients of the product A (ω) B (ω) are obtained by convolving the coefficients of the individual spectra.

Since the coefficients of the product of two spectra can be obtained by a convolution operation, they can also be obtained by a multiplication of Fourier transforms. One can construct pulse trains of the form

$$a_p(x) = \sum_{n=0}^{N} a_n \text{ rect } (x - 2n)$$

$$b_p(x) = \sum_{n=0}^{N} b_n \text{ rect } (x - 2n) \qquad (4\text{-}25)$$

where

$$\text{rect } (x) = \begin{cases} 1 , & 0 \leq x \leq 1 \\ 0 , & x < 0, \; x > 1 . \end{cases} \qquad (4\text{-}26)$$

Then

$$c_p(x) = a_p(x) * b_p(x)$$

$$= \sum_{n=0}^{2N} c_n \text{ tri } (x - n) \qquad (4\text{-}27)$$

4.4 --Continued.

where

$$\text{tri}(x) = \begin{cases} x, & 0 \le x \le 1 \\ 2 - x, & 1 \le x \le 2 \\ 0, & x < 0,\ x > 2 . \end{cases} \tag{4-28}$$

The coefficients c_n in (4-27) are given by (4-24). To obtain these coefficients more easily, one can compute $A_p(\omega)$ and $B_p(\omega)$, the Fourier transforms of $a_p(x)$ and $b_p(x)$. The function $c_p(x)$ is the inverse Fourier transform of $A_p(\omega) \times B_p(\omega)$.

As in the more conventional analysis of linear systems utilizing sine waves, Fourier transformation is seen to be a valuable tool. Usually, Fourier transforms are multiplied in order to compute convolutions that describe time functions. In the above analysis, Fourier transforms are again utilized to compute convolutions. For Taylor series spectral analysis, however, the convolutions describe functions in the frequency domain. Convolution of two time functions is equivalent to convolution of their Taylor series spectral coefficients.

4.5 Detection of a Signal F (ω) with Known Coefficients.

In order to detect a known signal F (ω) (rather than F (ω) U (ω))with spectral coefficients $\underline{f}$, Equation (4-18) implies that the filter responses $\underline{r}$ should be correlated with $\underline{\hat{h}}$, i.e. ,

4.5 --Continued.

$$\ell(R) = \sum_{n=0}^{N} r_n \hat{h}_n \qquad (4\text{-}29)$$

where, from (4-8),

$$\hat{h}_n = C(n)\, E_n^{1/2}\, h_n \qquad (4\text{-}30)$$

so that

$$\ell(\underline{R}) = \sum_{n=0}^{N} r_n\, C(n)\, E_n^{1/2}\, h_n \quad . \qquad (4\text{-}31)$$

The vector $\underline{h}$ corresponds to the coefficients of $H(\omega)$, where

$$F(\omega) \equiv H(\omega)\, U(\omega) \quad . \qquad (4\text{-}32)$$

If $U(\omega)$ has coefficients $\underline{u}$, then according to (4-26),

4.5 --Continued.

$$\begin{bmatrix} f_o \\ f_1 \\ f_2 \\ \cdot \\ \cdot \\ \cdot \\ \cdot \\ f_N \end{bmatrix} \cdot \simeq \begin{bmatrix} u_o & 0 & 0 & \cdots & 0 \\ u_1 & u_o & 0 & \cdots & 0 \\ u_2 & u_1 & u_o & \cdots & 0 \\ \cdot & \cdot & \cdot & & \\ \cdot & \cdot & & \cdot & \\ \cdot & \cdot & & & \cdot \\ \cdot & \cdot & & & \cdot \\ u_N & u_{N-1} & \cdots & & u_o \end{bmatrix} \begin{bmatrix} h_o \\ h_1 \\ h_2 \\ \cdot \\ \cdot \\ \cdot \\ \cdot \\ h_N \end{bmatrix} \tag{4-33}$$

where the approximation is obtained by representing U (ω) in terms of a polynomial with N coefficients on a bounded frequency interval.

Notice that the form (4-33) would not exist if U (ω) were defined in terms of an infinite number of coefficients. When U (ω) is approximated by a finite number N of coefficients, the frequency interval over which the approximation is accurate must always be bounded.* By the same argument, if the input function F (ω) is square integrable and is described in terms of N coefficients (N bounded), the analysis must apply to a bounded frequency interval rather than to the semi-infinite interval.

*A finite order polynomial in ω becomes unbounded as $\omega \to \infty$, whereas (2-8) implies that U (ω) $\to$ 0 as $\omega \to \infty$.

4.5 --Continued.

Equation (4-33) can be written

$$\underline{f} \approx \underline{u} * \underline{h} = \underline{\underline{T}}_{u} \underline{h}, \qquad (4\text{-}34)$$

where $\underline{\underline{T}}_{u}$ is the square (N x N) matrix in (4-33). The filter outputs in Equation (4-31) should therefore be correlated with $C(n) E_n^{1/2} b_n$, where

$$\underline{h} \approx \underline{\underline{T}}_{u}^{-1} \underline{f} \qquad (4\text{-}35)$$

and $\underline{f}$ corresponds to the known coefficients of the input signal spectrum (or approximations to these coefficients that are valid over a bounded frequency interval).

The process is shown in Figure 4-2. In terms of Figure 4-1, $F(\omega)$ is written as $H(\omega) U(\omega)$. The receiver then works to detect $H(\omega)$ as in Figure 4-1, where $H(\omega) = [\, U(\omega) \,]^{-1} F(\omega)$ or $\underline{h} = \underline{\underline{T}}_{u}^{-1} \underline{f}$.

4.6 Estimation of Unknown Spectral Coefficients.

If the signal coefficients are unknown, they can be estimated by determining the maximum value of the probability density function of the output observations when the signal is present. Letting $p(\underline{R} \mid H_1)$ be the probability density function

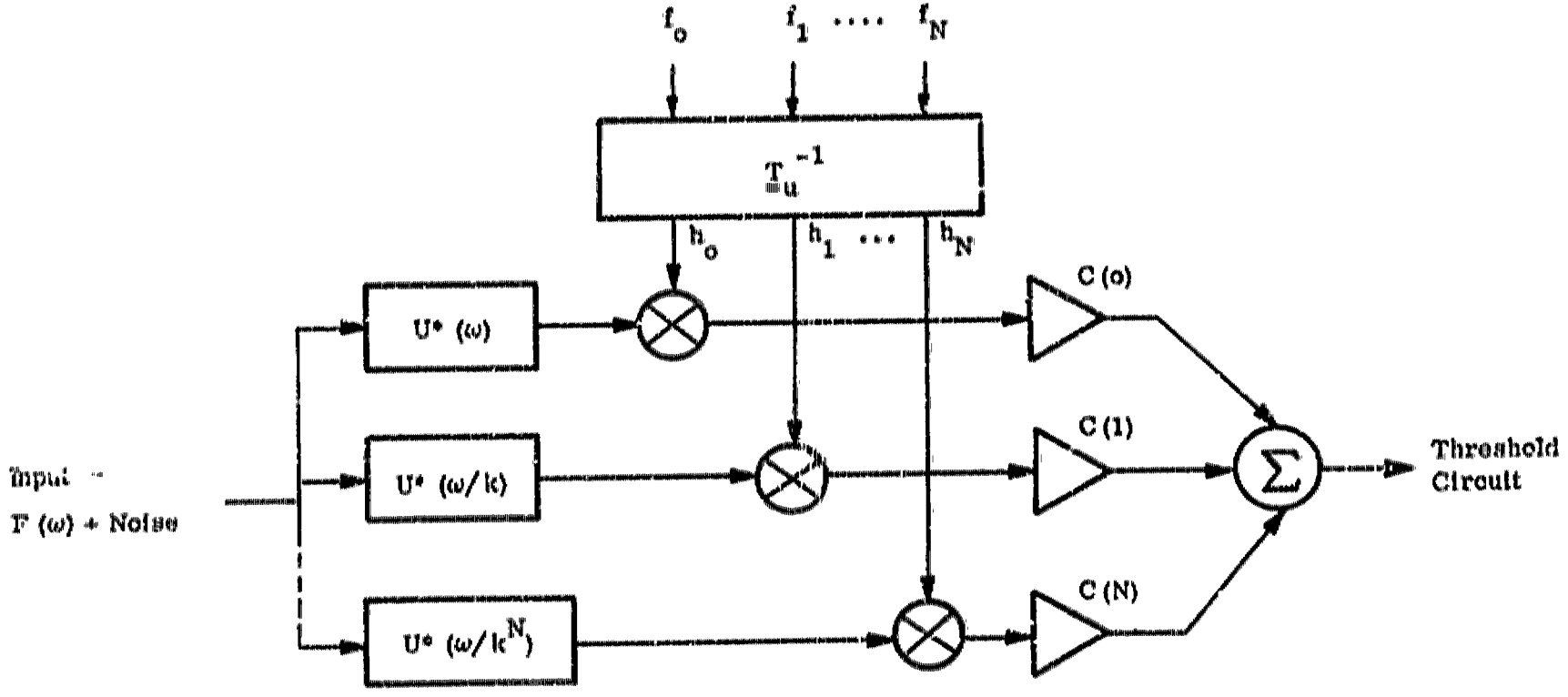

Figure 4-2. Detection of a signal with Spectrum F (ω) When the Taylor Series Coefficients of F (ω) are known.

4.6 --Continued.

describing the filter outputs in the presence of a signal,* the coefficients g_n (Equation 4-7) can be estimated by setting

$$\frac{\partial}{\partial g_n} \log \left[p\left(\underline{R} \mid H_1\right) \right] = 0 \ . \tag{4-36}$$

Equation (4-36) leads to a maximum likelihood (M L) estimate[33] of the $\underline{g}$ coefficients.

Once again, the fact that $\underline{f}$ is determined from $\underline{g}$ by computing $\underline{\underline{Q}}_o \underline{g}$ (Equations 4-17 and 4-8) results in considerable simplification. Consider an M L estimate performed on $\underline{\underline{Q}}_o \underline{r}$, rather than on $\underline{r}$ itself. The transformation $\underline{\underline{Q}}_o$ causes the noise readings to be statistically independent. In the presence of signal, $\underline{\underline{Q}}_o \underline{R}$ is a vector of independent Gaussian random variables with means given by $\underline{\underline{Q}}_o \underline{g} = (2/N_o) \hat{\underline{f}}$, from Equations (4-7) and (4-17). The distribution $p\left(\underline{\underline{Q}}_o \underline{R} \mid H_1\right)$ is therefore maximized by determining the mean value of each element of the output vector $\underline{\underline{Q}}_o \underline{r}$:

$$E\left\{\underline{\underline{Q}}_o \underline{R} \mid H_1\right\} = (2/N_o) \hat{\underline{f}}$$

$$\longrightarrow \text{ M L estimate of } \underline{f} \ , \tag{4-37}$$

---

* The notation used in this section is from Van Trees' book[32]. By using capital $\underline{R}$ and lower case $\underline{r}$, Van Trees distinquishes between a random variable ($\underline{R}$) and sample values of a random process ($\underline{r}$).

4.6 --Continued.

where, from (4-8),

$$f_n = [\, C(n)\ E_n^{1/2}\,]^{-1}\ \hat{f}_n \quad . \tag{4-38}$$

The above process is illustrated in Figure 4-3.

The processor in Figure 4-3 estimates the coefficients of F (ω), where the received signal is F (ω) U (ω). If the received signal is F (ω) alone, one can use the same procedure to estimate the coefficients of H (ω), where F (ω) = H (ω) U (ω). To obtain the coefficients of F (ω) from those of H (ω), Equation (4-34) can be invoked. The resulting process is shown in Figure 4-4 .

4.7 Relaxing the Decorrelation Requirement.

Equation (4-17) implies that the Taylor coefficients of an incoming spectrum can be estimated if the $\underset{=}{K}_o$ matrix (the covariance matrix of the noise responses) can be inverted. Inversion of $\underset{=}{K}_o$ is possible if its determinant is nonzero, i.e., if the parameter k in (2-3) and (4-10) is greater than one. In other words,

$$k^{(n-m)^2/4} = \chi_{uu}(0,\ k^{n-m}) < 1 \quad . \tag{4-39}$$

It has already been remarked that complete decorrelation of filter transfer functions is unnecessary. It is not necessarily required that $|\chi_{uu}(0,\ k^{n-m})|^2$ be <u>much</u> less than one ; a simple "less than" sign is sufficient.

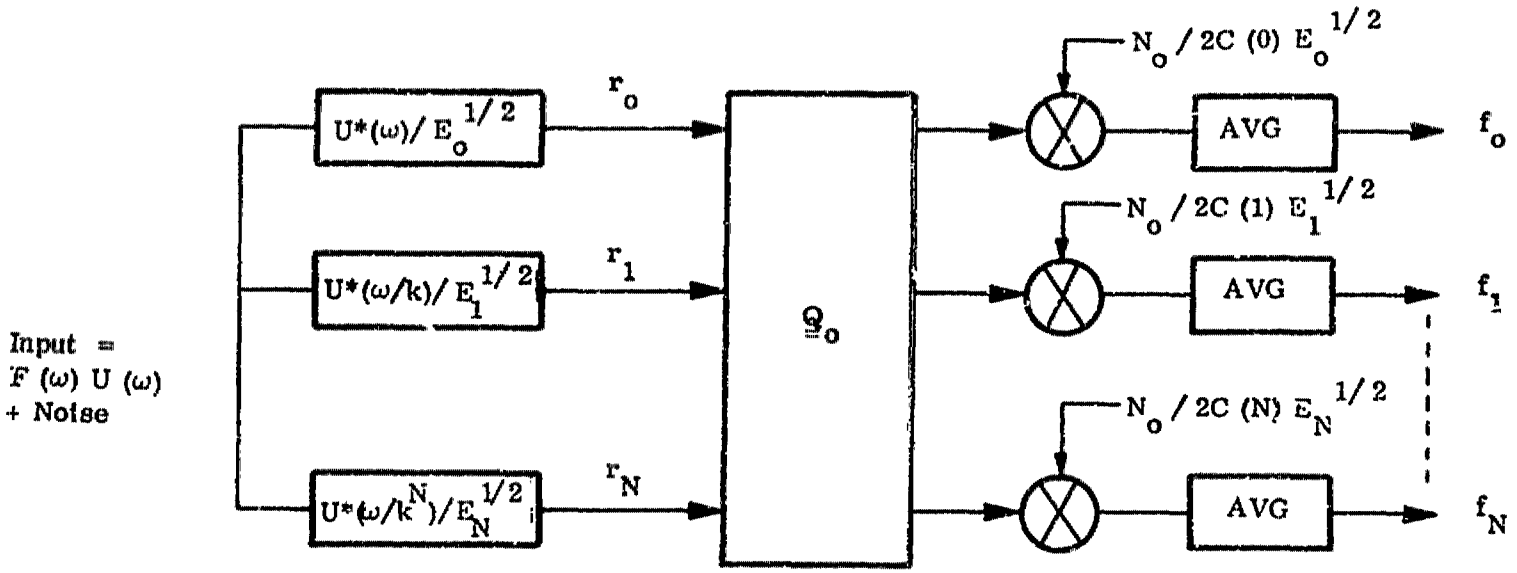

Figure 4-3. Maximum Likelihood Estimation of the Taylor Series Coefficients (f_o, f_1, . . . , f_N) of F (ω), when the Input Signal is F (ω) U (ω).

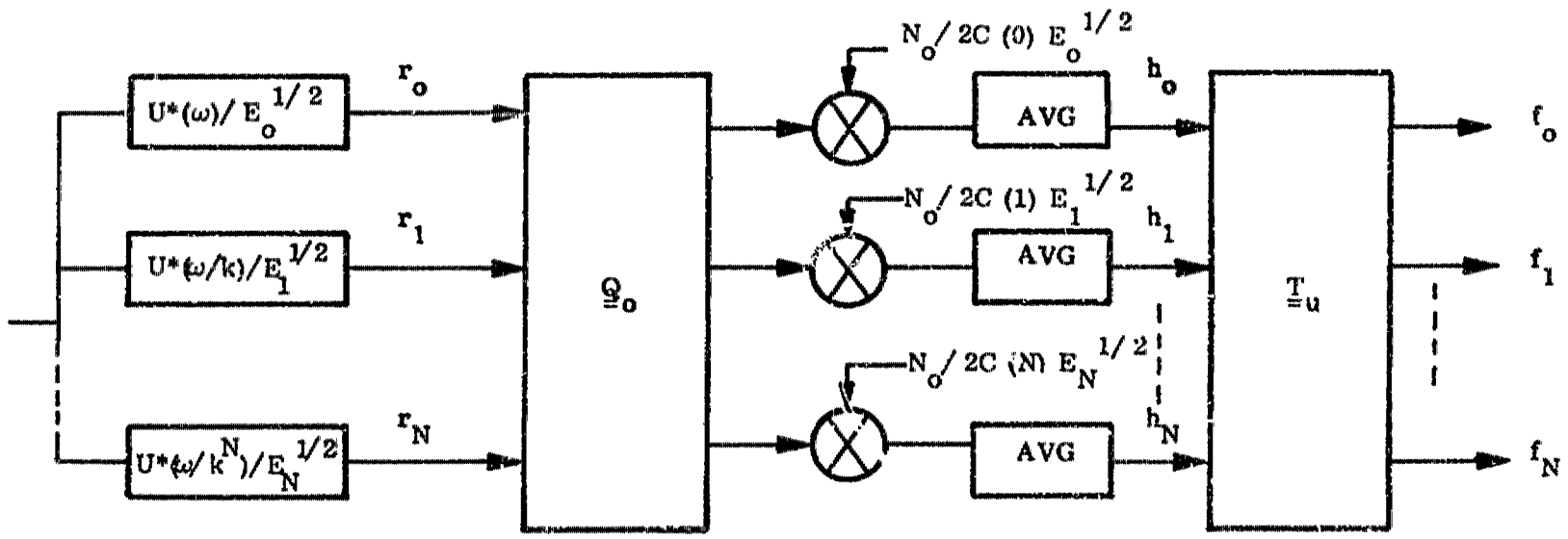

Figure 4-4. Maximum Likelihood Estimation of the Taylor Series Coefficients of F (ω), when the Input Signal is F (ω).

4.8 Detection of a Signal with Spectrum F (ω) U (ω) when the Power Series Coefficients of F (ω) are Random Variables.

The receiver in Figure 4-1 is easily generalized to the case where each coefficient f_n is a random variable with its own probability density function (pdf). Target coefficients that are random variables can result from the aspect dependence of a given reflector and/or the differences between individual members of a single target set, e.g., the set of dangerous sharks.

Unless a reflector is extremely symmetrical, its transfer function F (ω) will be dependent upon the position from which the reflector is observed. The Taylor series coefficients of F (ω) are therefore dependent upon aspect angle*, θ. Let $P(f_n|\theta)$ be the pdf describing the aspect dependence of each coefficient f_n. For a particular target, $P(f_n \mid \theta)$ equals $\delta [f_n - f_n(\theta)]$, where $f_n(\theta)$ is a deterministic function describing the aspect dependence of f_n. For a set of similar but not identical targets, $P(f_n \mid \theta)$ has a nonzero variance. Let P (θ) be the probability of encountering the target from a particular aspect angle, θ. Then the pdf associated with the random coefficient f_n is

$$P(f_n) = \int_0^{2\pi} P(f_n \mid \theta)\ P(\theta)\, d\theta \qquad (4\text{-}40)$$

Figure 4-1 summarizes the analysis in Section 4-3, where a likelihood ratio test is applied to a receiver with filters $Z_m(\omega) = U^*(\omega / k^m) / E_m^{1/2}$. The test consists of correlating the filter outputs with the numbers $\{C(n)\, E_n^{1/2} f_n\}$, where $\{f_n\}$ is a set of N power series coefficients describing F (ω).

*The aspect angle θ is a scalar if the problem is considered in two dimensions; θ is a two term vector for three dimensional problems.

4.8 --Continued.

When the coefficients $\{f_n\}$ are random variables, it can be shown[72] that

$$\ell(\underline{R}) = \int_{-\infty}^{\infty} \ell(\underline{R} \mid \underline{f})\, P(\underline{f})\, d\underline{f} \qquad (4\text{-}41)$$

where, from (4-18),

$$\ell(\underline{R} \mid \underline{f}) = \sum_{n=0}^{N} C(n)\, E_n^{1/2}\, r_n f_n \quad . \qquad (4\text{-}42)$$

Therefore,

$$\ell(\underline{R}) = \sum_{n=0}^{N} C(n)\, E_n^{1/2}\, r_n \overline{f_n} \qquad (4\text{-}43)$$

where

$$\overline{f_n} = \int_{-\infty}^{\infty} f_n\, P(f_n)\, df_n \quad . \qquad (4\text{-}44)$$

Substituting (4-40) into (4-44),

4.8 --Continued.

$$\overline{f_n} = \int_{-\infty}^{\infty} \int_{0}^{2\pi} f_n \, P(f_n \mid \theta) \, P(\theta) \, d\theta \, df_n$$

$$= \int_{0}^{2\pi} E\{f_n \mid \theta\} \, P(\theta) \, d\theta \qquad (4\text{-}45)$$

where the conditional expected value is

$$E\{f_n \mid \theta\} = \int_{-\infty}^{\infty} f_n \, P(f_n \mid \theta) \, df_n \, . \qquad (4\text{-}46)$$

If the problem is to detect a single, well-specified target, $E\{f_n \mid \theta\}$ is just the function $f_n(\theta)$ describing the dependence of each coefficient upon aspect angle. In this case,

$$\overline{f_n} = \int_{0}^{2\pi} f_n(\theta) \, P(\theta) \, d\theta \qquad (4\text{-}47)$$

and

$$\ell(R) = \sum_{n=0}^{N} C(n) \, E_n^{1/2} \, \epsilon_n \int_{0}^{2\pi} f_n(\theta) \, P(\theta) \, d\theta \, . \qquad (4\text{-}48)$$

4.8 --Continued.

Once again, P (θ) represents the sonar's probability of viewing the target from a particular aspect angle, θ.

5. SIGNAL TO INTERFERENCE RATIO (SIR) MAXIMIZATION USING LINEAR DETECTION.

5.1 Linear Detection of Received Signals.

In radar systems, decisions are usually based upon an envelope detected or squared version of correlator response. The reason for such nonlinear processing is the elimination of "fine structure" [76] within the autocorrelation function. This fine structure results from modulation of the baseband signal. If the signal u (t) modulates a carrier with frequency ω_o, the autocorrelation function of the modulated signal has the same envelope as the autocorrelation function of u (t). The phase of the autocorrelation function varies as $\omega_o t$. This phase variation is the so-called "fine structure" which is eliminated in order to feed a "cleaner" signal into the threshold detector.

An important difference between wideband sonar and radar (or narrowband sonar) is that the baseband signal is actually transmitted without modulating a carrier. All operations can therefore be carried out at baseband frequencies, and the autocorrelation function (for a properly designed signal) is no longer corrupted by the "fine structure" of radar theory.

Decisions can therefore be based upon the response of a completely linear system. Complete linearity is advantageous because phase differences can be exploited for both clutter suppression and enhancement of signal to noise ratio.

For clutter suppression, one can design a filter so that the maximum response to an unwanted reflector echo is negative, whereas the maximum response

5.1 --Continued.

to the desired target is positive. Square-law detectors would require the unwanted reflector to invoke a filter response whose magnitude was small.

For noise suppression, one can ignore large-negative filter outputs if the response to the desired signal is positive. Half of the noise-induced peaks of the squared filter response are thus ignored. As one would expect, the resulting signal to noise ratio is doubled, just as in comparisons of coherent vs. noncoherent detection.

5.2 Signal Design for Linear Detection.

If linear detection is to be used, the autocorrelation function should ideally have only one positive peak. It would seem, however, that large negative sidelobes are permissible. The large negative sidelobes of the autocorrelation functions* in Figures 5-1 and 5-2 will not not induce false triggering or range ambiquities if linear detection is used. These autocorrelation functions correspond to k = 1.5 and k = 2 in Equation (2-8), where $|G(\omega)| = 1$. These k-values bound most of the animal signals that have been studied thus far. In Tables 2-1 and 2-2, for example, $k \approx 1.65$.

Although large negative sidelobes are permissible from the viewpoint of range ambiguity peaks, such sidelobes are apparently not desirable for the resolution of two closely spaced targets. A small positive peak can be masked by a larger negative peak, corresponding to a large nearby reflector. The peak to sidelobe ratio improves as k is made larger, as shown in Figure 5-3.

* The functions in Figures 5-1 through 5-3 were computed and plotted by R.V. Jones of ESL.

Figure 5-1. The Autocorrelation Function Corresponding to U (ω) in Equation (2-8), with $|U(\omega)| = 1$ and $k = 1.6$.

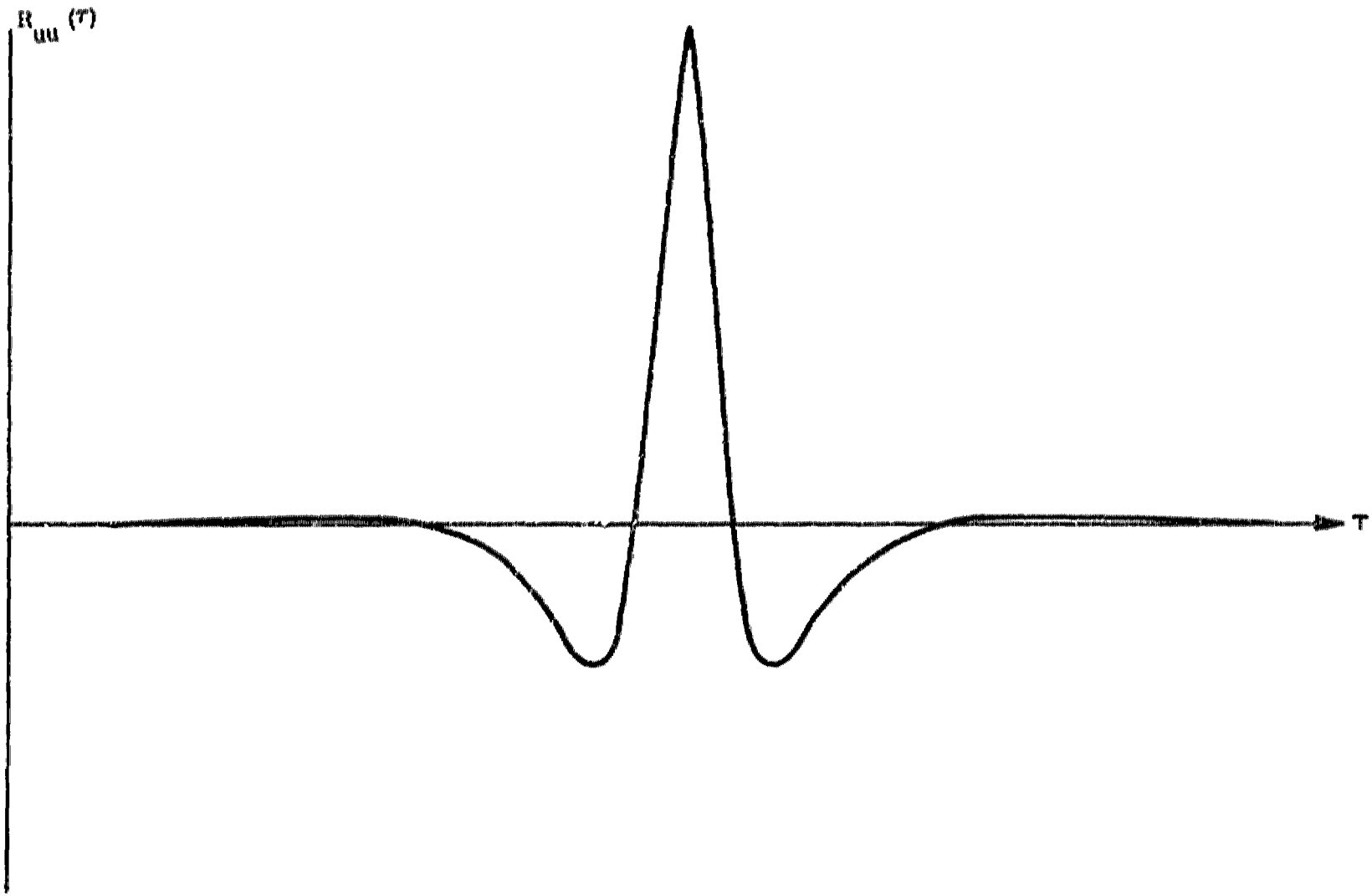

Figure 5-2. The Autocorrelation Function Corresponding to U (ω) in Equation (2-8), with | G (ω) | = 1 and k = 2.

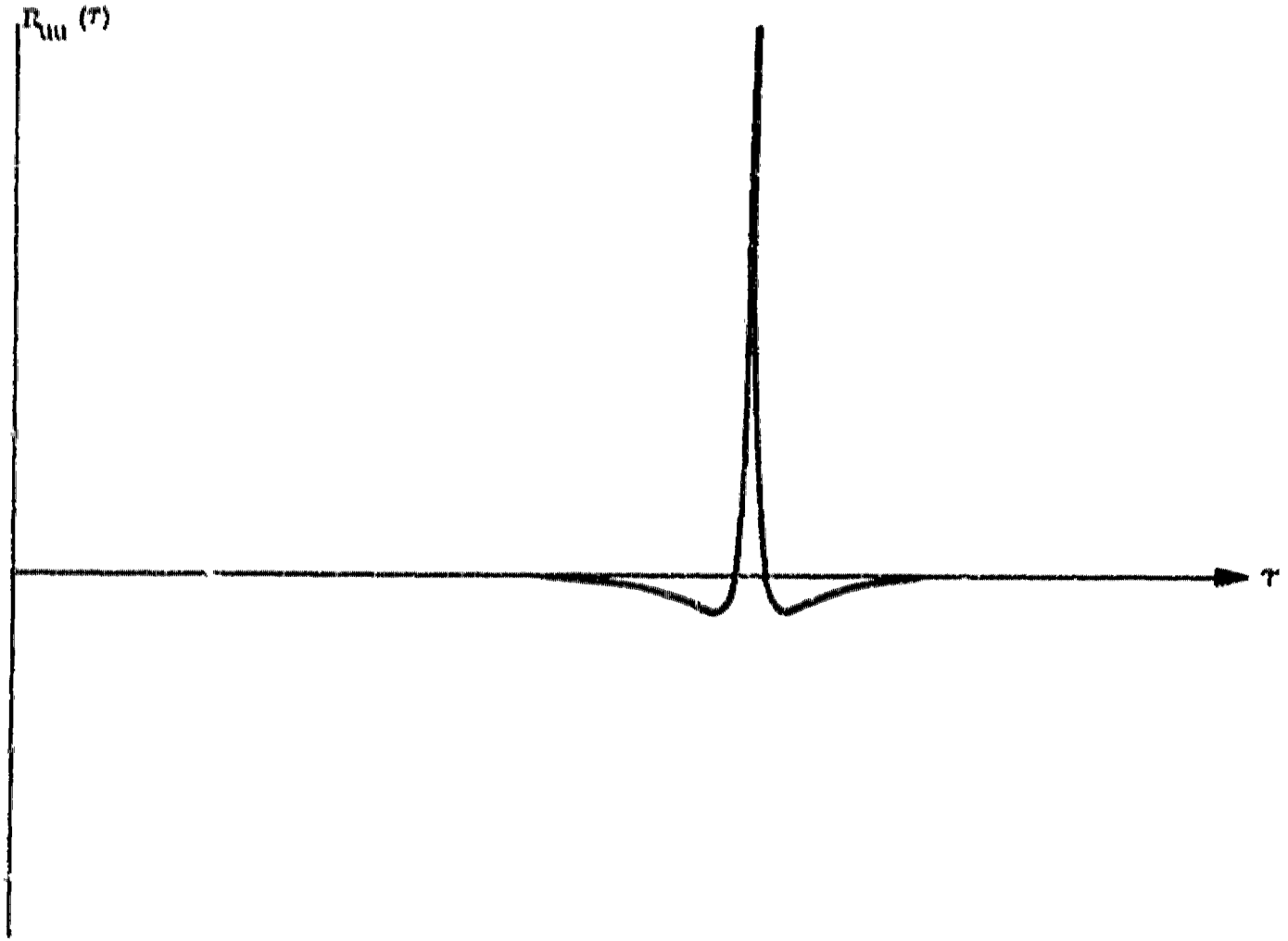

Figure 5-3. The Autocorrelation Function Corresponding to U (ω) in Equation (2-8), with | G (ω) | = 1 and k = 10.

5.2 --Continued.

A small target near a large one will not be detectable in terms of the magnitude of a single matched filter's response. The presence of an additional target, however, will change the shape of the filter response. This shape change should be detectable by filtering with scaled versions of the transmitted spectrum, as discussed in Sections 3 and 4.

When linear detection is used in conjunction with the signals (2-8), the resolution of closely spaced reflectors is accomplished by describing the two reflectors as one complex target. The existence of two targets is then determined by Taylor series spectral analysis. From this viewpoint, signals with large negative autocorrelation sidelobes are again permissible.

5.3 Signal-filter Optimation for Maximum SIR, using Linear Detection.

The transmitted signal is modelled as a linear combination of stretched versions of the signal (2-8) ;

$$U_{Trans}(\omega) = u_0 U(\omega) + u_1 \omega U(\omega) + u_2 \omega^2 U(\omega) + \ldots + u_N \omega^N U(\omega) \qquad (5\text{-}1)$$

where

$$\sum_{n=0}^{N} |u_N|^2 = 1$$

5.3 --Continued.

and where the parameter k is sufficiently large so that

$$\max_{\tau} \left| \chi_{uu} (\tau, k^{n-m}) \right|^2 \approx \delta_{nm} \quad . \tag{5-2}$$

The filter is modelled as a bank of matched filters with transfer functions

$$Z_n (\omega) = \omega^n U^* (\omega) / E_n \quad . \tag{5-3}$$

A weighted sum of the filter outputs is used to determine the presence of a target, as shown in Figure 5-4. The weights $\underline{v}$ are constrained so that

$$\sum_{n=0}^{N} \left| v_n \right|^2 = 1 \quad . \tag{5-4}$$

The target transfer function is defined as

$$F (\omega) \approx \sum_{n=0}^{N} f_n \omega^n \tag{5-5}$$

and the average clutter transfer function is

$$C (\omega) \approx \sum_{n=0}^{\infty} c_n \omega^n \quad . \tag{5-6}$$

The target echo is

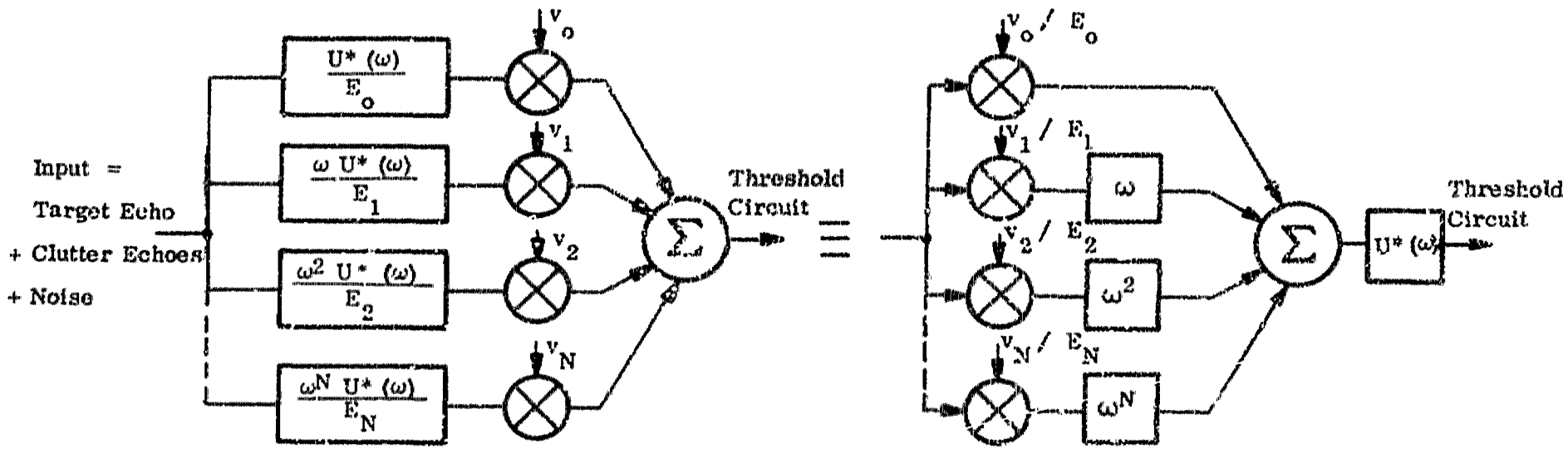

Figure 5-4. Equivalent Configurations of a Linear Receiver Utilizing the Functions in Equation (2-8). Signal to Interference Ratio is Maximized by Adjusting the Filter Weights $(v_o, v_1, \ldots, v_N)$ and the Transmitted Signal Weights $(u_o, u_1, \ldots, u_N)$, where the Fourier Transform of the Transmitted Signal is $U_{Trans}(\omega) = \sum_{n=0}^{N} u_n \omega^n U(\omega)$. The energy of $\omega^n U(\omega)$ is E_n.

5.3 --Continued.

$$F(\omega)\ U_{Trans}(\omega) = \sum_{n=0}^{N} \sum_{m=0}^{N} f_n u_m \omega^{n+m} U(\omega)$$

$$= f_o u_o U(\omega) + (f_o u_1 + f_1 u_o)\ \omega\ U(\omega)$$

$$+ (f_o u_2 + f_1 u_1 + f_2 u_o)\ \omega^2 U(\omega) + \ldots . \qquad (5\text{-}7)$$

The clutter echo is

$$C(\omega)\ U_{Trans}(\omega) = \sum_{n=0}^{N} \sum_{m=0}^{N} c_n u_m \omega^{n+m} U(\omega)$$

$$= c_o u_o U(\omega) + (c_o u_1 + c_1 u_o)\ \omega\ U(\omega)$$

$$+ (c_o u_2 + c_1 u_1 + c_2 u_o)\ \omega^2 U(\omega) + \ldots . \qquad (5\text{-}8)$$

The weighted sum of the filter outputs is

$$\Sigma_T = (f_o u_o) v_o + (f_o u_1 + f_1 u_o) v_1 + (f_o u_2 + f_1 u_1 + f_2 u_o) v_2 + \ldots . \qquad (5\text{-}9)$$

5.3 --Continued.

for the target and

$$\sum_c = (c_o u_o) v_o + (c_o u_1 + c_1 u_o) v_1 + (c_o u_2 + c_1 u_1 + c_2 u_o) v_2 + \ldots . \qquad (5\text{-}10)$$

for the clutter.

To maximize the signal to clutter ratio, one can maximize the difference $\sum_T - \sum_c$ with constraints on $\sum_{n=0}^{N} |u_n|^2$ and $\sum_{n=0}^{N} |v_n|^2$. In other words, one can maximize the quantity

$$J(\underline{u}, \underline{v}) = \sum_T - \sum_c - \lambda \left(\sum_{n=0}^{N} |u_n|^2 + \sum_{n=0}^{N} |v_n|^2 \right) . \qquad (5\text{-}11)$$

Differentiating $J(\underline{u}, \underline{v})$ with respect to v_n and setting the result equal to zero gives

$$\sum_{\substack{i,j \\ i+j=n}} (f_i - c_i) u_j - 2\lambda v_n^* = 0$$

or

$$v_n = \frac{1}{2\lambda} \sum_{\substack{i,j \\ i+j=n}} (f_i - c_i)^* u_j^* . \qquad (5\text{-}12)$$

5.3 --Continued.

In matrix notation, with $\lambda \equiv 1/2$,

$$\begin{bmatrix} v_o \\ v_1 \\ \cdot \\ \cdot \\ \cdot \\ \cdot \\ \cdot \\ v_N \end{bmatrix} = \begin{bmatrix} (f_o - c_o)^* & 0 & \cdots & 0 \\ (f_1 - c_1)^* & (f_o - c_o)^* & 0 \cdots & 0 \\ \cdot & \cdot & & \\ \cdot & \cdot & \cdot & \\ \cdot & \cdot & & \cdot \\ \cdot & \vdots & & \\ \cdot & \cdot & & \\ (f_N - c_N)^* & (f_{N-1} - C_{N-1})^* & \cdots & (f_o - c_o)^* \end{bmatrix} \begin{bmatrix} u_o^* \\ u_1^* \\ \\ \\ \\ \\ u_N^* \end{bmatrix} \qquad (5\text{-}13)$$

Differentiating $J(\underline{u}, \underline{v})$ with respect to u_n and setting the result equal to zero gives (with $\lambda \equiv 1/2$),

$$\begin{bmatrix} u_o \\ u_1 \\ \cdot \\ \cdot \\ \cdot \\ \cdot \\ \cdot \\ u_N \end{bmatrix} = \begin{bmatrix} (f_o - c_o)^* & (f_1 - c_1)^* & (f_2 - C_2)^* & \cdots & (f_N - C_N)^* \\ 0 & (f_o - c_o)^* & (f_1 - C_1)^* & \cdots & (f_{N-1} - C_{N-1})^* \\ \cdot & \cdot & & & \\ \cdot & \cdot & \cdot & & \\ \cdot & \cdot & & \cdot & \\ \cdot & \cdot & & & \cdot \\ \cdot & \cdot & & & \\ 0 & 0 & \cdots & 0 & (f_o - C_o)^* \end{bmatrix} \begin{bmatrix} v_o^* \\ v_1^* \\ \\ \\ \\ \\ v_N^* \end{bmatrix} \qquad (5\text{-}14)$$

5.3 --Continued.

In other words,

$$\underline{u} = \underline{\underline{A}}^T \underline{v}^* \quad \text{and} \quad \underline{v} = \underline{\underline{A}}\ \underline{u}^* \tag{5-15}$$

where $\underline{\underline{A}}$ is the N x N matrix in (5-13). It follows from (5-15) that

$$\underline{u} = \underline{\underline{A}}^T\ \underline{\underline{A}}^*\ \underline{u} \tag{5-16}$$

and

$$\underline{v} = \underline{\underline{A}}\ \underline{\underline{A}}^{*T}\ \underline{v} \tag{5-17}$$

so that $\underline{u}$ and $\underline{v}$ are eigenvectors of the transformations $\underline{\underline{A}}^T\ \underline{\underline{A}}^*$ and $\underline{\underline{A}}\ \underline{\underline{A}}^{*T}$ respectively.

For example, suppose that we wish to detect a planar reflector with $F(\omega) = 1$ amid clutter with $C(\omega) = \omega^3$. Then, for N = 5,

$$\underline{\underline{A}} = \begin{bmatrix} 1 & 0 & 0 & 0 & 0 \\ 0 & 1 & 0 & 0 & 0 \\ 0 & 0 & 1 & 0 & 0 \\ -1 & 0 & 0 & 1 & 0 \\ 0 & -1 & 0 & 0 & 1 \end{bmatrix} \tag{5-18}$$

5.3 --Continued.

$$\underline{\underline{A}}^T \underline{\underline{A}}^* = \begin{bmatrix} 2 & 0 & 0 & -1 & 0 \\ 0 & 2 & 0 & 0 & -1 \\ 0 & 0 & 1 & 0 & 0 \\ -1 & 0 & 0 & 1 & 0 \\ 0 & -1 & 0 & 0 & 1 \end{bmatrix} \qquad (5\text{-}19)$$

$$A\,A^{*T} = \begin{bmatrix} 1 & 0 & 0 & -1 & 0 \\ 0 & 1 & 0 & 0 & -1 \\ 0 & 0 & 1 & 0 & 0 \\ -1 & 0 & 0 & 2 & 0 \\ 0 & -1 & 0 & 0 & 2 \end{bmatrix} \qquad (5\text{-}20)$$

An eigenvector of both (5-19) and (5-20) is

$$\underline{u} = \underline{v} = \begin{bmatrix} 0 \\ 0 \\ 1 \\ 0 \\ 0 \end{bmatrix} . \qquad (5\text{-}21)$$

Notice, however, that the same matrices $\underline{\underline{A}}^T \underline{\underline{A}}^*$ and $\underline{\underline{A}}\ \underline{\underline{A}}^{*T}$ would result if $F(\omega) = \omega^3$ and $C(\omega) = 1$. One must therefore check to see whether the SIR has been maximized or minimized. A simple check is to compute $\sum_T$ and $\sum_c$

5.4 Advantages of a Basis Set of Wideband Functions over a Sinusoidal Basis.

It is interesting to recast the problem of SIR maximization in terms of a basis consisting of time limited sinusoids. The advantages of the functions (2-8) for clutter suppression are clearly pointed out by this procedure.

The first realization concerning sinusoids is that their autocorrelation functions are unsuited to linear detection because of large, positive sidelobes. One must assume that the ranges of target and clutter are known a priori. Alternatively, one can follow the usual practice of envelope detecting the filter outputs.

A second discouraging feature of sinusoids is that they are sensitive to target motion. Any attempt at a fine-grain analysis of echo spectra must use long duration sinusoids which are seriously affected by unforeseen motion of target or clutter. The wideband signals (2-8) are generally insensitive to small stretch factors induced by reflector motion, i.e., they are doppler tolerant.

The problem will therefore be restricted to stationary targets and clutter reflectors whose ranges are known a priori. Even with such restrictions, a sinusoidal basis leads to solutions that may be difficult to use in practice.

Since sinusoids are eigenfunctions of linear systems, there can be no energy transfer between basis functions when targets are stationary. In other words, if

$$U_{Trans}(\omega) = \sum_{n=0}^{N} u_n \, \text{rect}\left[(\omega - n W) / W \right] \qquad (5\text{-}22)$$

5.4 ---Continued.

where the rect (•) function is defined in (4-26), then

$$F(\omega)\, U_{Trans}(\omega) = \sum_{n=0}^{N} f_n u_n \,\mathrm{rect}\left[(\omega - nW) / W \right], \qquad (5\text{-}23)$$

where

$$F(\omega) = \sum_{n=0}^{N} f_n \,\mathrm{rect}\left[(\omega - nW) / W \right] . \qquad (5\text{-}24)$$

If (5-7) were written

$$F(\omega)\, U_{Trans}(\omega) = \sum_{n=0}^{N} e_n e^{jn} U(\omega) , \qquad (5\text{-}25)$$

then

$$\underline{e} = \underline{\underline{A}} \; \underline{u} \qquad (5\text{-}26)$$

where $\underline{\underline{A}}^{*}$ is the NxN matrix in (5-13) with $c_0 = c_1 = \ldots = c_N = 0$, i.e.,

5.4 --Continued.

$$A = \begin{bmatrix} f_o & 0 & \cdots & 0 \\ f_1 & f_o & 0 & \cdots & 0 \\ \cdot & & \cdot & & \\ \cdot & & & \cdot & \\ \cdot & & & & \cdot \\ \cdot & & & & \cdot \\ \cdot & & & & \cdot \\ f_N & f_{N-1} & \cdots & & f_o \end{bmatrix} \qquad (5\text{-}27)$$

According to Equations (5-22) through (5-24), $\underline{\underline{A}}$ is always diagonal for sinusoidal basis vectors. This diagonal property is just another manifestation of the fact that there is no energy transfer between sinusoidal basis functions when they are passed through a linear system.

Since $\underline{\underline{A}}$ is a diagonal matrix, $\underline{\underline{A}}^* \underline{\underline{A}}^T$ and $\underline{\underline{A}}\, \underline{\underline{A}}^{*T}$ are also diagonal matrices. Unless two diagonal elements have the same value, the eigenvectors of such matrices are

5.4 --Continued.

$$\underline{u} = \begin{bmatrix} 1 \\ 0 \\ 0 \\ . \\ . \\ . \\ 0 \end{bmatrix}, \begin{bmatrix} 0 \\ 1 \\ 0 \\ . \\ . \\ . \\ 0 \end{bmatrix}, \ldots, \begin{bmatrix} 0 \\ 0 \\ . \\ . \\ . \\ 0 \\ 1 \end{bmatrix} . \qquad (5\text{-}28)$$

The eigenvalues associated with these eigenvectors are $|a_{11}|^2, |a_{22}|^2, |a_{NN}|^2$, since

$$[\underline{\underline{A}}^* \underline{\underline{A}}^T - \lambda \underline{\underline{I}}]\, \underline{u} = 0$$

or

$$\begin{bmatrix} |a_{11}|^2 - \lambda & & & O \\ & |a_{22}|^2 - \lambda & & \\ & & . & \\ O & & & |a_{NN}|^2 - \lambda \end{bmatrix} \begin{bmatrix} u_1 \\ u_2 \\ . \\ . \\ u_N \end{bmatrix} = 0 \; . \qquad (5\text{-}29)$$

The unit vectors in (5-28) correspond to constant frequency pulses. Such signals are very sensitive to unforeseen changes in target and clutter. Furthermore,

5.4 --Continued.

the use of a single frequency prevents the receiver from gathering information concerning target response at other frequencies. Finally, as the duration of the constant frequency pulse is increased to obtain a better SIR, the range resolution becomes much poorer, so that more clutter contributes to the filter response and SIR actually decreases.

From the above analysis, it is clear that the solution of the SIR problem for linear systems depends upon the basis set that is used. A basis set of constant frequency pulses leads to a solution that (i) has unacceptable sidelobes associated with its autocorrelation function, (ii) is easily perturbed by motion of the environment or the receiver, (iii) is very sensitive to slight transfer function changes, and (iv) does not provide any indication that such changes have occured. It should also be mentioned that, when multipath effects are introduced, a narrowband signal experiences more serious fading problems than a wideband signal. [20]

5.5 Interpretation of the New SIR Results in Terms of Signal Design for Maximum Reflected Energy.

If a point target analysis is used, maximum correlator response is proportional to signal energy. The maximum response occurs when perfect hypotheses have been made concerning the range and velocity of the planar target.

If the linear transform hypothesis is substituted for the point target assumption, then a correct guess concerning the target transfer function $F(\omega)$ leads to an echo autocorrelation function $R_{ee}(\tau)$ whose maximum value is

5.5 --Continued.

$$R_{ee}(0) = \frac{1}{2\pi} \int_{-\infty}^{\infty} |U(\omega) F(\omega)|^2 d\omega$$

$$= \frac{1}{2\pi} \int_{-\infty}^{\infty} |E(\omega)|^2 d\omega , \qquad (5\text{-}30)$$

where $E(\omega) = F(\omega) U(\omega)$ is the echo spectrum.

Just as in the point target case, maximum correlator response is proportional to echo energy. It is therefore relevant to derive a signal u (t) that maximizes the reflected energy from a given target.

Writing (5-30) in terms of u (t) and changing the order of integration gives[34, 35]

$$\int_{-\infty}^{\infty} |e(t)|^2 dt = \int_{-\infty}^{\infty} \int_{-\infty}^{\infty} u(x) u^*(y) \left[\frac{1}{2\pi} \int_{-\infty}^{\infty} |F(\omega)|^2 e^{j\omega(y-x)} d\omega \right] dxdy$$

$$= \int_{-\infty}^{\infty} \int_{-\infty}^{\infty} u(x) u^*(y) R_{ff}(y-x) dxdy \qquad (5\text{-}31)$$

where $R_{ff}(\tau)$ is the autocorrelation function of the target impulse response f (t), i.e.,

5.5 --Continued.

$$R_{ff}(\tau) = \int_{-\infty}^{\infty} f(t)\, f^{*}(t+\tau)\, dt \quad . \tag{5-32}$$

Letting

$$z(y) = \int_{-\infty}^{\infty} u(x)\, R_{ff}(y-x)\, dx \tag{5-33}$$

gives

$$\int_{-\infty}^{\infty} |e(t)|^2\, dt = \int_{-\infty}^{\infty} u^{*}(y)\, z(y)\, dy \quad . \tag{5-34}$$

The left hand side of (5-31) and (5-34) is the energy of the echo waveform, e (t). Assuming that both z (y) and u (y) are normalized to contain unit energy, (5-34) can be maximized via the Schwarz inequality. The right hand side of (5-34) is maximized when

$$z(y) = \lambda\, u(y) \tag{5-35}$$

or

$$\lambda\, u(y) = \int_{-\infty}^{\infty} u(x)\, R_{ff}(y-x)\, dx \tag{5-36}$$

where λ is constant.

5.5 --Continued.

If u (t) is time limited to the interval [0, T], then (5-36) becomes a homogeneous Fredholm integral equation whose solutions are the eigenfunctions of $R_{ff}(\tau)$.

The signal that maximizes the echo energy for a particular target is the solution of (5-36) with maximum eigenvalue, λ_{max}. For this signal, the echo energy is $\lambda_{max} E_u$.

If the transmitted signal is not theoretically time limited (for example, if u (t) is a CW signal with Gaussian envelope) then the Fourier transform of (5-36) is

$$\lambda U(\omega) = U(\omega) \mid F(\omega) \mid^2 \qquad (5\text{-}37)$$

If U (ω) is sufficiently narrowband, then

$$\lambda U(\omega) \approx \mid F(\omega_o) \mid^2 U(\omega) \qquad (5\text{-}38)$$

where ω_o is the carrier frequency of U (ω). The narrowband signal's carrier frequency should therefore correspond to a maximum on the curve of backscattered power versus frequency. Such a waveform is optimum for the maximization of echo energy.

For a point target,

$$R_{ff}(y - x) = \delta(y - x) \qquad (5\text{-}39)$$

5.5 --Continued.

and (5-26) is identically satisfied for all admissible waveforms. A planar target does not favor one signal over another as far as returned energy is concerned. For a non-planar target, however, both echo energy and maximum echo power depend upon the transmitted waveform.

Equation (5-38) is equivalent to Equation (5-29), where U (ω) is described by one of the eigenvectors in (5-28). The optimum eigenvector is the one with the maximum eigenvalue, λ_{max}. Just as

$$\lambda_{max} = \max_{\omega_o} | F(\omega_o) |^2 \qquad (5\text{-}40)$$

in (5-38), Equation (5-29) implies that

$$\lambda_{max} = \max (| a_{11} |^2, | a_{22} |^2, \ldots, | a_{NN} |^2) . \qquad (5\text{-}41)$$

For a sinusoidal basis,

$$| a_{nn} |^2 = | F(\omega_n) |^2 . \qquad (5\text{-}42)$$

The above equivalence is not surprising. In the absence of clutter, the SIR is maximized by maximizing $\sum_T$, with constraints upon signal energy, $\sum_n | u_n |^2$ and upon the energy of the filter's impulse response, $\sum_n | v_n |^2$. Since $\sum_T$, the magnitude of the filter's response to the target echo, is bounded by the energy of the echo,

5.5 --Continued.

the SIR maximization problem is identical to maximizing the quantity in (5-30) with equivalent energy constraints.

The equivalence between SIR maximization and maximization of echo energy shows that the eigenfunction equation (5-16) is analogous to Equation (5-36). It follows that the matrix $\underline{\underline{A}}^T \underline{\underline{A}}^*$ is analogous to $R_{ff}(y - x)$. Indeed, f (t) is the target's impulse response, the function that is convolved with the signal u (t) in order to form the echo. Similiarly, the vector $\underline{\underline{A}}\,\underline{u}$ describes the first N terms of a convolution process, as indicated by Equations (4-19) - (4-24).

One can further exploit the equivalence by noting that the general SIR problem defines $\underline{\underline{A}}$ as in (5-13). Each element in (5-13) involves the difference between target and clutter components. The analogous result is to rewrite (5-36) as

$$\lambda\, u(y) = \int_{-\infty}^{\infty} u(x)\; R_{f-c,\; f-c}(y - x)\; dx \qquad (5\text{-}43)$$

where $R_{f-c,\; f-c}(\tau)$ is the autocorrelation function corresponding to F (ω) - C (ω), the difference between target and clutter transfer functions.

5.6 Summary of Section 5.

The use of certain wideband signals allows for the elimination of nonlinear operations in sonar receivers. Once such operations are eliminated, the maximization

5.6 --Continued.

of SIR becomes much simpler. The determination of an optimum signal-filter pair, however, still depends upon the basis that is chosen to describe the relevant functions. A basis composed of the functions (2-8) seems to produce much more practical solutions than a basis of narrowband sinusoids.

The solution to the SIR problem is similar to the solution of a related problem, i.e., maximizing the energy of the target echo. The energy maximization problem becomes identical to the SIR problem if the target transfer function $F(\omega)$ is replaced by $F(\omega) - C(\omega)$, the difference between target and clutter transfer functions. Both problems reduce to the solution of an eigenfunction equation. This result suggests that the functions (2-8) could prove useful in providing alternative solutions to such equations.

In order to maximize SIR, the approaches in Sections 2.3 and 5.3 both maximize the difference between target and clutter responses, while constraining the response to noise. For square law detection, uniformly distributed clutter has the same effect as noise, i.e., undesired responses occuring at random times. Clutter is thus treated as though it were noise. For linear detection, the difference between target and clutter responses is the same as the response of the linear filter to a signal that is the difference between target and clutter echoes. The optimum receiver therefore acts as a matched filter -- matched to the difference between signal and expected clutter returns.

The above observations are easily applied to the receiver in Figure 4-1. If square law detection is used, one should first determine the expected output power of each filter with noise and clutter echoes at the input. In order to whiten the response to interference, each energy normalized filter output should then be divided by its own measured

5.6 --Continued.

response to noise and clutter. (If the interference has constant power spectral density, all energy normalized filter outputs will be divided by the same number.) This procedure results in a correlation of echoes with $\hat{f}_n / I(\omega)$, where $I(\omega)$ is the response to interference, as in Equation 2-35. For linear detection, one should replace the gains $\hat{f}_n$ in Figure 4-1 by $\hat{f}_n - \hat{c}_n$, where the $\hat{f}_n$ coefficients correspond to the target transfer function and the $\hat{c}_n$ coefficients correspond to the average clutter transfer function.

6. BAT WAVEFORMS AND THE SIMILARITIES BETWEEN AMPLITUDE MODULATION AND LINEAR FILTERING FOR CHIRPED PULSES.

6.1 Bat Signals and Amplitude Modulation.

The experimental work of Griffin, Friend, and Webster[34, 35] seems to suggest that the bat Myotis lucifugus may use amplitude modulation differences to distinguish between different target shapes. If the theory presented in Section 2 is applied to products in the time domain (rather than in the frequency domain) one arrives at an optimum time function $U_1(t)$ for Taylor series characterization of the modulating signal a (t). This function, $U_1(t)$, is identical to the function in Equation (2-8), provided the independent variable is time rather than frequency.

It has been found[3] that the signals $U_1(t)$ can be matched to bat signals if $U_1(t)$ is premultiplied by a truncating function $y_1(t)$, where

$$y_1(t) = 1 + \sum_{n=M}^{\infty} y_n t^n \quad . \tag{6-1}$$

When the signal $U_1(t)\, y_1(t)$ is used for target characterization, the first M coefficients of the modulation a (t) are unaffected by the truncation. The truncating function that has been used is

$$y_1(t) = \exp\left[- (\beta t)^M \right] = 1 + \sum_{n=1}^{\infty} \frac{(-1)^n (\beta^M)^n}{n!} (t^M)^n \quad . \tag{6-2}$$

6.1 --Continued.

Some examples of the functions $U_1(t)\ y_1(t)$ are shown in Table 6-1. The corresponding signals are shown in Figures 6-1 and 6-2. These signals compare favorably with the Myotis crusing and pursuit pulses[36] shown in Figures 6-3 and 6-4.

6.2 The Fourier Transforms of Bat-Like Signals.

The analysis in the Appendix indicates that the inverse Fourier transforms of the functions $U(\omega)$ in (2-5) have approximately the same mathematical form as the frequency domain functions. This similarity implies that any given signal $U_1(t)$ can be approximated by the inverse Fourier transform of $U_2(\omega)$, where $U_1(\bullet)$ and $U_2(\bullet)$ belong to the class of functions described by Equation (2-5).

Figures 6-1 through 6-4 demonstrate that some bat signals can be matched to the functions $U_1(t)\ y_1(t)$. The similarity between $U_1(t)$ and the inverse Fourier transform of $U_2(\omega)$ would seem to imply that the same bat signals can be matched to the inverse Fourier transform of $U_2(\omega)$ multiplied by an appropriate truncating function, $y_2(\omega)$. Such matches can indeed be made, provided

$$y_2(\omega) = \exp\left[-(\beta\omega)^{-M}\right] = 1 + \sum_{n=1}^{\infty} \frac{(-1)^n (\omega^{-M})^n}{n!\ (\beta^M)^n} . \qquad (6\text{-}3)$$

In (6-3), $y(\omega)$ acts as a high pass function. The first M Taylor series coefficients corresponding to $F(\omega)\ y_2(\omega)$ will be those of $F(\omega)$ alone if $F(\omega)$ has no more than M significant terms, since

Table 6-1. Examples of the Signals $U_1(t)\, y_1(t)$, where $U_1(t)$ is Given by Equation (2-8) and $y_1(t)$ is an Appropriate Truncation Function. When these Waveforms are Amplitude Modulated, they Convey Information about the Taylor Series Coefficients of the Modulating Time Function.

1. $U_1(t)\, y_1(t) = t^{-2.5} e^{-(\log t)^2} \cos [\, 400\, \pi\, (\log t)\,]\, e^{-(3t)^{20}}$

2. $U_1(t)\, y_1(t) = t^{-1.2} e^{-.5\,(\log t)^2} \cos [\, 160\, \pi\, (\log t)\,]\, e^{-(2t)^{30}}$

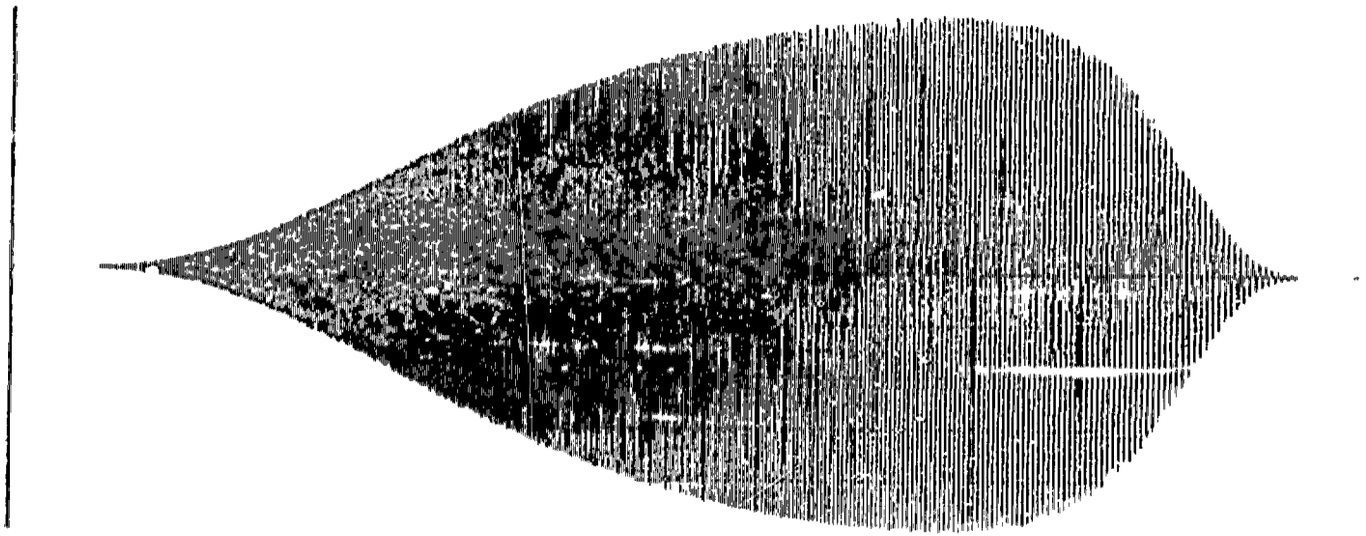

Figure 6-1. Graph of the First Function in Table 6-1. This Signal is Designed for Characterization of Amplitude Modulation Induced by a Nonplanar Target. Instantaneous Period Increases Linearly with Time. Compare with Figures 6-3 and 6-5.

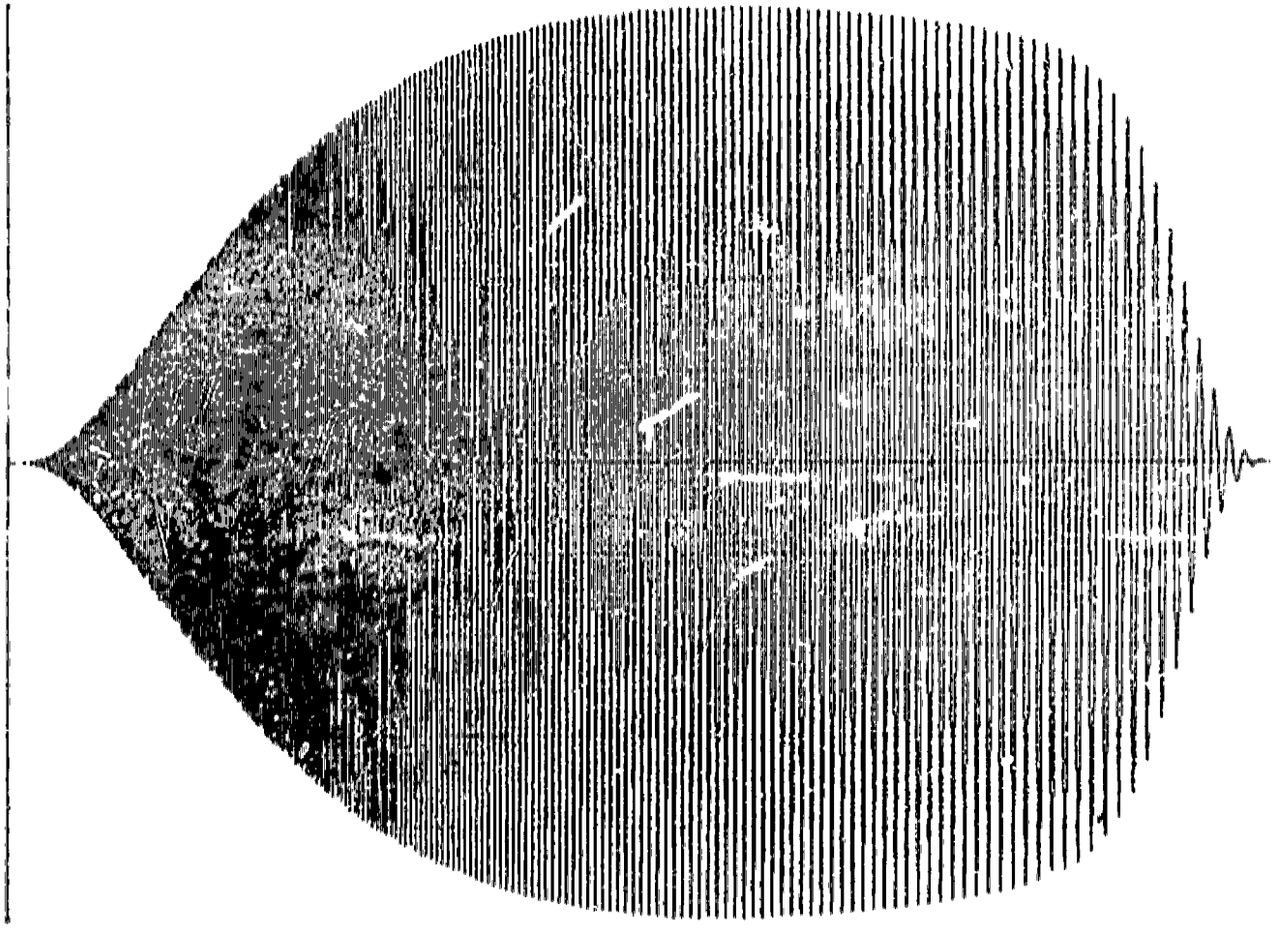

Figure 6-2. Graph of the Second Function in Table 6-1. This Signal is Designed for Characterization of Amplitude Modulation Induced by a Nonplanar Target. Instantaneous Period Increases Linearly with Time. Compare with Figures 6-4 and 6-6.

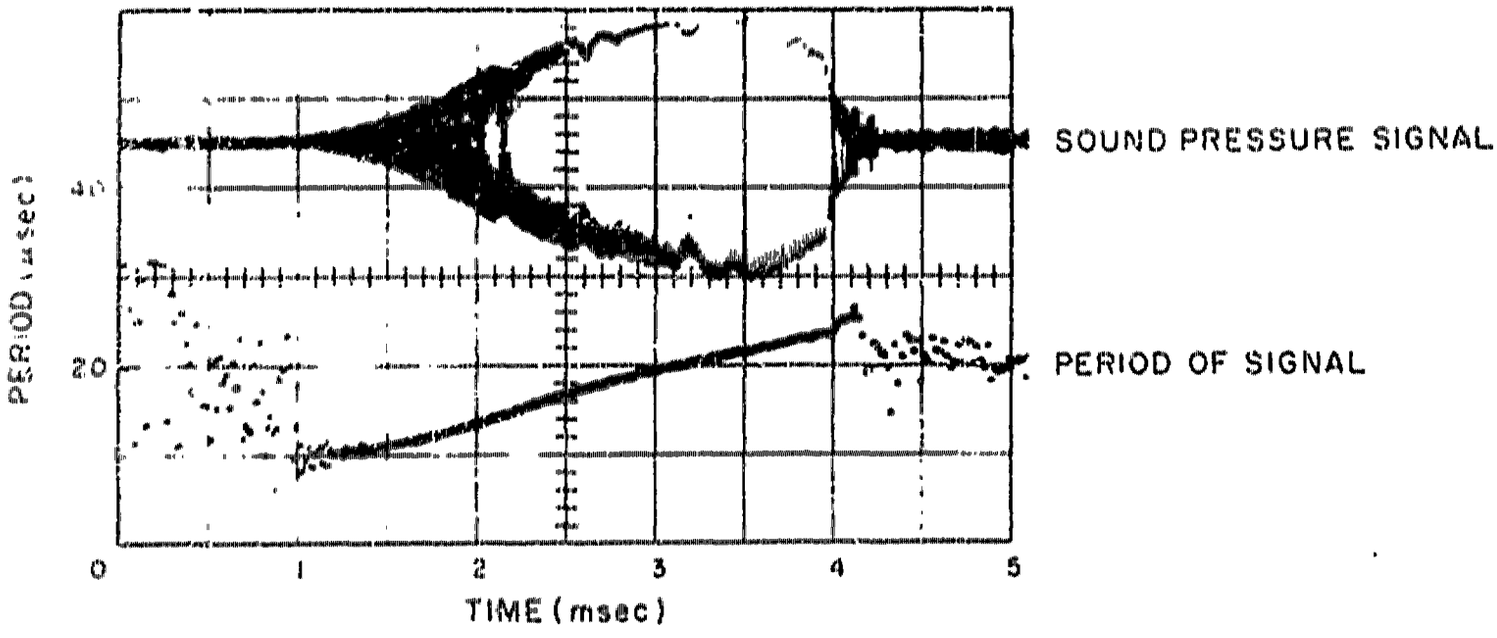

Figure 6-3. Cruising Pulse of the Little Brown Bat, Myotis lucifugus, Measured by D. A. Cahlander and J. J. G. McCue at MIT Lincoln Laboratory.

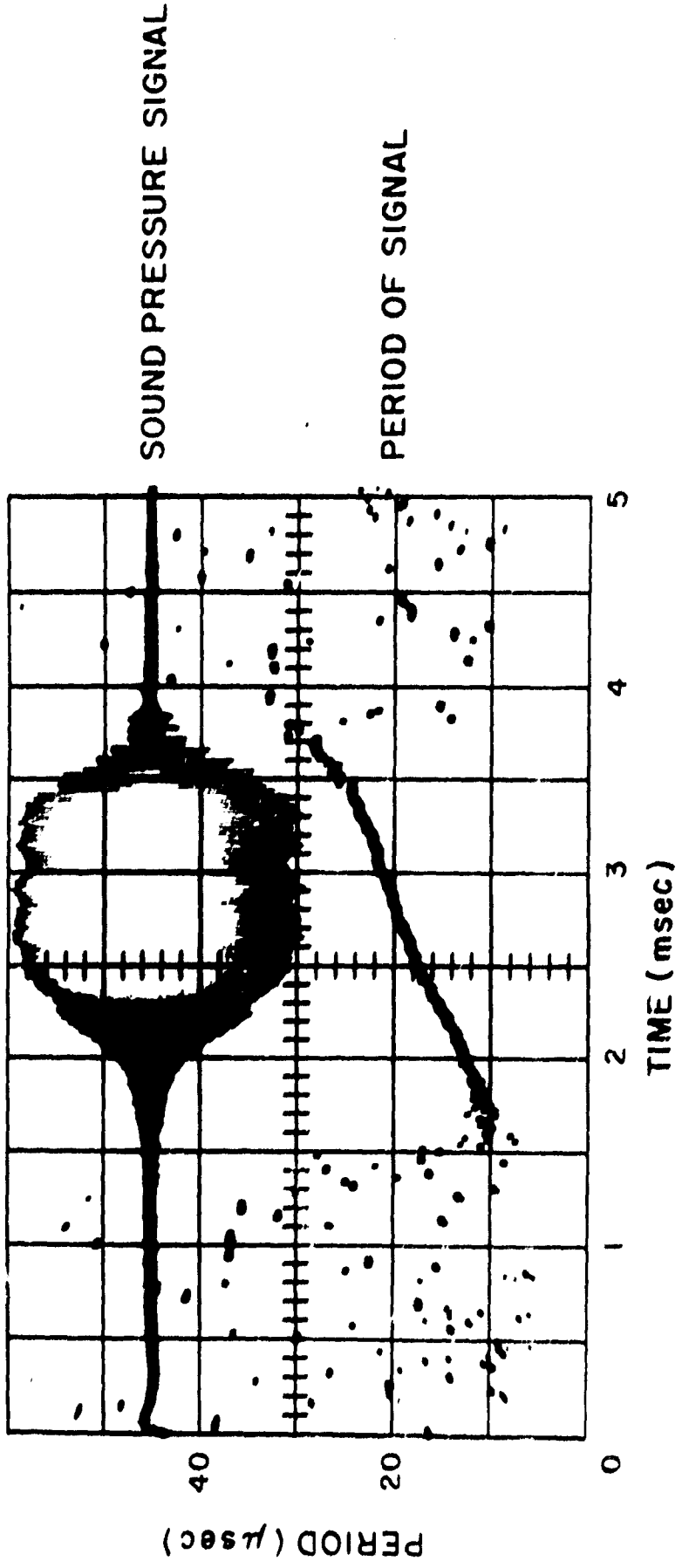

Figure 6-4. Pursuit Pulse of Myotis lucifugus. Measured by D.A. Cahlander and J.J.G. McCue at MIT Lincoln Laboratory.

6.2 --Continued.

$$F(\omega)\, y_2(\omega) = \sum_{n=0}^{\infty} f_n \omega^n - (1/\beta^M) \sum_{n=0}^{\infty} f_n \omega^{n-M} + (1/2\beta^{2M}) \sum_{n=0}^{\infty} f_n \omega^{n-2M} + \ldots .$$

$$= \sum_{n=-\infty}^{\infty} b_n \omega^n \quad . \tag{6-4}$$

In (6-4), $(b_o, b_1, \ldots, b_{M-1}) \approx (f_o, f_1, \ldots, f_{M-1})$ if

$$f_n / \beta^M \approx 0 , \quad n \geq M . \tag{6-5}$$

Alternatively, if the target transfer function is described as a combination of integrators, i.e., if

$$F(\omega) = \sum_{n=0}^{\infty} f_n \omega^{-n} , \tag{6-6}$$

then

$$F(\omega)\, y_2(\omega) = \sum_{n=0}^{\infty} f_n \omega^{-n} - (1/\beta^M) \sum_{n=0}^{\infty} f_n \omega^{-(n+M)} + \ldots . \tag{6-7}$$

6.2 --Continued.

and the first M terms of a power series expansion of $F(\omega)\, y_2(\omega)$ are identical with those of $F(\omega)$, even if condition (6-5) does not hold true.

The functions $U_2(\omega)\, y_2(\omega)$ whose inverse Fourier transforms match the Myotis pulses are shown in Table 6-2, and the inverse Fourier transforms are illustrated in Figures 6-5 and 6-6. The value of β^M for the second function in Table 6-2 (the pursuit pulse) indicates that the function in Figure 6-6 is capable of nearly undistorted characterization of all the power series coefficients f_n corresponding to the target transfer function, $F(\omega)$.

6.3 Discussion of the Myotis Results.

Figures 6-1 through 6-6 demonstrate that two different hypotheses can be used to explain the Myotis crusing and pursuit pulses. One hypothesis is based upon the observation that different targets cause the echo of a chirped pulse to acquire different amplitude modulations.[35] The other hypothesis is based upon the idea that targets act as linear filters.

These hypotheses lead to similar signal design problems. The problems are similar because a duality exists between (i) amplitude modulation, which multiplies the transmitted time signal $u(t)$ by a time function $a(t)$, and (ii) linear filtering, which multiplies the spectrum $U(\omega)$ of the transmitted signal by a frequency function $F(\omega)$.

One would expect the solutions of the two problems to be dissimilar, since comparatively few functions are identical in time and frequency (i.e., only a restricted

Table 6-2. Examples of the Transforms $U_2(\omega)\, y_2(\omega)$, where $U_2(\omega)$ is Given by Equation (2-8) and $y_2(\omega)$ is an Appropriate Truncating Function. When the Inverse Fourier Transforms of $U_2(\omega)\, y_2(\omega)$ are Passed Through a Linear Filter, they Convey Information about the Taylor Series Coefficients of the Filter's Transfer Function.

1. $U_2(\omega)\, y_2(\omega) = \omega^{-0.7}\, e^{-0.9 (\log \omega)^2}\, e^{-j 241.2 \pi \log \omega}\, e^{-(.9\omega)^{-20}}$

2. $U_2(\omega)\, y_2(\omega) = \omega^{-1.1}\, e^{-0.5 (\log \omega)^2}\, e^{-j 80 \pi \log \omega}\, e^{-(1.8\,\omega)^{-22}}$

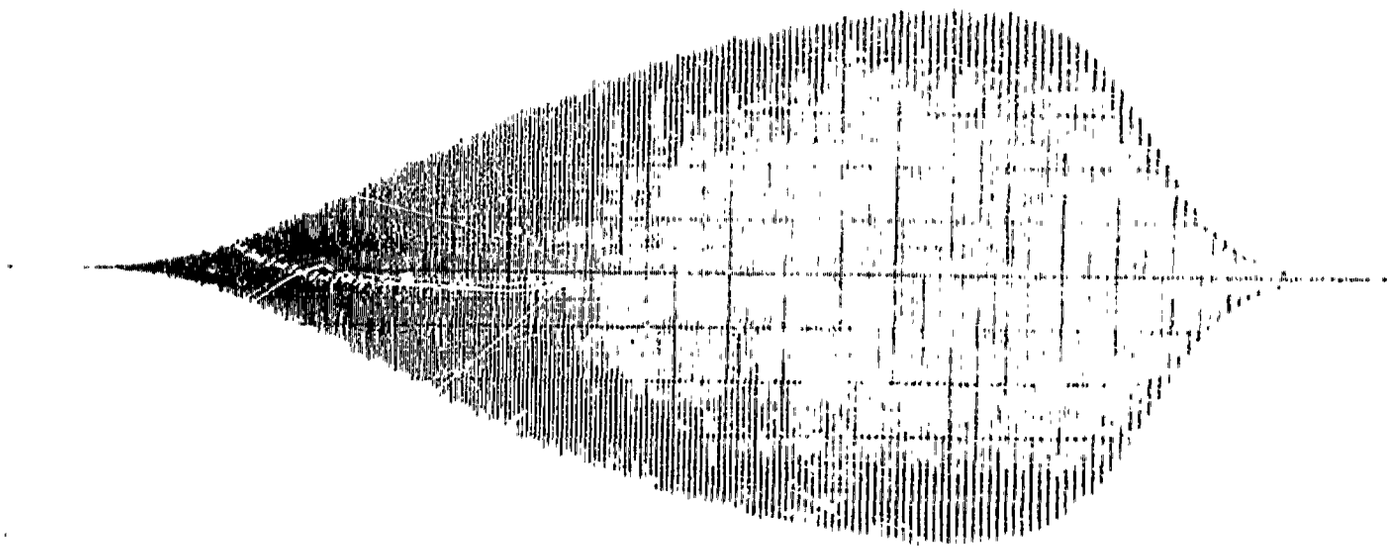

Figure 6-5. The Inverse Fourier Transform of the First Function in Table 6-2. Like the Porpoise Waveforms in Figure 2-6, This Signal is Designed for Characterization of a Linear Filter Via Spectral Power Series Coefficients. Instantaneous Period Increases Linearly with Time. Compare with Figures 6-1 and 6-3.

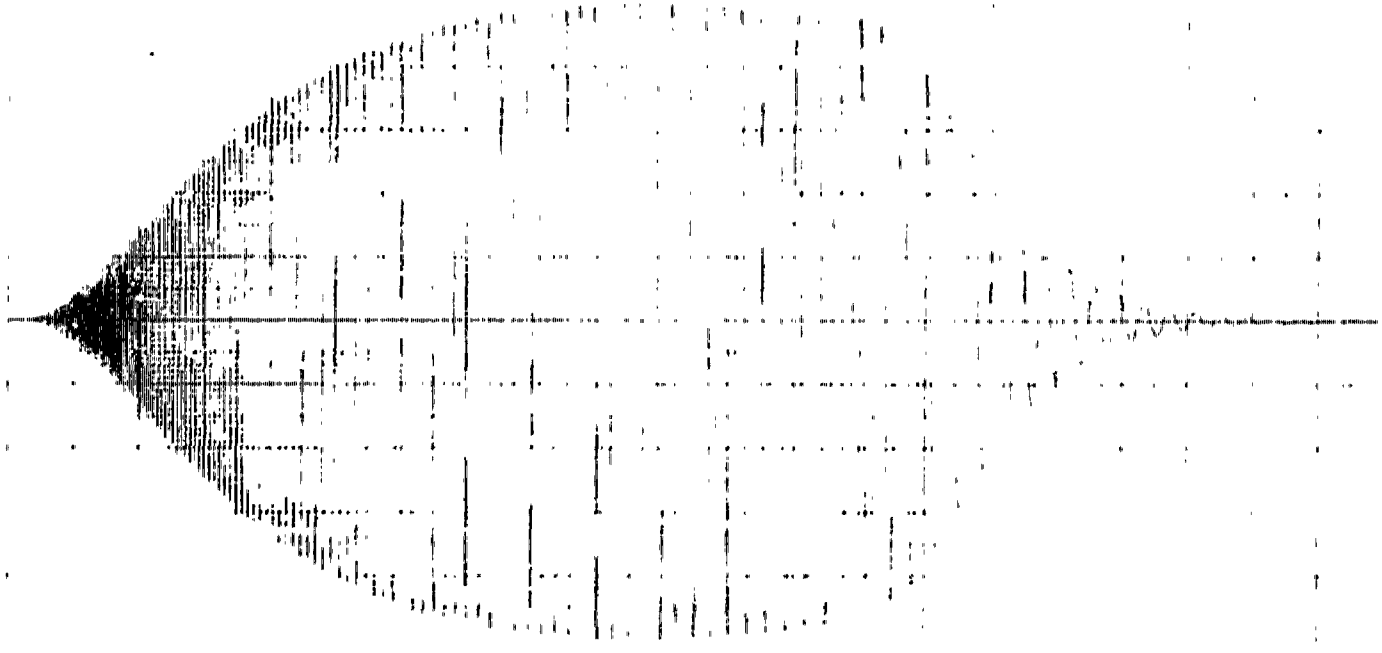

Figure 6-6. The Inverse Fourier Transform of the Second Function in Table 6-2. Like the Porpoise Waveforms in Figure 2-6, This Signal is Designed for Charactertization of a Linear Filter Via Spectral Power Series Coefficients. Instantaneous Period Increases Linearly with Time. Compare with Figures 6-2 and 6-4.

6.3 --Continued.

class of functions are exact eigenvalues of the Fourier transform). Chirped signals, however, are often approximate eigenvalues of the Fourier transform. Linear chirp is the best known case, but the stationary phase approach (see the Appendix) implies that some other chirped waveforms have the same property.

Given that two mathematical hypotheses result in approximately the same correspondence with reality, one must seek further data to determine which hypothesis is correct, or whether there exists an equivalence of the hypotheses that has been overlooked.

The hypothesis that bat signals are designed to analyze amplitude modulation is re-enforced by some neurophysiological work. In studies of bats' auditory neural processing, N. Suga[37] and A. Grinnell[38] have found many neurons which are tuned to particular frequency intervals. Since neuronal excitation is a function of amplitude as well as frequency, each tuned neuron can act as an AM demodulator over a particular frequency range. Tuned neurons therefore provide a means for determining the echo amplitude at any given frequency.

The hypothesis that bat signals are designed to convey information about the target qua linear filter is strengthened by the observations in Sections 2 through 4. The psychoacoustic excitation functions can theoretically be invoked to explain not only porpoise echolocation clicks, but those of any other mammal.

A supporter of the amplitude modulation hypothesis would have to concede that there is considerable evidence to support the critical bandwidth theory. Nevertheless, he could point out that N. Suga has found no evidence of a dispersive delay pulse

6.3 --Continued.

compression mechanism in his years of studying the FM bats.[39] One could therefore claim that the auditory filters do not implement the log phase necessary for true pulse compression[40] and efficient linear filter characterization.

It is possible, however, that FM bats may use a pulse compression mechanism that does not involve a dispersive delay. For example, incoming signals may be repeatedly multiplied by stored versions of the transmitted waveform*, and the product integrated. The multiplication operation is particularly easy to perform with neural elements, since all signals are coded in terms of a positive quantity, the number of excitation pulses per second. Positive voltages can be interpreted as increased discharge rates (excitations) and negative voltages can be interpreted as decreased rates (inhibitions), relative to the spontaneous discharge rate of the unexcited neuron. In electronics, the multiplication of two positive voltages (single quadrant multiplication) is accomplished with a voltage variable amplifier. Any neuron with both excitatory and inhibitory synaptic connections to its dendrites provides the analog of such an amplifier. The integration process can be implemented by low pass filtering, which again is naturally realized by any neuron; all neurons have a recovery time that limits the maximum discharge rate, so that they act as low pass filters.

A supporter of the hypothesis that targets are characterized as linear filters can therefore still insist that the appropriate filtering process (Figure 4-1) is implemented by Myotis. He can point out that only 100 neurons are required for the whole correlation process.** Furthermore, he can remark that the reference signal

* For a 20 KHz bandwidth, this method would require a new multiplication to commence every 50 microseconds.

** Any one correlator can be reused after it has performed multiplication and integration over the expected signal duration. For a 3 msec, 20 kHz wide signal, the receiver could thus be implemented with 100 multiplication-integration circuits.

6.3 --Continued.

is based upon an efferent input from a higher part of the neural processor, i.e., a part of the brain that could be incapacitated by anesthesia.[41] These observations could explain the lack of success that has been encountered in searching for a pulse compression mechanism via neural probes on anesthetized animals.

6.4 The Equivalence of the Amplitude Modulation and Linear Filtering Hypotheses.

Since additional evidence can be found to favor either hypothesis, let us reconsider the possibility that the hypotheses are equivalent. As it turns out, there is considerable evidence favoring this point of view:

First, there is the fact that if the chirp rate is sufficiently slow, the FM signal determines the response of a linear filter to each frequency, and this response is manifested as an amplitude modulation of the chirped waveform.

Second, the amplitude of a chirped signal in time is easily related to its amplitude in frequency, if the stationary phase approximation is valid (see the Appendix.) It follows that a given amplitude modulation in time results in a corresponding amplitude modulation in frequency (linear filtering), i.e., there is an equivalent linear filter for any amplitude modulation imparted to the chirped signal.

Third, the matched filtering shown in Figure 4-1 results in a process that is similar to sampling the magnitude of an echo over different segments of the returned waveform. The signals $u^*(k^n t)$ are compressed when n is positive, so that echoes are

6.4 --Continued.

correlated with functions whose maxima occur closer and closer to the beginning of the pulse as n increases. The same signals are stretched when n is negative, so that echoes are correlated with functions whose maxima occur further and further toward the end of the pulse as n decreases.* This effect will be demonstrated in Section 7. The effect may also indicate a scheme by which the tuned neurons found by Suga and Grinnell can act as the equivalent of a bank of matched filters or correlators.

Fourth, the two derivations of Myotis signals hinge upon the use of power series to describe the amplitude modulation function a (t) or the linear filter function F (ω). It has already been shown (Section 4.4) that linear filtering results in a convolution of filter coefficients with the spectral coefficients of the processed signal. In fact, amplitude modulation can also be written as a convolution operation involving the spectral coefficients of the processed signal. This effect is discussed below.

6.5 A Mathematical Relation between Amplitude Modulation and Linear Filtering.

Consider the product of two functions a (t) and u (t). On a finite time interval (0 , T) , a (t) can be represented by an N^{th} order polynomial,**

$$a(t) = A_o + A_1 t + A_2 t^2 + \ldots + A_N t^N \quad . \qquad (6\text{-}8)$$

* The signals (2-8) have no range-doppler coupling, so that $u^*(k^n t) \leftrightarrow U^*(\omega/k^n) / k^n$ correlates with u (t) for zero delay. Zero delay implies that $u^*(k^n t)$ and u (t) have the same time origin (t=0) for maximum correlator response. Plots of $u^*(k^n t)$ for different values of n reveal maxima whose locations depend upon n.

** As in (6-1), we represent power series coefficients of time domain functions by capital letters and coefficients of frequency domain functions by lower case letters.

6.5 --Continued.

Let

$$a(t)\,u(t) = c(t) \tag{6-9}$$

and

$$c(t) \longleftrightarrow C(\omega) \tag{6-10}$$

where the double arrow indicates a Fourier transform pair. The problem is to find the power series coefficients c_n of $C(\omega)$.

According to (3-3), one way to find the c_n's is to form the integral

$$\int_0^T t^m c(t)\,dt = (m!/j^m)\,c_m \,. \tag{6-11}$$

Substituting (6-8) into (6-9) and (6-9) into (6-11),

$$(m!/j^m)\,c_m = \sum_{n=0}^{N} A_n \int_0^T t^{n+m}\,u(t)\,dt \,. \tag{6-12}$$

Now

$$\int_0^T t^{n+m}\,u(t)\,dt = \left[(n+m)!/j^{m+n}\right] u_{n+m} \,, \tag{6-13}$$

6.5 --Continued.

where

$$u(t) \longleftrightarrow U(\omega) = \sum_{n=0}^{N} u_n \omega^n \quad . \tag{6-14}$$

The finite order polynomial representation of $U(\omega)$ is, of course, only valid over a restricted frequency interval $(0, W)$ if $U(\omega)$ is given by (2-8).

According to (6-12) and (6-13),

$$(m!/j^m)\ c_m = \sum_{n=0}^{N} [(n+m)!/j^{m+n}]\ A_n\ u_{n+m} \quad . \tag{6-15}$$

Letting

$$\begin{aligned} c_m' &= (m!/j^m)\ c_m \\ u_m' &= (m!/j^m)\ u_m \end{aligned} \tag{6-16}$$

we have

$$c_m' = \sum_{n=0}^{N} A_n\ u_{n+m}' \quad . \tag{6-17}$$

6.5 --Continued.

In matrix notation,

$$\begin{bmatrix} c'_{-N} \\ c'_{-N+1} \\ \vdots \\ c'_{-1} \\ c'_{0} \\ c'_{1} \\ \vdots \\ c'_{N-1} \\ c'_{N} \end{bmatrix} = \begin{bmatrix} A_N & 0 & 0 & \cdots & 0 & 0 \\ A_{N-1} & A_N & 0 & & & \\ \vdots & & \ddots & & & \\ A_1 & A_2 & A_3 & \cdots & A_N & 0 \\ A_0 & A_1 & A_2 & \cdots & A_{N-1} & A_N \\ 0 & A_0 & A_1 & \cdots & A_{N-2} & A_{N-1} \\ \vdots & & & & & \\ 0 & 0 & 0 & & A_0 & A_1 \\ 0 & 0 & 0 & & 0 & A_0 \end{bmatrix} \begin{bmatrix} u'_0 \\ u'_1 \\ \vdots \\ u'_N \end{bmatrix} . \qquad (6\text{-}18)$$

In (6-18), c_n for $n < 0$ is included strictly as a formality. It is apparent from (6-16) that these coefficients are in fact undefined.

By comparing (6-18) with (4-24), we see that

$$c' = A_r * u' \qquad (6\text{-}19)$$

6.5 --Continued.

where $\underline{A}$ is the vector of coefficients defined by (6-8) and $\underline{A}_T$ is the same vector with the order of its elements reversed, i.e.,

$$\underline{A} = \begin{bmatrix} A_0 \\ A_1 \\ \cdot \\ \cdot \\ \cdot \\ A_N \end{bmatrix} \quad \text{and} \quad \underline{A}_T = \begin{bmatrix} A_N \\ A_{N-1} \\ \cdot \\ \cdot \\ \cdot \\ A_0 \end{bmatrix} . \qquad (6\text{-}20)$$

In (6-19), the asterisk symbolizes convolution, as defined by Equations (4-23) and (4-24).

Since

$$c(t) = a(t)\, u(t) \longleftrightarrow C(\omega) = A(\omega) * U(\omega) , \qquad (6\text{-}21)$$

we see that multiplication in time or convolution in frequency can be represented by a convolution operation involving both time coefficients and frequency coefficients. From (4-21) through (4-24), multiplication in frequency or convolution in time can be represented by a convolution operation involving two sets of frequency coefficients.

6.3 Finding the AM Equivalent to any Measured Transfer Function.

Using (6-16), Equation (6-18) can be rewritten:

$$\begin{bmatrix} 1 & 0 & 0 \cdot \cdot \cdot 0 \\ 0 & 1!/j^1 & 0 \cdot \cdot \cdot 0 \\ 0 & 0 & 2!/j^2 \cdot \cdot \cdot 0 \\ \cdot & & \\ \cdot & & \\ \cdot & & \\ 0 & 0 \cdot \cdot \cdot 0 & N!/j^N \end{bmatrix} \begin{bmatrix} c_0 \\ c_1 \\ c_2 \\ \cdot \\ \cdot \\ \cdot \\ c_N \end{bmatrix}$$

$$= \begin{bmatrix} \frac{N!}{j^N} u_N & \frac{(N-1)!}{j^{N-1}} u_{N-1} \cdot \cdot \cdot \frac{1!}{j^1} u_1 & u_0 \\ 0 & \frac{N!}{j^N} u_N \cdot \cdot \cdot \frac{2!}{j^2} u_2 & \frac{1!}{j^1} u_1 \\ \cdot & & \\ \cdot & & \\ \cdot & & \\ 0 & 0 \cdot \cdot \cdot & \frac{N!}{j^N} u_N \end{bmatrix} \begin{bmatrix} A_N \\ A_{N-1} \\ \cdot \\ \cdot \\ \cdot \\ A_0 \end{bmatrix} \qquad (6\text{-}19)$$

6.6 --Continued.

or

$$\begin{bmatrix} c_0 \\ c_1 \\ c_2 \\ \vdots \\ c_N \end{bmatrix} = \begin{bmatrix} \frac{N!}{j^N} u_N & \frac{(N-1)!}{j^{N-1}} u_{N-1} & \cdots & \frac{1!}{j^1} u_1 & u_0 & A_N \\ 0 & \frac{j^1}{1!}\frac{N!}{j^N} u_N & \cdots & \frac{j^1}{1!}\frac{2!}{j^2} u_2 & u_1 & A_{N-1} \\ 0 & 0 & \cdots & \frac{j^2}{2!}\frac{3!}{j^2} u_3 & u_2 & A_{N-2} \\ \vdots & \vdots & & & & \vdots \\ 0 & 0 & \cdots & & u_N & A_0 \end{bmatrix} \tag{6-20}$$

Equation (6-20) can be abbreviated

$$\underline{c} = \underline{\underline{M}}_u \, \underline{A}_r \, . \tag{6-21}$$

so that

$$\underline{A}_r = \underline{\underline{M}}_u^{-1} \, \underline{c} \, . \tag{6-22}$$

6.6 --Continued.

Recall that the coefficients $\underline{c}$ correspond to the spectrum C (ω), where C (ω) is the Fourier transform of a (t) u (t). The coefficients $\underline{c}$ can be estimated with the processor in Figure 4-4.

If C (ω) results from the linear filtering process

$$C(\omega) = F(\omega)\ U(\omega) \quad , \tag{6-23}$$

then the power series spectral coefficients of F (ω) can be derived by computing $\underline{\underline{T}}_u^{-1}\ \underline{c}$, where $\underline{\underline{T}}_u$ is the NxN matrix in (4-33).

If C (ω) results from amplitude modulation of the signal u (t), i.e., if

$$C(\omega) \longleftrightarrow c(t) = a(t)\ u(t) \longleftrightarrow A(\omega) * U(\omega) \quad , \tag{6-24}$$

then the power series temporal coefficients of a (t) can be derived by computing $\underline{\underline{M}}_u^{-1}\ \underline{c}$, where $\underline{\underline{M}}_u$ is the NxN matrix in Equation (6-20).

The above two processes are shown in Figure 6-7. The first process gives the transfer function coefficients corresponding to a filtered version of the transmitted signal u (t). The second process gives the equivalent amplitude modulation coefficients for the same received signal.

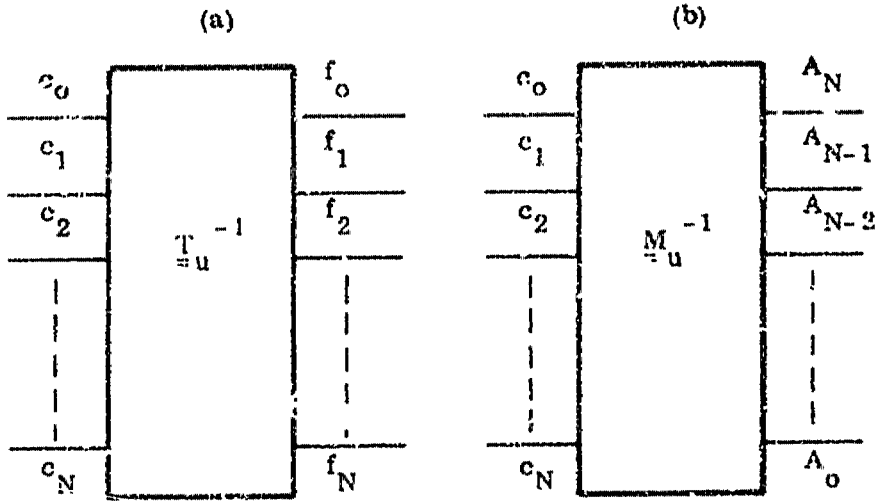

Figure 6-7. Manipulations of the Output Coefficients Determined by the Estimator in Figure 4-4, when Input = C (ω) + NOISE. In (a), the Numbers are Processed to Give the Spectral Coefficients Corresponding to F (ω), where C (ω) = F (ω) U (ω). The Resulting Processor is Identical to that in Figure 4-3. In (b), the Same Numbers are Processed to Give the Temporal Coefficients Corresponding to a (t), where C (ω) = A (ω) * U (ω) or c (t) = a (t) u (t).

6.7 Estimation of Amplitude Modulation Parameters on the Basis of More Than One Pulse.

When a pulse train is transmitted, different received pulses will generally have different amplitude modulating functions. These functions can be related, however, since they are presumably determined by the same continuous amplitude modulation, a(t). If the interpulse interval is T_o and the modulation of the first pulse is given by (6-8), then the modulation of the second pulse is given by

$$a(t - T_o) = \sum_{n=0}^{N} [a^{(n)}(T_o) / n!] (t - T_o)^n , \qquad (6-25)$$

where $a^{(n)}(T_o)$ is determined by differentiating both sides of (6-8) and letting $t = T_o$:

$$a^{(n)}(T_o) = \sum_{m=n}^{N} (m! A_m) T_o^{m-n} / (m-n)! . \qquad (6-26)$$

Substituting (6-26) into (6-25),

$$a(t - T_o) = \sum_{n=0}^{N} \frac{(t - T_o)^n}{n!} \sum_{m=n}^{N} \frac{m!}{(m-n)!} A_m T_o^{m-n}$$

$$= \sum_{n=0}^{N} A_{n1} (t - T_o)^n . \qquad (6-27)$$

6.7 --Continued.

In (6-27),

$$A_{n1} = \frac{1}{n!} \sum_{m=n}^{N} \frac{m!}{(m-n)!} A_m T_o^{m-n} \quad . \qquad (6\text{-}28)$$

In matrix notation,

$$\begin{bmatrix} A_{o1} \\ A_{11} \\ A_{21} \\ \cdot \\ \cdot \\ \cdot \\ A_{N1} \end{bmatrix} = \begin{bmatrix} 1 & T_o & T_o^2 & \cdots & T_o^N \\ 0 & \frac{1}{1!} & \frac{2T_o}{1!} & \cdots & \frac{NT_o^{N-1}}{1!} \\ 0 & 0 & \frac{1}{2!} & \cdots & \frac{N(N-1)T_o^{N-2}}{2!} \\ \cdot & \cdot & & & \\ \cdot & \cdot & & & \\ \cdot & \cdot & & & \\ 0 & 0 & 0 & \cdots & 1 \end{bmatrix} \begin{bmatrix} A_o \\ A_1 \\ A_2 \\ \cdot \\ \cdot \\ \cdot \\ A_N \end{bmatrix} . \qquad (6\text{-}29)$$

Defining

$$a(t - 2T_o) = \sum_{n=0}^{N} A_{n2} (t - 2T_c)^n$$

$$= \sum_{n=0}^{N} [a^{(n)}(2T_o) / n!] (t - 2T_o)^n \quad , \qquad (6\text{-}30)$$

6.7 --Continued.

we can determine $a^{(n)}(2T_o)$ by differentiating both sides of (6-27) and letting $t = 3T_o$;

$$a^{(n)}(2T_o) = \sum_{m=n}^{N} m!\, A_{m1}\, T_o^{m-n} / (m-n)! \qquad (6\text{-}31)$$

Substituting (6-31) into (6-30),

$$a(t-2T_o) = \sum_{n=0}^{N} A_{n2}\,(t-2T_o)^n$$

$$= \sum_{n=0}^{N} \left[\frac{1}{n!} \sum_{m=n}^{N} \frac{m!}{(m-n)!}\, T_o^{m-n}\, A_{m1}\right](t-2T_o)^n ,$$

(6-32)

so that

$$\begin{bmatrix} A_{02} \\ A_{12} \\ A_{22} \\ \vdots \\ A_{N2} \end{bmatrix} = \begin{bmatrix} 1 & T_o & T_o^2 & \cdots & T_o^N \\ 0 & \frac{1}{1!} & \frac{2T_o}{1!} & \cdots & \frac{NT_o^{N-1}}{1!} \\ 0 & 0 & \frac{1}{2!} & \cdots & \frac{N(N-1)\,T_o^{N-2}}{2!} \\ \vdots & & & & \\ 0 & 0 & 0 & \cdots & 1 \end{bmatrix} \begin{bmatrix} A_{01} \\ A_{11} \\ A_{21} \\ \vdots \\ A_{N1} \end{bmatrix} . \qquad (6\text{-}33)$$

6.7 --Continued.

Letting

$$\underline{\underline{P}} = \begin{bmatrix} 1 & T_o & T_o^2 & \cdots & T_o^N \\ 0 & 1 & 2T_o & \cdots & NT_o^{N-1} \\ 0 & 0 & \frac{1}{2!} & \cdots & \frac{N(N-1)T_o^{N-2}}{2!} \\ \vdots & & & & \\ 0 & 0 & 0 & \cdots & 1 \end{bmatrix} \tag{6-34}$$

we have, from (6-29) and (6-33),

$$\begin{aligned} \underline{A}_1 &= \underline{\underline{P}}\,\underline{A} \\ \underline{A}_2 &= \underline{\underline{P}}\,\underline{A}_1 = \underline{\underline{P}}^2\,\underline{A} \\ \underline{A}_n &= \underline{\underline{P}}^n\,\underline{A} \end{aligned} \tag{6-35}$$

so that

$$\underline{A} = \underline{\underline{P}}^{-n}\,\underline{A}_n \quad . \tag{6-36}$$

6.7 --Continued.

In (6-36),

$$\underline{\underline{P}}^{-n} = [\underline{\underline{P}}^{n}]^{-1} \tag{6-37}$$

and

$$\underline{A}_n = \begin{bmatrix} A_{on} \\ A_{1n} \\ \cdot \\ \cdot \\ \cdot \\ A_{Nn} \end{bmatrix} \tag{6-38}$$

is the vector of time series coefficients measured from the $n^{\underline{th}}$ received pulse.

The coefficients measured for <u>all</u> the received pulses can, mutatis mutandis, be used to estimate the time series coefficients in (6-8). Each pulse is processed as in Figure 6-7 (the second process). The resulting coefficients can then be used to estimate A_0, A_1, ... A_N in (6-8) by means of the transformation (6-36).

6.8 Discussion and Summary of Section 6.

The theory of target description that has been derived to explain cetacean echolocation has been applied to bats. The theoretical signals can be matched to Myotis pulses* as well as to those of Tursiops. To match the bat pulses, the theoretical waveforms must be high pass filtered in a special way. The high pass filter must not disturb the ability to determine at least twenty Taylor coefficients of a target's transfer function.

The above results constitute the first mathematical evidence that a unified theory of animal echolocation exists. The theory also provides a measure of the maximum number of spectral coefficients that can conveniently be estimated by the animals.

Because of similarities between the theoretical waveforms and their Fourier transforms, one can interpret the bat signals (and possibly the porpoise signals as well) in terms of time domain characterization of an unknown amplitude modulation. This alternate interpretation is interesting from several viewpoints:

(i) It implies that, for certain classes of signals, one can find a time invariant, linear filtering operation that is equivalent to any amplitude modulation. This equivalence implies (Section 10) the existence of a time invariant filter which has the same effect as any time varying linear transformation of a given pulse.

* The theoretical signals have also been matched to echolocation pulses of Eptesicus fuscus and Lasiurus borealis. These matches will be discussed in a future report.

6.8 --Continued.

(ii) The AM interpretation provides insights into the possible functions of various neurological processes which have been discovered in the auditory pathways of bats and other animals. Specifically, one can interpret the functions of neurons which respond to specific frequencies or chirp rates.

(iii) The AM interpretation illustrates another virtue of power series spectral analysis, viz., that both multiplication and convolution in the time domain can be represented by the same operation (convolution of appropriate coefficients) in the frequency domain.

In a discussion of neural processing (as seen from the viewpoints of amplitude demodulation vs. linear filter characterization) it was pointed out that a single matched filter could be implemented with 100 neurons, provided suitable inputs were available. It would seem that the proper input signals can be made available via the parallel connection of neurons to carry high frequency information. This concept is discussed further in Section 8.

It is possible that correlation using a single nerve cell could be performed at a very peripheral level, perhaps at the location where pressure waves are first converted into chemical-electrical signals. Such a hypothesis would require (i) that optimum filtering be detectable at the peripheral level if anesthetic is not used[41],

6.8 --Continued.

(ii) that efferent nerve fibers extend all the way to the vicinity of the hair cells[74], and (iii) that the correlation processing of a wideband signal be divided into a sequence of narrowband correlations over restricted frequency ranges.[75]

7. AN EXPERIMENT TO TEST THE THEORY.

7.1 The Physical Implementation.

In order to gain further insight into the theory and how it works in practice, a sonar experiment is being carried out with high frequency sound.* Although the experiment was funded by ESL as a reduction to practice for a patent application, it is reported here in order to augment the reader's comprehension of the theory.

The ultrasonic transducers that were used for the experiment were built to the specifications given by J. J. G. Mc Cue and A. Bertolini[42]. Although the transducers were designed as receivers, one was used as a transmitter. The two transducers are shown in a bistatic configuration in Figure 7-1. The target is the plane in the foreground; it is perpendicular to the line that bisects the angle between the transducers.

The signal that is being used has a Fourier transform as in Equation (2-8). Specifically, the signal has Fourier transform

$$U(\omega) = \omega^{.85} \, e^{-(\log \omega)^2 / 2\log k} \, e^{-j\, 16\, \pi \log \omega / \log k} \qquad (7\text{-}1)$$

where $k = 2.06$. This value of k is slightly higher than the values usually employed by bats and dolphins. The reason for such a large value was to obtain better isolation between coefficients, since we planned to measure only six different target coefficients.

---

* The experiment was designed by R. Altes; the electronic equipment was built by P. Keleshian; data is being gathered and processed by W. Reese.

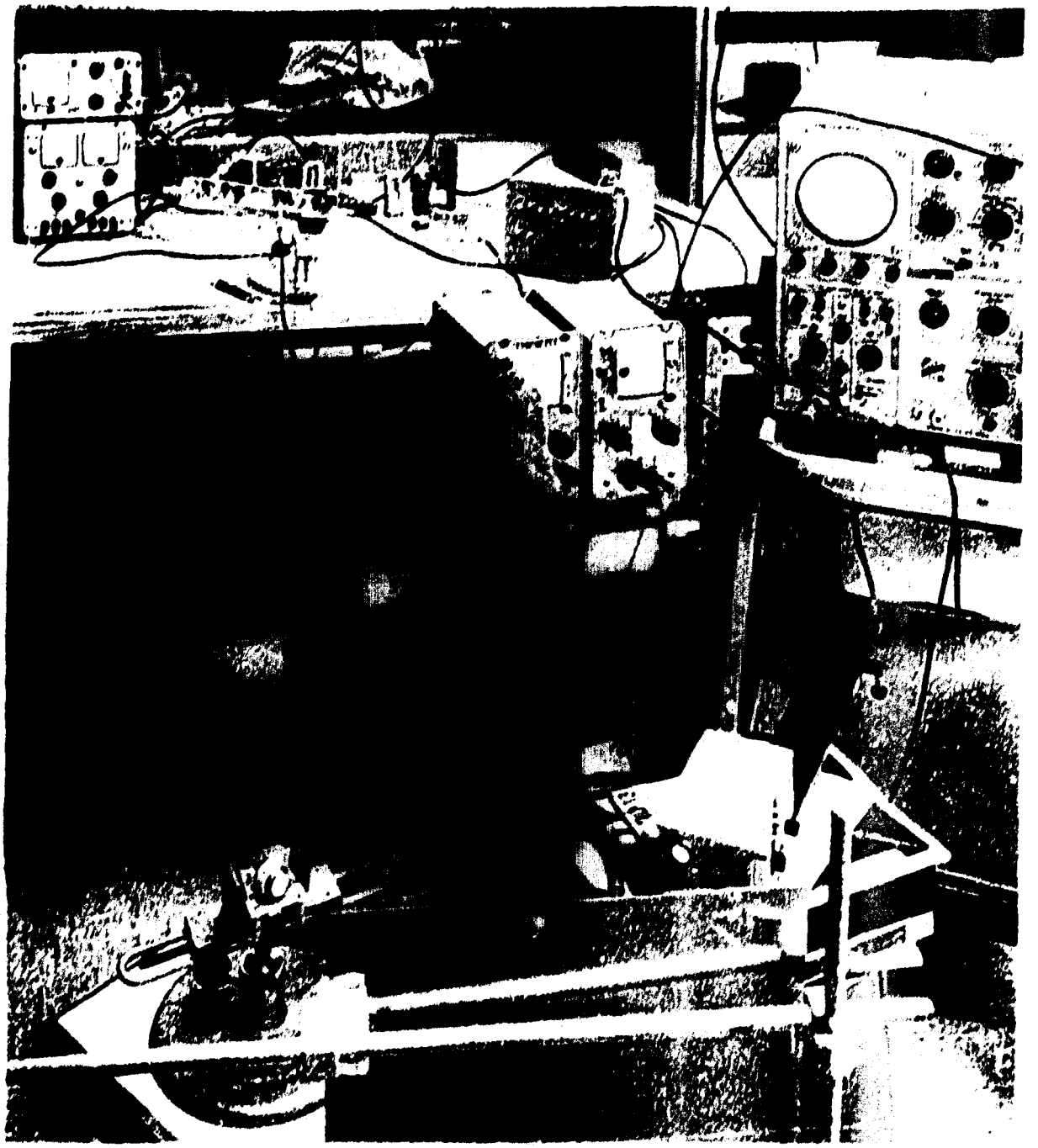

Figure 7-1. Ultrasonic Equipment to Implement the Method of Target Description Discussed in this Report. Target and Two Transducers are in Foreground. Reflected Pulses are Shown on the Oscilloscope Screen. A Transmitted Pulse is Shown in Figure 7-2.

7.1 --Continued.

The signal was chosen to be a compromise between bat and porpoise echolocation waveforms. Like dolphin signals, no truncation function was applied in the frequency domain. Like bat signals, the phase factor was made large enough to produce a significant number of zero crossings, i.e., a recognizable chirp. The phase factor, although large enough to produce a chirp, is still not as large that employed by Myotis, but much larger than that employed by Tursiops.

The transmitted signal is shown in Figure 7-2. The waveform is generated in the laboratory by using a read-only memory (ROM) device. By varying the clock rate, i.e., the rate at which the sampled signal is read out of the ROM, the waveform can be stretched or compressed. Notice that the signal in Figure 7-2 is truncated at its low frequency end. This truncation was decided upon because the low frequency end has comparatively little energy and is greatly over sampled. The samples could better be utilized at the high frequency end of the pulse.*

The correlation operation is performed with analog differentiators and integrators and an analog multiplier. The reference signal is obtained by generating a second waveform with the ROM. The second waveform is generated at the right time so that it coincides with the target echo. The reference signal is then differentiated once, twice, or three times, integrated once or twice, or left alone. The resulting waveforms are, theoretically, time scaled versions of the transmitted signal. The extent to which differentiation or integration reproduces a scaled version of the signal is determined by the similarity between the analog operations and their mathematical

* For efficient sampling of a chirped signal, one should really use a variable clock rate, so that many samples are not wasted in oversampling the low frequency portion of the signal.

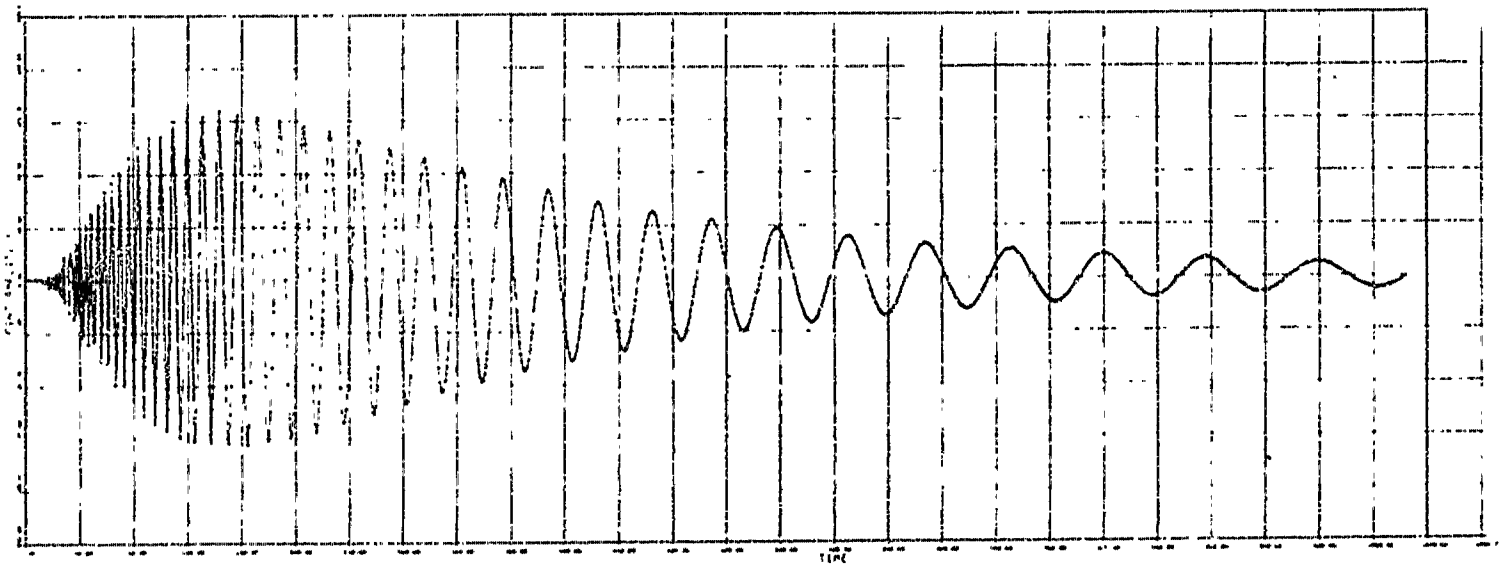

Figure 7-2. Transmitted Signal for the Ultrasonic Experiment. The Signal is Generated by a ROM (Read-Only Memory) Device that was Programmed with a Computer.

7.1 --Continued.

counterparts, and by the similarity of the signal to its mathematical counterpart. Figure 7-3 shows that two analog differentiations and one analog integration are reasonably well behaved. The second integration is imperfect because of low frequency distortion (integrators are low pass filters) and because the pulse is truncated for efficient ROM utilization.**

A scaled reference signal is correlated with the target echo by multiplication and integration. The maximum output of the correlator is determined for each reference signal. The maximum outputs are related to the target power series coefficients by the analysis in Section 4.

7.2 Some Qualitative Results.

The most important results of this experiment are the qualitative observations and insights that are obtained before one even begins to collect numerical data.

Echo differences for different objects are easily observed on the oscilloscope screen. These differences seem to be manifested as different amplitude modulations imparted to the returning pulse. This observation has already been reported by Griffin[35].

Figure 7-3 illustrates that the scaled signals have their maxima at different times, relative to the returning echo. When the scaled reference signals are correlated

** A better (but more expensive) way to produce the reference signals is to use a different clock rate for the second ROM pulse.

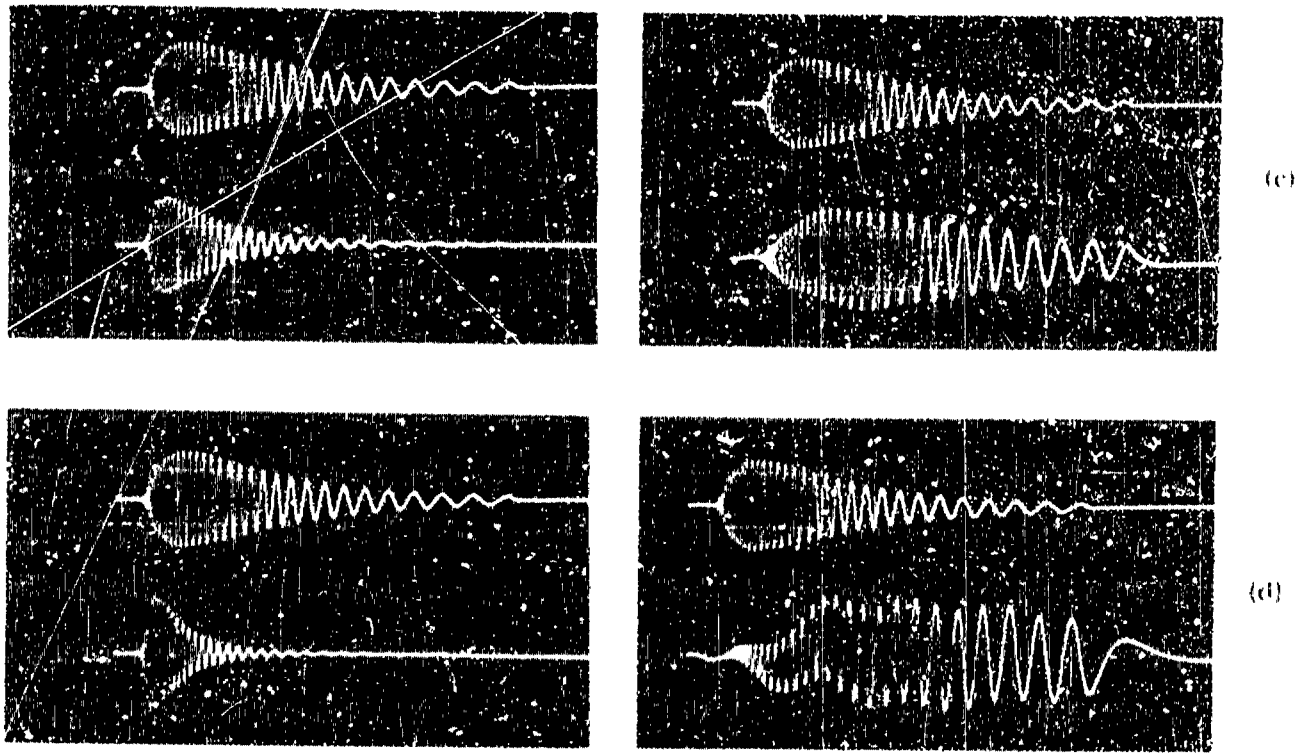

Figure 7-3. The Top Waveform in All Four Pictures is the Transmitted Signal (Output of ROM). The Bottom Signals are: (a) The Top Waveform After Being Processed with An Analog Differentiator. Differentiation Should Cause Compression by a Factor of 2.06. (b) The Top Waveform After Double Differentiation with an Analog Device. Compression Factor Should Be $(2.06)^2$. (c) The Top Waveform After Analog Integration. Truncation of the Top Waveform Prevents a Complete Version of the Stretched Signal from Being Formed. (d) The Top Waveform After Double Analog Integration. Low Frequency Distortion and Signal Truncation Cause Significant Differences Between the Output Signal and Its Theoretical Counterpart, i.e., a Stretched Version of the Top Waveform.

7.2 --Continued.

with an echo, the correlator output is very dependent upon the amplitude of the echo at the peak of the reference signal. Matched filtering for power series target characterization is thus equivalent to amplitude demodulation of various portions of the reflected pulse. This equivalence has been explored in Section 6.

Further insight is obtained when one realizes that the reference signals which "look" at the leading edge of the echo pulse are the differentiated or shortened versions of the transmitted signal. Differentiated reference signals are therefore used to characterize the leading edge of an echo, which is related to initial curvature and "hardness" of the material.*

Conversely, integrated (stretched) reference signals characterize the trailing part of the echo, and are thus related to the range extent of the target. Experimentally, targets that are extended in range cause the echo to be stretched. This stretching can be characterized by an integration process when the appropriate signals are used.

---

* T. R. Bullock and S. Ridgway[43] have found a dichotomy in Tursiops' neural processing of acoustic data. Signals with fast rise times are processed in a different part of the brain than signals with slow rise times. Since transmitted echolocation clicks generally have fast rise times, Bullock and Ridgway chose to classify the fast rise time analyzer as the sonar processor. Slow rise time echoes, however, are still possible with fast rise time signals. Such echoes would occur for targets with gradual changes in acoustic impedance or cross section, such as a large tilted plane or a soft, waterlogged object, and for all targets that are far away, since the channel acts as a low pass filter. It is therefore tempting to reclassify the fast rise time analyzer as the "sonar processor for close, hard targets." Reflections from such targets may require quick, decisive action, whereas other targets can be contemplated at leisure. This reaction time consideration may explain the dichotomy found by Bullock and Ridgway. An interesting behavioral experiment would be the measurement of reaction time as a function of signal shape.

7.2 --Continued.

The author has often been asked about the correlation of spectral power series coefficients with target shape. The above observations supply a partial answer. Small, hard targets with limited range extent will have comparatively large coefficients for $n > 0$, where $F(\omega) = \sum_{-N/2}^{N/2} f_n \omega^n$. Targets with large range extent or slow changes in acoustic impedance will have comparatively large coefficients for $n < 0$.

7.3 Some Quantitative Results.

A schematic diagram of the experiment is shown in Figure 7-4. The second ROM pulse is correlated with the echo, after being passed through a differentiator or integrator. The maximum correlator response magnitude determines a coefficient that helps to characterize the target transfer function. The filter outputs should be processed as in Section 4, Figure 4-3. For our purposes, however, it suffices to show that the correlator outputs are indeed different for different targets.

All correlator responses should be normalized. Each response should be divided by the output of the autocorrelator, i.e., the correlator response when the reference signal is the same as the transmitted signal.

Three targets have been used: A steel cylinder with a 3/8 inch diameter, a metal plate oriented perpendicular to the angle bisecting the two transducers (the "perpendicular plane"), and the same plane tilted thirty degrees, with the closest edge toward the transmitter.

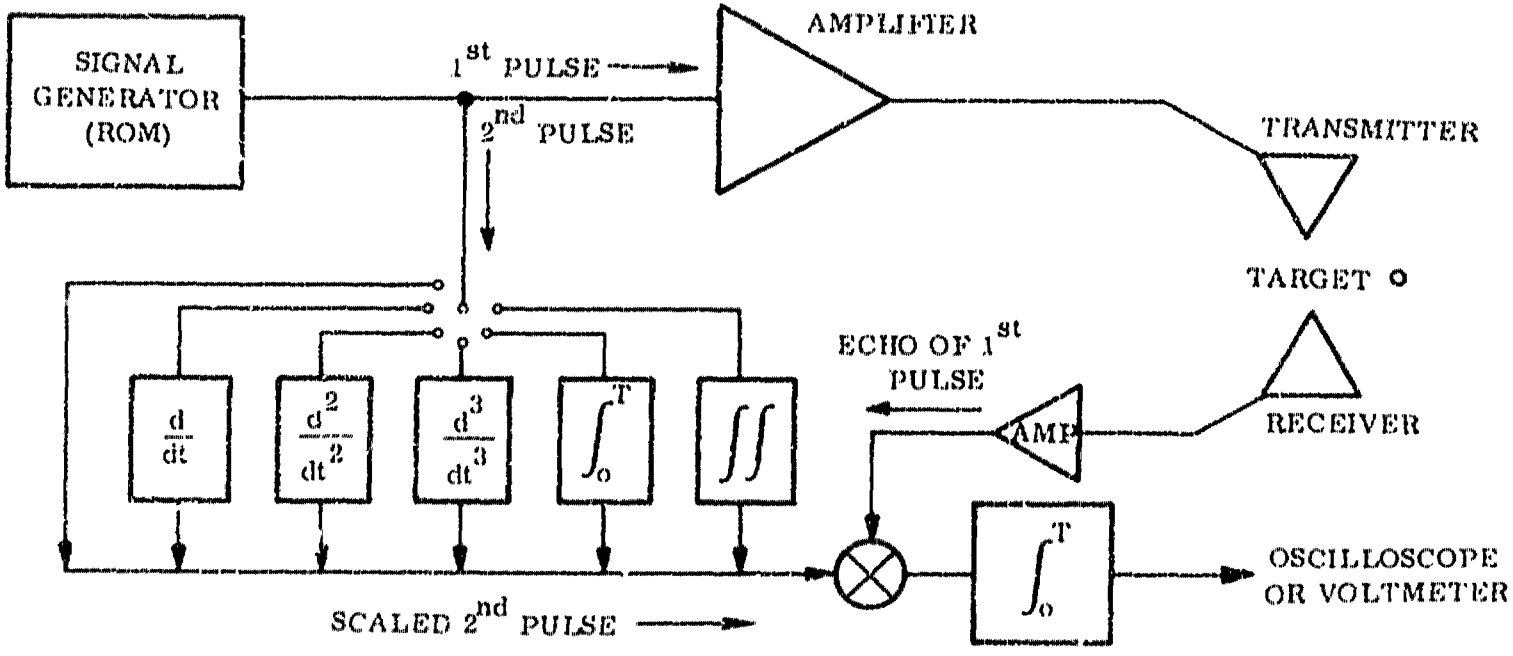

Figure 7-4. Block Diagram of Experimental System. The ROM Generates Two Identical Pulses. Echo of First Pulse is Correlated with a Scaled Version of Second Pulse. Delay between Generated Pulses is Set to Maximize Correlator Output.

7.3 --Continued.

The data is presented as reflected signals and numbers in Figure 7-5 and Table 7-1. Figure 7-5 shows the echoes from the three different targets. Table 7-1 illustrates that one can indeed obtain different normalized correlator responses for different target shapes.

7.4 Future Experimentation.

Some of the data gathered in future experiments will be digitized and processed by computer. Computer filtering will eliminate the uncertainties caused by imperfections of the analog equipment.

Experiments are currently under way to gather data when receiver and transmitter are colocated, rather than separated as in Figure 7-1. We are also discriminating between cylinders of different size, in an attempt to simulate some of the behavioral experiments that have been performed with cetaceans.

It is hoped that the experiment will soon be set up to discriminate targets in water, using small, off-the-shelf wideband transducers. It would also be interesting to detect small disturbances on the air-water interface, as Noctilio leporinus (the fishing bat) apparently does.[44] One could set up the capacitive (air) transducers to look at the surface of an aquarium containing fish, and electronically trigger a camera to record the fishes' positions when an appropriate set of filter responses is observed.

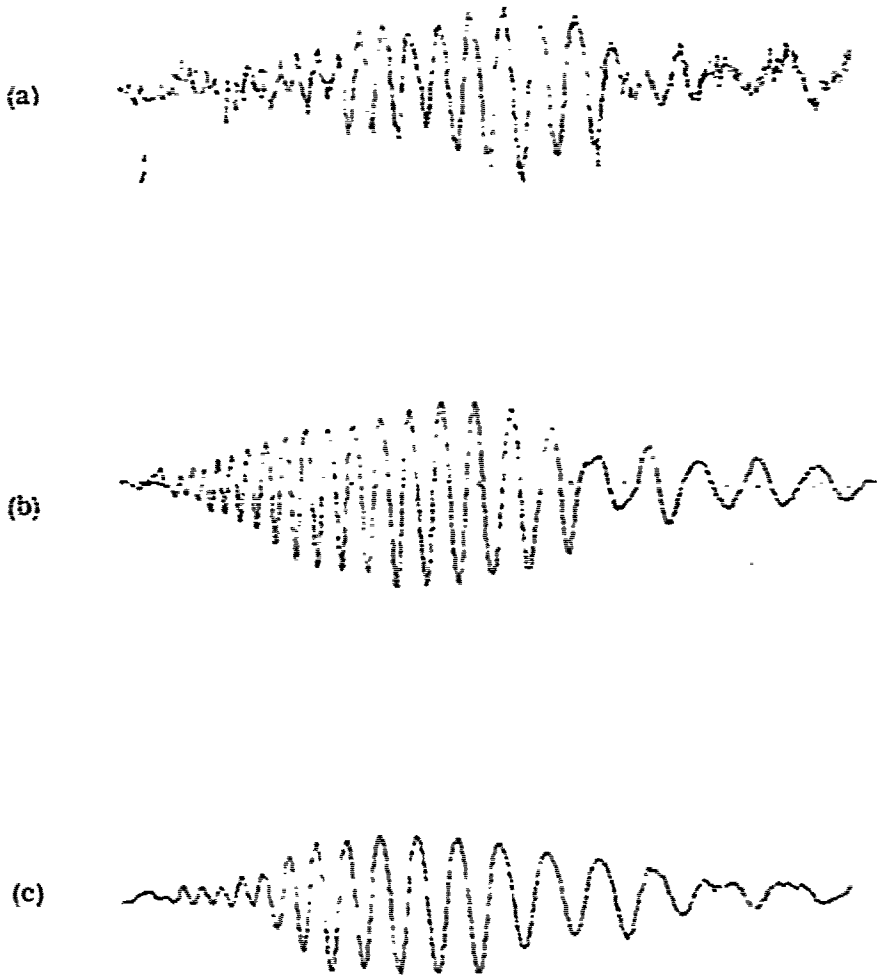

Figure 7-5. Graphs of the Echoes from Three Different Reflectors: (a) the 3/8" Diameter Cylinder, (b) the Perpendicular Plane, (c) the Tilted Plane. The Coefficients in Table 7-1 are Determined by Correlating these Echoes with the Signals in Figure 7-3.

Input to Correlator	3/8" Diameter Cylinder	Perpendicular Plane	Tilted Plane
Trans. Signal	1.0	1.0	1.0
1st Deriv.	0.65	0.46	0.43
2nd Deriv.	0.45	0.21	0.29
3rd Deriv.	0.30	0.17	0.14
Integral	1.0	0.96	1.1
Double Int'l.	0.95	1.2	1.6

Table 7-1. Table of Experimentally Determined Coefficients

8. TWO MODELS OF THE AUDITORY SIGNAL PROCESSOR.

8.1 Experimental Results.

Measurements of auditory threshold as a function of tone duration have been made for dolphins[45] and humans[46]. For all audible frequencies, these measurements indicate an increase in sensitivity for pulse durations up to approximately 0.2 seconds. For tones longer than 0.2 seconds, the threshold stays approximately constant.

Measurements of just noticeable frequency difference have been made for human listeners.[47] These measurements indicate sensitivity to a 3 Hz frequency change for tones with frequency less than 2 KHz. Above 2 KHz, the minimum detectable frequency change becomes larger: 10 Hz at 4 KHz, 22 Hz at 8 KHz.

Masking of pure tones by narrowband noise has led to a model of the ear as a spectrum analyzer. This model uses filters whose bandwidths are approximately proportional to their center frequencies. These so-called critical bandwidths are approximately twenty times the minimum perceptible frequency difference[24] discussed above.

Physiological experiments performed by von Bekesy and reported in Fletcher's book[48] show a relation between number of nerve endings attached to the basilar membrane at a given position and the resonant frequency at that position (Figures 8-1 and 8-2). The curves imply that a narrowband masking signal offset by Δf from a pure tone will succeed in masking the tone if Δf is sufficiently small. At the higher frequencies, Δf can be increased and masking will still occur. This observation is intimately related to the concept of critical bandwidth, as indicated by the masking data curves in Figure 8-2.

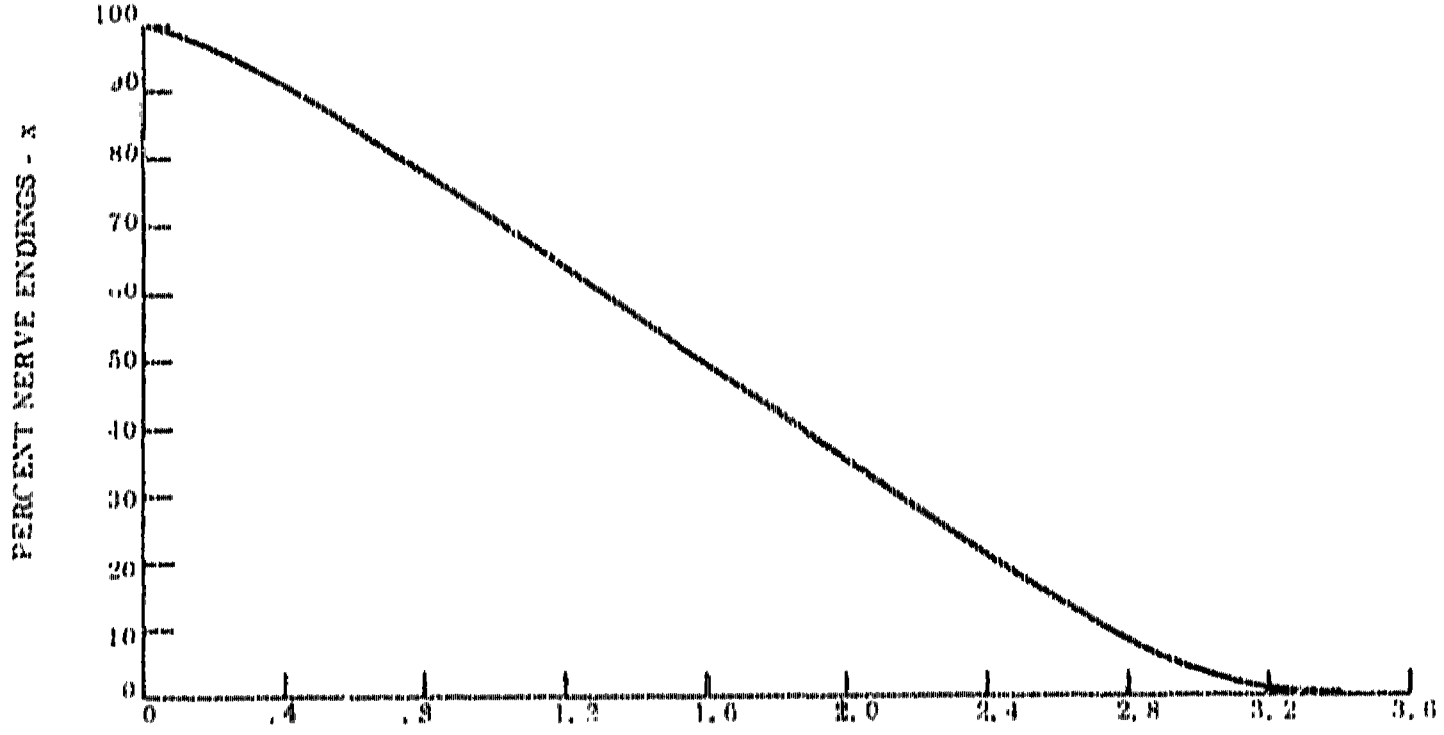

Figure 8-1. The Relation Between the Percent x of Nerve Endings and the Distance z Passed Over in Going From the Stapes to the Helicotrema End of the Basilar Membrane.

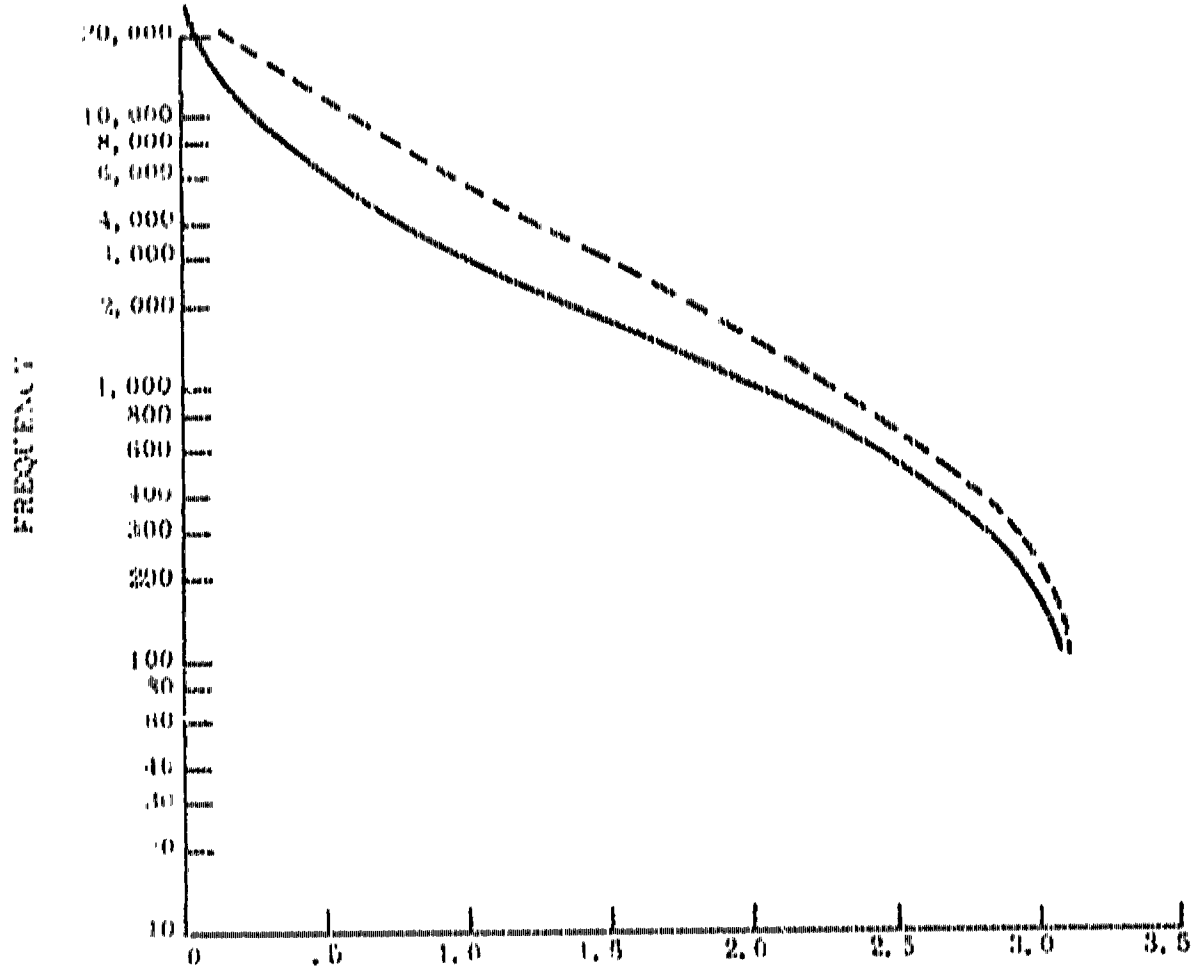

Figure 8-7. The Calculated Relation between the Resonant Frequency f_0 and the Distance From the Stapes. Solid Line and Dotted Line Symbolize Calculations Based upon Two Different Sets of Masking Data.

8.2 Fletcher's Model of the Auditory Processor.

R.S. Gales[49] has pointed out that the above measurements can all be explained in terms of Fletcher's model. This model involves a parallel connection of critical bandwidth filters. Connected to each filter output is a rectifier and an integrator. The integrator acts as a low pass filter with a 5 Hz bandwidth, i.e., the effective integration time is 0.2 seconds.

The integration time of 0.2 seconds is consistent with the duration dependence of auditory threshold. The critical bandwidths are consistent with the masking data and with Figures 8-1 and 8-2. The just noticeable frequency differences are explained[50] in terms of translating the tone away from the center frequency of a critical band filter. As the frequency of the tone changes, the magnitude of the filter response changes. The theoretical change in amplitude of filter response for a frequency translation equal to the just noticeable frequency difference is closely related to the just noticeable amplitude change at the appropriate frequency.

8.3 A Linear Model*

An alternate model of the auditory system starts with a series of probes which extend into a resonant cavity of variable cross section (the cochlea). Each probe is associated with a hair cell (each of which actually has more than ten cilia extending into the liquid of the cochlea[51]). Each probe is connected to a band pass filter. All the band pass filters are assumed to have the same bandwidth, i.e., 5 Hz.

---

* This model is a slightly revised version of a model suggested in Reference 3.

8.3 --Continued.

The outputs of N (f_o) adjacent filters are combined (summed), where N(f_o) is the next highest integer corresponding to f_o, the center frequency of the filter in KHz. The center frequency f_o corresponds to the resonant frequency of the cavity (cochlea) at the filter's probe location. In other words, separate filter outputs are available (N(f_o) = 1) for $f_o \leq 1$ KHz. For $1 < f_o \leq 2$ KHz, two filter outputs are combined. For $f_o = 8$ KHz, eight filter outputs are combined. The combined filter outputs are then further manipulated in order to optimally detect various signals.

The above model is again consistent with the experimental results in Section 5.1, as well as with some additional results. Notice in Figures 8-1 and 8-2 that the value of $\Delta f_o / \Delta N$, the resonant frequency change divided by the number of nerve endings associated with this change, is maximized at the stapes, the high frequency end of the cochlea. The maximum frequency change per hair cell can be determined from the fact that there are 23,500 hair cells in total.[52] The maximum frequency change per hair cell is approximately

$$\frac{\Delta f_o}{\Delta N} \approx \frac{20,000 \text{ Hz} - 10,000 \text{ Hz}}{10\% \text{ of } 23,500 \text{ hair cells}}$$

$$\approx \frac{10,000}{2,350} \approx 5 \text{ Hz / hair cell} . \qquad (8\text{-}1)$$

S 3 --Continued.

The combination of N (f_o) filters explains the just noticeable frequency difference data. To translate a CW tone from one filter combination to the next, the frequency must be shifted by ⌈ N (f_o) × 5 Hz ⌉ / 2, i.e., half the total bandwidth. For $f_o \leq 1$ KHz, ⌈ N (f_o) × 5 ⌉ / 2 = 2.5 Hz; at f_o = 4 KHz the required translation is 10 Hz; at f_o = 8 KHz, the required translation is 20 Hz. These numbers correlate closely with the just noticeable frequency differences.

The tone duration data is also explained by the new model, since signals are convolved with a filter impulse response that is 0.2 seconds long. The maximum response to an input pulse of constant frequency will thus increase linearly with pulse duration until the pulse becomes longer than 0.2 seconds. At this point, the maximum response remains constant, even when the input pulse duration is increased.

The new model is also consistent with the capacity of neurons to transmit a signal. The refractory period of a typical neuron lasts approximately one millisecond.[53] Because of this refractory period, a tone with more than one maximum per millisecond (1 KHz) can only be transmitted if the burden is shared by other neurons. Assume that these neurons are connected to adjacent 5 Hz filters. Spontaneous discharges of different neurons will cause them to be excited at different times, since the excitation of one neuron may occur during the refractory period of another. If each neuron triggers on a different signal peak, then a combination of four neurons can handle a 4 KHz signal, eight neurons can handle an 8 KHz signal, etc. In general, a combination of N (f_o) neurons can handle a signal with frequency f_o, where N (f_o) was defined above. If the N (f_o) neurons are connected to adjacent 5 Hz filters, the just noticeable frequency difference will be ⌈ N (f_o) × 5 Hz ⌉ / 2.

8.3 --Continued.

C. S. Johnson[54] has pointed out that the new model can also explain the rapid cutoff of marine mammals' auditory thresholds at the high frequency end. The model can also explain changes that occur in the auditory spectrum analyzer for wide-band signals. D. M. Green has found that "critical bands are not fixed in width but are adjustable so as to match the particular detection situation."[55]

The most important aspect of the new model is that it allows for faithful transmission of a complete signal without the information - destroying, nonlinear rectifier-integrator (envelope detector) as a necessary component of initial processing. The receiver can thus operate upon the spectral phase of a signal, as well as its spectral amplitude. In terms of the theory in Sections 2 through 4, the phase as well as the magnitude of spectral Taylor series coefficients can be determined. In terms of matched filter theory, true pulse compression becomes possible.[56]

A disconcerting property of Fletcher's model is its behavior when it is utilized as a sonar signal processor. The low pass filter or integrator at the output of each critical bandwidth filter results in an output pulse that is at least 0.2 seconds in duration, regardless of the bandwidth of the input signal. The range resolution of a sonar processor equipped with such an envelope detector is on the order of 220 feet in air, or 900 feet in water.

It is obvious that animal echolocation systems have much better resolution. In fact, J. Simmons' experiments[56] show that the range resolution of the FM bat Eptesicus fuscus is predicted by the autocorrelation function of the bat's sonar pulse. This resolution is approximately determined by the reciprocal of the bat's signal bandwidth, and is equivalent to about half an inch.

8.3 --Continued.

If animal sonar data is to be explained by Fletcher's model, the envelope detectors must be altered to shorten the integration time. A shorter integration time, however, does not provide an adequate explanation for the measured tone duration dependence of the auditory threshold.

The linear model does not suffer from the above problem. Although the impulse response of each 5 Hz filter is 0.2 seconds long, a linear combination of these responses can produce a pulse with a much shorter duration. The minimum width of such a pulse is approximately the reciprocal of the total bandwidth of all the signals that are added together.

Envelope detecting the output of each 5 Hz filter is only legitimate if one assumes that the signal is a tone with a bandwidth that is less than 5 Hz wide.

The new model allows for linear signal analysis and reasonable range resolution, but does not offer a completely satisfying explanation of critical bandwidth data. It would seem that a minimum number (twenty) of the $N(f_o)$ combined 5 Hz filter outputs must be further combined when narrowband masking noise is introduced. Perhaps a stimulus with a bandwidth exceeding some minimum level elicits power series spectral analysis, while a narrowband tone is subjected to ordinary spectrum analysis. This dichotomy could explain the division of many bat signals into narrowband tones and wideband chirps.

9. MINIMIZING THE VOLUME OF THE WIDEBAND AMBIGUITY FUNCTION.

The volume of the wideband ambiguity function is not fixed as in the narrowband case,[77] even though signals are defined to have unit energy. It is still possible, however, to define a set of signals such that all members of the set have the same wideband ambiguity volume. A relevant example[57] is the set of signals with Fourier transforms

$$U(\omega) = \omega^{-1/4} \; e^{-(\log \omega)^2 \,/\, 2 \log k} \; e^{j \phi(\omega)} \qquad (9\text{-}1)$$

where $\phi(\omega)$ can be any continuous function and k can be any constant greater than one. All signals whose spectra can be described by (9-1) have a wideband ambiguity function with the same volume as the narrowband ambiguity function[57], i.e.,

$$\text{Volume} = \int_0^\infty \int_{-\infty}^{\infty} \left| \chi_{uu}(\tau, s) \right|^2 d\tau \, ds = 2\pi E^2, \qquad (9\text{-}2)$$

where E is the energy of the signal.

For good range and doppler resolution, the volume under the ambiguity function should be made as small as possible. The volume depends upon $|U(\omega)| = A(\omega)$, since[57]

$$\text{Volume} = E \int_0^\infty \frac{A^2(\omega)}{\omega} \, d\omega \; . \qquad (9\text{-}3)$$

The dependence of volume upon $|U(\omega)|$ explains why $\phi(\omega)$ can remain unspecified in (9-1).

9. --Continued.

An undesirable way to minimize the volume is indicated by the inequality[58]

$$\int_{s_1}^{s_2} \int_{-\infty}^{\infty} | \chi_{uu}(\tau, s) |^2 \, d\tau \, ds \leq \frac{4\pi}{3^{1/2}} \left[\frac{1}{2\pi} \int_0^{\infty} [\dot{A}(\omega)]^2 \, d\omega \right]^{1/2} \times (s_2^{1/2} - s_1^{1/2}) \qquad (9\text{-}4)$$

where

$$\frac{1}{2\pi} \int_0^{\infty} [\dot{A}(\omega)]^2 \, d\omega \leq \frac{1}{2\pi} \int_0^{\infty} | \dot{U}(\omega) |^2 \, d\omega = \int_{-\infty}^{\infty} t^2 | u(t) |^2 \, dt \equiv D_t^2 , \qquad (9\text{-}5)$$

the mean square duration. If D_t^2 is made small, the volume will be made small. For a given energy, however, making D_t^2 small implies a large maximum power, a quantity which is always constrained in any practical system.

A meaningful volume minimization problem is then to find the function $A(\omega)$ that minimizes $\int_0^{\infty} [A^2(\omega) / \omega] \, d\omega$ as in (9-3), with constraints that (i) E, the signal energy be kept large, and (ii) $\int_0^{\infty} [\dot{A}(\omega)]^2 \, d\omega$, a lower bound for D_t^2, be kept large

9. --Continued.

The functional to be minimized is therefore

$$J\,[\,A(\omega)\,] = \int_0^\infty [\,A^2(\omega)/\omega\,]\,d\omega + \lambda_E \int_0^\infty A^2(\omega)\,d\omega + \lambda_T \int_0^\infty [\,\dot{A}(\omega)\,]^2\,d\omega$$

$$= \int_0^\infty F(\omega, A, \dot{A})\,d\omega \quad . \tag{9-6}$$

where λ_E and λ_T are Lagrange multipliers for the energy and time duration constraints.

The Euler-Lagrange equation provides a necessary condition for the function $A(\omega)$ to be an extremaloid of the functional (9-6) :

$$\frac{\partial F}{\partial A} - \frac{d}{d\omega}\left[\frac{\partial F}{\partial \dot{A}}\right] = 0\,, \tag{9-7}$$

or

$$\ddot{A} - [\,(\lambda_E/\lambda_T) + 1/(\omega\lambda_T)\,]\,A = 0\,. \tag{9-8}$$

9. --Continued.

The Legendre necessary condition requires that

$$\frac{\delta^2 F}{\delta \dot{A}^2} \geq 0 \qquad (9\text{-}9)$$

in order that the extremaloid be such that the functional (9-6) is minimized. Equation (9-9) requires that

$$\lambda_T \geq 0 \ . \qquad (9\text{-}10)$$

Equation (9-8) can be written in the same form as the Coulomb wave equation[59]:

$$\ddot{A} + [\, 1 - (2\eta/\omega) - L(L+1)/\omega^2 \,]\, A = 0 \ . \qquad (9\text{-}10)$$

To make (9-8) identical with (9-10), let

$$\lambda_T = 1/2\eta \ : \ \lambda_E = -\lambda_T \qquad (9\text{-}11)$$

The two equations are then identical if $L = 0$ or $L = 1$. The solutions are the Coulomb wave functions[59]

$$F_o(\eta, \omega) \text{ and } F_{-1}(\eta, \omega) \ .$$

9. --Continued.

Since both $F_o(\eta, \omega)$ and $F_{-1}(\eta, \omega)$ are solutions of the same differential equation, they must be equal. Indeed, if $L = 0$ is substituted into the recurrence relation[59]

$$L\left[d F_L(\eta, \omega)/d\omega\right] = (L^2+\eta^2)^{1/2} F_{L-1}(\eta, \omega) - (\eta + L^2/\omega) F_L(\eta, \omega), \tag{9-12}$$

one comes to the conclusion that

$$F_o(\eta, \omega) = F_{-1}(\eta, \omega) . \tag{9-13}$$

The functions $A(\omega)$ that minimize ambiguity volume while constraining energy and time duration to remain large are therefore Coulomb wave functions with $L = 0$.

Since $A(\omega)$ is defined as the magnitude of the spectrum $U(\omega)$, we require that $A(\omega) \geq 0$. Furthermore, we require that $A(\omega)$ be continuous, so that the integral in (9-5) is defined. These two implicit constraints imply that

$$A(\omega) = \begin{cases} 0 , & \omega \leq 0 \\ F_o(\eta, \omega), & 0 \leq \omega \leq z_1 \\ 0 , & \omega \geq z_1 \end{cases} \tag{9-14}$$

where z_1 is the first zero of $F_o(\eta, \omega)$ for $\omega > 0$. For example, Figure 9-1 shows $A(\omega)$ for $\eta = 1$, $\eta = 5$, and $\eta = 10$. For energy normalized signals, it is clear

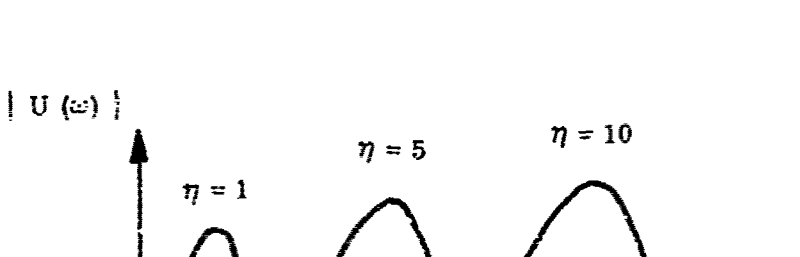

Figure 9 1. Unnormalized Graphs of $F_o(\eta, \omega)$ for $\eta = 1, 5, 10$. The Functions are Truncated at their First Zero Crossings, in Accordance with Continuity and Positive Semidefiniteness Requirements.

9. --Continued.

from (9-3) that the volume decreases as η is increased. The minimum attainable volume is therefore determined by the maximum frequency that can be obtained with a given system.

Equation (9-14) defines the amplitude of the signal's spectrum, but what about the associated phase? From the viewpoint of volume minimization, the phase is arbitrary. From the viewpoint of pulse compression techniques, however, a nonlinear (chirped) phase function is desirable. It can be shown[57] that range-doppler coupling will be avoided if a log phase function is used with the positive semidefinite function described by (9-14)*.

* In general, it is shown in reference 57 that any positive semidefinite, Analytic, real frequency function can be multiplied by a log phase function, and the resulting transform will correspond to a signal that has no range doppler coupling. Another example is found in Section 6, where some Myoti. signals were matched to real, positive semidefinite spectra with log phase functions. The Myotis signals therefore have no range-doppler coupling, a result that was determined experimentally by R. A. Johnson.[10]

10. FURTHER ANALYSIS INVOLVING THE EQUIVALENCE OF AMPLITUDE MODULATION AND LINEAR FILTERING.

10.1 Characterization of Time Varying Linear Systems.

In Section 6, it was shown that amplitude modulation of the pulsed signals u (t), with Fourier transforms given by (2-8), could be viewed as a linear filtering process. Heuristic justification for this equivalence was presented in Section 7.

Figure 10-1 shows a linear system which can be made equivalent to any other linear system* over a given frequency interval. The differentiators are preceded by gains that determine the power series spectral coefficients of F (ω), the system transfer function. To characterize a time varying linear system, the power series spectral coefficients are allowed to change with time, as indicated in Figure 10-1.

When a pulsed signal u (t) with Fourier transform (2-8) is introduced at the input of the system in Figure 10-1, the modulation functions $a_n(t)$ have the effect shown in Section 6. In other words, the product $a_n(t)\, u(t)$ can be described as a linear time invariant transformation of u (t).

A linear time invariant transformation can again be characterized by a sequence of differentiators, provided an appropriate time invariant gain is associated with each differentiation. For an input pulse described by (2-8), the time varying linear system in Figure 10-1 is thus equivalent to the time invariant system in Figure 10-2. This system can again be characterized by the methods in Section 4. Specifically, one can design a time invariant receiver to detect echoes from a target whose shape and/or aspect is time varying.

*More precisely, any other linear system with a transfer function that is analytic at ω = 0. The argument can be generalized to other systems by including integrators, as well as differentiators, in Figure 10-1.

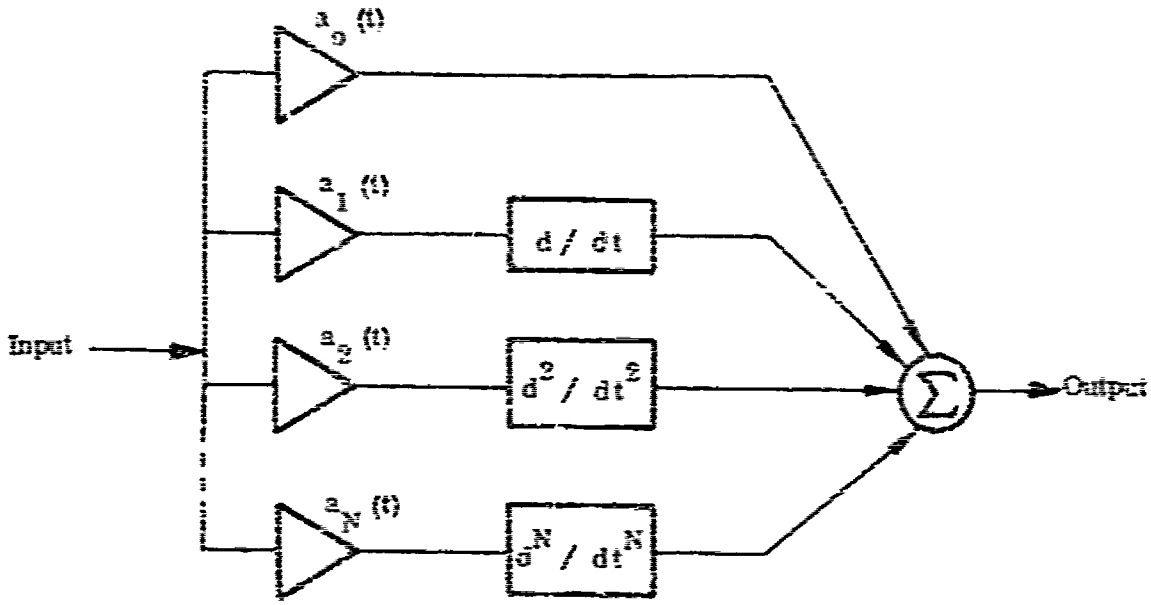

Figure 10-1. A System whose Transfer Function can be Made Identical to that of Any Linear System with Transfer Function $\sum_0^N a_n(t)\,\omega^N$, over a Given Frequency Interval $[\omega, W]$. The Gains $a_n(t)$ can be Complex, i.e., they each have an Associated Phase Shift.

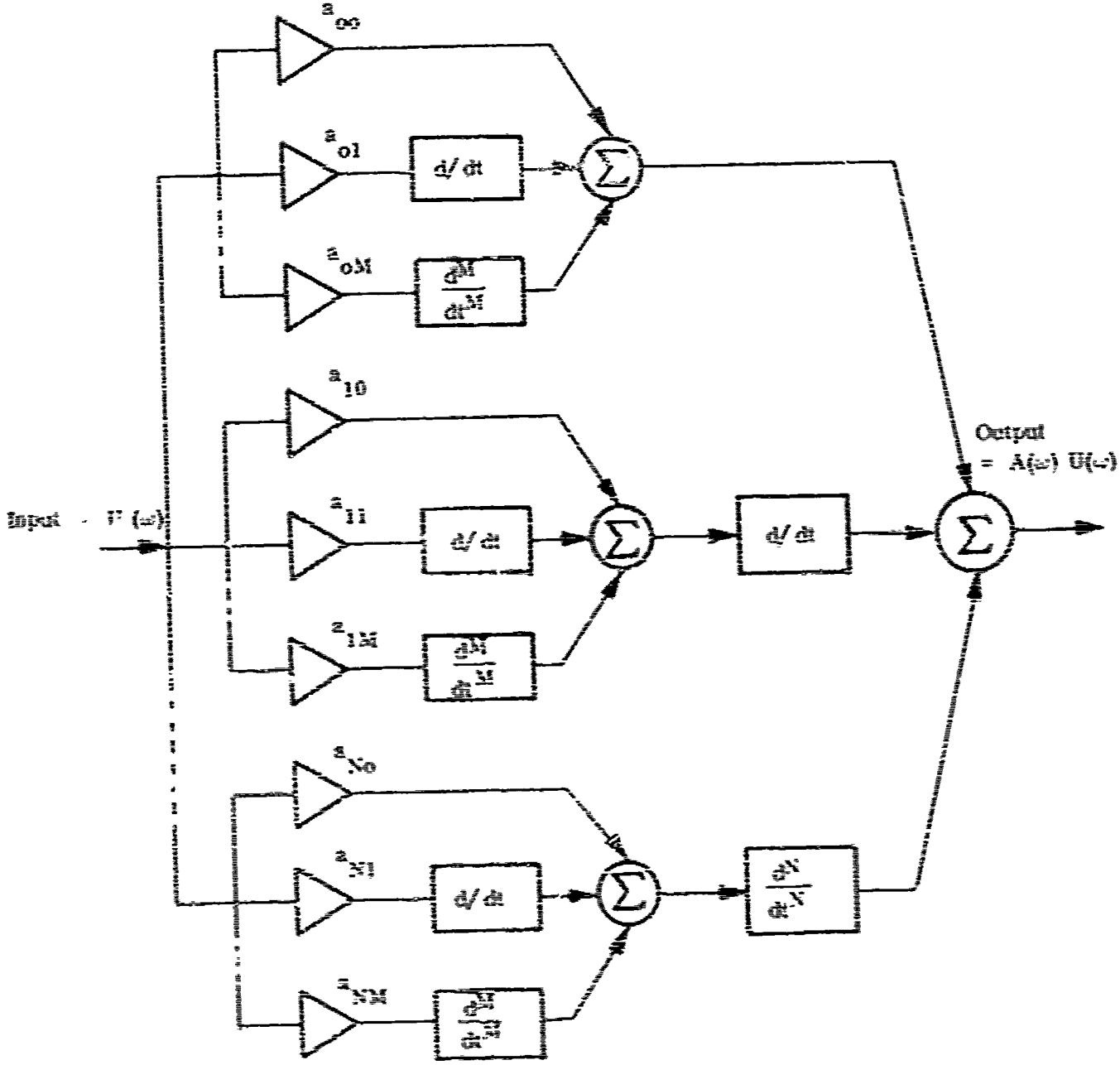

Figure 10-2.

When the Input to the System in Figure 10-1 is a Pulse with Transform U (ω) as in Equation 2-8, the Amplitude Modulations $a_{ij}(t)$ Can be Modelled as Linear Filtering Processes. The Time-Varying System in Figure 10-1 Can Therefore be Modelled as a Time Invariant System when Input U (ω), as Shown Here. Therefore, Any Time Varying Linear System with Transfer Function $\sum_{n}^{N} a_n(t) \omega^N$ Can be Modelled as a Time Invariant System with Appropriate Constant Coefficients, if the Signal U (ω) is used.

10.1 —Continued.

The equivalence between time varying and time invariant systems may be very useful for bats and porpoises. It is interesting (and intuitively obvious) that when a time varying target is held still, its transfer function can generally be modelled with fewer differentiators than are necessary for characterization of the scintillating target. A larger number of significant power series coefficients results from changes in target shape or aspect. These higher order coefficients may serve to identify targets with the proper dynamic behavior,* as observed in the experiments of Griffin, Friend, and Webster[34]. These experiments involved Myotis' ability to discriminate between tumbling mealworms and other targets.

10.2 Channel Equalization.

Another application of the equivalence between modulation and linear filtering involves the channel equalization problem. Many communication channels can be modelled as time varying linear filters, sometimes with spurious FM. Such channels are encountered in underwater sound propagation, long range radio links, and some long distance telephone lines.

If the appropriate signals (2-8) and receivers (Section 4) are used, one can treat both modulation effects and time varying linear transfer function distortion in the same manner. The effects can be measured by a series of probe pulses that occur at regular intervals, interspersed with the data. The coefficients induced by channel imperfections can then be subtracted from the data coefficients. Such a scheme provides an easy method of equalization for both linear and nonlinear effects.

*At a meeting of the Acoustical Society of America, Dr. A. Novick mentioned that a Myotis could distinguish a live legless roach amid a pile of dead legless roaches.

10.2 --Continued.

One way to transmit binary data with the signals (2-8) is to use linear increasing period modulation for one signal and linear decreasing period modulation for the other. These modulations are induced by using a frequency phase function equal to exp [-j 2πn log ω / log k] and exp [+ j 2πn log ω / log k] , respectively. These signals are excellent probes to determine the effective transfer function of the channel qua linear system. Therefore, if the receivers in Section 4 are used (rather than only two matched filters), one can characterize the channel at the same time as data is being transmitted.

If the channel is stochastically time varying, one can estimate the expected values of the coefficients for a linear filter model. These expected values are related to the coefficients A_n that describe the time varying gains in Figure 10-1, i.e.,

$$a_n(t) = \sum_{m=0}^{\infty} A_{nm} t^m \quad . \tag{10-1}$$

In this case, $a_n(t)$ is a stochastic process which we represent by the expected values of A_{nm} , where

$$A_{nm} = \left[d^m a_n(t) / dt^m \Big|_{t=0} \right] \times 1/m! \quad . \tag{10-2}$$

The expected values of A_{nm} are related to moments of the power spectrum of the process $a_n(t)$. For a stationary stochastic process,[60]

10.2 --Continued.

$$E\left\{\left[\, d^m a_n(t) / dt^m \,\big|_{t=0}\,\right]^2\right\} = (-1)^m d^{2m} R_{a_n}(\tau) / d\tau^{2m} \,\big|_{\tau=0}$$

$$= \frac{1}{2\pi} \int_{-\infty}^{\infty} \omega^{2m} S_{a_n}(\omega)\, d\omega \,, \qquad (10\text{-}3)$$

where $R_{a_n}(\tau) \longleftrightarrow S_{a_n}(\omega)$ are the autocorrelation function and power spectrum of the stochastic process $a_n(t)$.

10.3 Simplification of Complicated Sonar and Communication Problems ; A Return to the Planar Target/ Perfect Channel Situation.

Radar/ sonar operation for perfect all-pass channels and planar ("point") targets is well understood. This report has considered nonplanar targets whose shapes change rapidly with time, and time varying, imperfect channel transfer functions. To the extent that target and channel transfer functions are predictable, appropriate signals and filters for detection of a target and analysis of its transfer function have been derived.

It is evident, however, that there is considerable unpredictability in detection of a target from a specific aspect angle at any given time. Stochastically time

10.3 --Continued.

varying targets can be treated via the analysis in Section 10.2, and random aspect angles can be dealt with as in Section 4-8. These approaches model the receiver in terms of the expected values of the random parameters. Although performance of the resulting system may be optimized in terms of many different observations, performance may be poor for a particular observation, e.g., an aspect angle such that the observed target parameters are very different from their mean values. In terms of detection theory, the variance of the sufficient statistic may be so large that the probability of false alarm is considerable when the threshold is set to give a reasonable probability of detection.

Given the above considerations, the sonar theorist (and echolocating animals) may yearn for the simplicity and demonstrated performance obtainable in the planar target/perfect channel situation. One way to achieve this simplicity is to use narrowband signals. These signals, however, are of little use for range resolution and suppression of clutter via range gating. One must therefore ask the question:

> "Does there exist a wideband signal such that the response of its matched filter is impervious to time varying linear transformations of the signal?"

A solution to the above problem is implicit in the results that have already been discussed in this report. In Section 10.1 it was demonstrated that time varying transfer functions have equivalent time invariant counterparts, if the functions $U(\omega)$ in Equation (2-8) are used. For a single pulse, any time varying nonplanar target or channel transfer function can therefore be modelled as a time invariant linear filter.

10.3 --Continued.

Furthermore, it was shown in Section 2.2 and in the Appendix that if the parameter k is sufficiently large, i.e., if $U(\omega)$ is sufficiently wideband*, then the additional echo components $a_1 \omega U(\omega) + a_2 \omega^2 U(\omega) + \ldots$ caused by time invariant filtering are uncorrelated with $U(\omega)$. For the signals defined by Equation (2-8), the added echo components introduced by nonplanar targets and imperfect channels do not affect the response of a filter that is matched to $U(\omega)$, if k is large.** This filter is matched to the transmitted signal, i.e., to the echo that would be conveyed through a perfect all-pass channel from a planar target.

For the signals (2-8) with sufficiently large k, the response of a single matched filter is therefore impervious to time varying linear transformations of the signal. Echoes can therefore be processed and interpreted in the same simple, straightforward way that would apply to planar 'target' perfect channel situations.

For communication systems, utilization of the signals (2-8) should result in minimum degradation of matched filter performance, even if the channel is rapidly time varying and unequalized. The wide bandwidth allows for resolution of multipath receptions.

---

* Note that the isolation between echo components increases with bandwidth. For the signals in Equation (2-8), the planar target model becomes more realistic as bandwidth is increased, rather than decreased.

** This result explains an observation made by E. I. Titlebaum[61] and R. A. Johnson[40], viz., that a Myotis pulse is nearly impervious to low pass filtering, so far as matched filter performance is concerned.

10.4 Application to Diagnostic Ultrasound.

If the wrong signals and filters are used, it is easy to see how a wider pulse bandwidth could introduce more confusion than it eliminates, especially if the planar target/perfect channel condition is explicitly or implicitly assumed.

An example of this confusion is to be found in diagnostic ultrasound research. When a constant frequency pulse (the favorite signal for diagnostic ultrasound[62, 63, 64, 65]) is made more narrow so that its bandwidth increases, "any difference in amplitude or velocity for the different frequency components within this bandwidth will distort the [filtered] pulse and generally widen it."[66]

Diagnostic ultrasound techniques are generally used to construct an image of an object by means of multiple reflections from the reflector's surface. For most wideband signals, this image is degraded by imperfect sound channels (intervening tissue) or by the curvature of the reflecting surface. This degradation occurs because of distorted pulses at the matched filter output. The distortion can be manifested as widening of the output pulse, unwanted ambiguity peaks, and a displaced maximum.

It has been shown (Section 10.3) that the increased resolution inherent in wideband signals (for the planar target/perfect channel situation) can still be obtained under imperfect conditions. A wideband signal can be used for ultrasonic diagnosis if the corresponding matched filter response is impervious to linear transformations of the signal. Equation (2-8) describes the Fourier transform of such a signal.*

* The dispersive effect of different propagation velocities at different frequencies can be modelled as a pulse compression or expansion. The Doppler tolerance of the signals (2-8) and their lack of range-Doppler coupling (Section 9, last paragraph) ensure that that such effects will not degrade the output of a filter that is matched to the transmitted waveform.

10.5 The FM Equivalent to any Measured Transfer Function ; FM Demodulation.

In Section 6, amplitude modulation functions were written as power series with complex coefficients. A frequency modulation function can be written in the same way. It would therefore seem that the receiver in Figure 6-7 can be adapted to estimate the coefficients of a function $\phi'(t)$ that is used to frequency modulate the signal u (t).

The frequency modulation process multiplies u (t), the inverse Fourier transform of one of the functions in (2-8), by exp [j ϕ(t)]. Although multiplication of u (t) by exp [j ϕ(t)] can be interpreted as an amplitude modulation process, a complex representation of u (t) gives

$$e^{j\phi(t)}\, u(t) = e^{j\phi(t)} \left[|u(t)|\, e^{j\phi_u(t)} \right]$$

$$= |u(t)|\, e^{j\left[\phi_u(t) + \phi(t)\right]} . \qquad (10\text{-}4)$$

The phase function associated with u (t) has an added information-carrying term. For standard FM, $(d/dt)\left[\phi_u(t) + \phi(t)\right] = \omega_o + \phi'(t)$, where ω_o is the carrier frequency and $\phi'(t)$ is the modulating signal.

The desired information is contained in the power series coefficients of $\phi'(t)$. The demodulation process should therefore provide estimates of D_0, D_1, D_2, ... , D_N, where

$$\phi'(t) = \sum_{n=0}^{N} D_n t^n . \qquad (10\text{-}5)$$

10.5 --Continued.

In Section 6.6, a method of finding the coefficients $\underline{A}$ corresponding to an amplitude modulating function was given. In terms of a modulating function $\exp [j \phi(t)]$, we have

$$e^{j \phi(t)} = \sum_{n=0}^{\infty} A_n t^n \quad . \tag{10-6}$$

The problem is to find a transformation that relates the $\underline{A}$ coefficients in (10-6) to the $\underline{D}$ coefficients in (10-5). Differentiating (10-6) gives

$$\frac{d}{dt} [e^{j \phi(t)}] = \sum_{n=0}^{\infty} n A_n t^{n-1} = \sum_{n=0}^{\infty} B_n t^n \tag{10-7}$$

where

$$B_n = (n+1) A_{n+1} \quad . \tag{10-8}$$

In matrix notation, (10-8) can be written

$$\underline{B} = \underline{\underline{H}} \ \underline{A} \tag{10-9} \tag{10-9}$$

where

10.3 --Continued.

$$\underline{\underline{H}} = \begin{bmatrix} 0 & 1 & 0 & 0 & \cdots & 0 & 0 \\ 0 & 0 & 2 & 0 & \cdots & 0 & 0 \\ 0 & 0 & 0 & 3 & \cdots & 0 & 0 \\ \cdot & & & \cdot & \cdot & & \\ \cdot & & & & \cdot & \cdot & \\ \cdot & & & & & \cdot & \cdot \\ \cdot & & & & & 0 & N+1 \\ 0 & 0 & 0 & \cdot & \cdot & \cdot & 0 \quad 0 \end{bmatrix} . \qquad (10\text{-}10)$$

Evaluating the left side of (10-7),

$$\sum_{n=0}^{\infty} B_n t^n = j \phi'(t)\, e^{j \phi(t)}$$

$$= j \sum_{n=0}^{N} D_n t^n \sum_{n=0}^{\infty} A_n t^n . \qquad (10\text{-}11)$$

Assuming that $\exp [\, j \phi(t) \,]$ can be approximated by its first N coefficients, we have

$$\underline{B} = j \underline{\underline{T}}_A \underline{D} \qquad (10\text{-}12)$$

10.5 --Continued.

where

$$\underline{\underline{T}}_A = \begin{bmatrix} A_o & O & O & \cdots & O \\ A_1 & A_o & O & \cdots & O \\ A_2 & A_1 & A_o & \cdots & O \\ \vdots & & & & \vdots \\ A_N & A_{N-1} & A_{N-2} & \cdots & A_o \end{bmatrix} \qquad (10\text{-}13)$$

In terms of the results in Section 4.4,

$$\underline{B} = j \underline{A} * \underline{D} \; . \qquad (10\text{-}14)$$

Solving (10-12) for $\underline{D}$ and using (10-9),

$$\underline{D} = -j \underline{\underline{T}}_A^{-1} \underline{B} = -j \underline{\underline{T}}_A^{-1} \underline{\underline{H}} \underline{A} \; . \qquad (10\text{-}15)$$

Equation (10-15) shows how the filter outputs can be processed in order to find the Taylor series coefficients of $\phi'(t)$. First the $\underline{A}$ coefficients are determined as in Figure 6-7 (maximum likelihood estimation), and then the operation in

10.3 --Continued.

(10-15) is implemented. Although the demodulation is accomplished by a matrix transformation, the transformation is nonlinear because $\underline{A}$ is processed with a matrix whose elements depend upon $\underline{A}$.

Notice that the inverse relation, $\underline{A} = j\left[\underline{\underline{T}}_A^{-1} \underline{\underline{H}}\right]^{-1} \underline{D}$, does not make sense, since A must already be known in order to calculate $\underline{\underline{T}}_A^{-1}$. This observation suggests that the demodulation process to obtain the coefficients of $\phi'(t)$ is irreversible (information is destroyed). Given $\underline{D}$, one cannot uniquely reconstruct the $\underline{A}$ coefficients which correspond to $\underline{D}$.

Equation (10-15) demonstrates that a linear filtering operation can be interpreted as a frequency modulation of the signal $u(t)$, provided the right hand side of (10-15) exists.

10.6 Taylor Expansions about Frequencies Other than Zero.

It has been shown that amplitude modulation and linear filtering can have identical effects upon spectral Taylor coefficients. These coefficients can be defined in terms of a Taylor expansion about any arbitrary frequency ω_o, as well as about $\omega = 0$. Returning to Section 4.4, we can redefine the functions U (ω) and F (ω) in terms of expansions about $\omega = \omega_o$:

$$U(\omega) = \sum_{n=0}^{N} \tilde{u}_n (\omega - \omega_o)^n = \sum_{n=0}^{N} u_n \omega^n \qquad (10\text{-}16)$$

$$F(\omega) = \sum_{n=0}^{N} \tilde{b}_n (\omega - \omega_o)^n = \sum_{n=0}^{N} b_n \omega^n \,. \qquad (10\text{-}17)$$

Now if

$$B(\omega) = F(\omega)\, U(\omega) = \sum_{n=0}^{N} b_n \omega^n$$

$$= \sum_{n=0}^{N} \tilde{b}_n (\omega - \omega_o)^n \qquad (10\text{-}18)$$

it follows that

$$\underline{b} \quad \underline{T}_u \quad \underline{f} \qquad (10\text{-}19)$$

10.6 --Continued.

where $\underline{\underline{T}}_u$ is the square matrix in (4-33).

Furthermore,

$$\underline{\tilde{b}} = \underline{\underline{T}}_u \, \underline{\tilde{a}} \tag{10-20}$$

so that the same result applies to coefficients of a Taylor expansion about $\omega_o \neq 0$.

Similarly, if

$$a(t) = \sum_{n=0}^{N} A_n t^n \tag{10-21}$$

as in (6-8), then

$$C(\omega) \longleftrightarrow a(t) \; u(t) \qquad c(t) \tag{10-22}$$

has coefficients

$$C(\omega) = \sum_{n=0}^{N} \tilde{c}_n (\omega - \omega_o)^n = \sum_{n=0}^{N} c_n \omega^n \tag{10-23}$$

where $\tilde{c}_n$ is proportional to the n^{th} derivative of $C(\omega)$ evaluated at $\omega = \omega_o$. In other words, (6-11) becomes

10.6 --Continued.

$$\Gamma(m+1)/(-j)^{m+1}\,\tilde{c}_m = \int_{-\infty}^{\infty} t^m c(t) e^{-j\omega_o t}\,dt$$

$$= \int_{-\infty}^{\infty} t^m \left[\left(\sum_{n=0}^{N} A_n t^n\right) u(t)\right] e^{-j\omega_o t}\,dt$$

$$= \sum_{n=0}^{N} A_n \int_{-\infty}^{\infty} t^{m+n} u(t) e^{-j\omega_o t}\,dt$$

$$= \sum_{n=0}^{N} A_n U^{(m+n)}(\omega_o)/(-j)^{m+n}$$

$$= \sum_{n=0}^{N} \Gamma(n+m+1)/(-j)^{m+n+1}\,\tilde{u}_{n+m}\,A_n \quad . \tag{10-24}$$

It follows that (6-21) can be written

$$\underline{\tilde{c}} = \underline{\underline{M}}_{\tilde{u}}\,\underline{A}_r \quad . \tag{10-25}$$

To find the coefficients $\tilde{f}$ of the linear time invariant filter that is equivalent to the amplitude modulation $a(t)\,u(t)$, set $\underline{\tilde{c}} = \underline{\tilde{b}}$, so that

$$\underline{\tilde{f}} = \underline{\underline{T}}_{\tilde{u}}^{-1}\,\underline{\underline{M}}_{\tilde{u}}\,\underline{A}_r \quad . \tag{10-26}$$

10.6 --Continued.

All the previous results therefore apply to coefficients that are defined in terms of $U^{(m)}(\omega_0)$, as well as to $U^{(m)}(0)$. This generalization is important because

$$\lim_{\omega \to 0} U^{(m)}(\omega) = 0 \qquad (10\text{-}27)$$

for all finite m, for the function $U(\omega)$ in (2-8).

10.7 Channels for which Matched Filter Response is Impervious to Channel Transfer Function.

In Section 10.3, it was argued that one can sometimes treat nonplanar targets and imperfect channels as if they were incapable of distorting the transmitted signal. It would seem that, if the parameter α is made large in (2-8), the resulting signals have matched filter responses that are impervious to imperfect channel transfer functions. This statement is true for a large class of transfer functions, but not to all possible functions.

A counter example constructed by E. L. Titlebaum* involves a dispersive channel with phase $\exp[j 2\pi n \log \omega / \log k]$. Such a phase function would distort the response of a filter that is matched to the spectrum $U(\omega)$ in (2-8).

The applicability of the results can be determined by examining the response of the matched filter $U^*(\omega)$ to the distorted signal spectrum $F(\omega) U(\omega)$:

* Private conversation at NRC, 22 August 1973.

10.7 ---Continued.

$$\text{Response} = F(\omega) \left| U(\omega) \right|^2$$

$$= \sum_{n=-\infty}^{\infty} f_n \omega^n \left| U(\omega) \right|^2$$

$$= \sum_{n=-\infty}^{\infty} f_n \left| C(n/2) \right|^2 \left| U(\omega/k^{n/2}) \right|^2 \quad . \tag{10-28}$$

This response is approximately equal to $f_o \left| U(\omega) \right|^2$ if

$$\left| f_n \right| \left| C(n/2) \right|^2 << \left| f_o \right| \tag{10-29}$$

for all $n \neq 0$, or

$$\left| f_n \right| << k^{-n\nu - n^2/4} \left| f_o \right| \quad . \tag{10-30}$$

Channel transfer functions $F(\omega)$ that satisfy the above inequality will not seriously affect the matched filter response. Notice, however, that Titlebaum's counter example does not satisfy the inequality. Condition (10-30) can therefore be used as a test to determine the applicability of the theory to any given situation.

11. SYNTHESIS, TRANSMISSION, AND UNDERSTANDING OF SPEECH.

Applications of the foregoing ideas to speech processing became obvious in the light of two observations:

1. The human and auditory spectrum analyzer is apparently set up to perform the operations discussed in Sections 3 and 4. Specifically, signals are analyzed to determine their spectral Taylor series coefficients. Receiver operations are greatly simplified when (i) the coefficients of interest are associated with a filter transfer function $F(\omega)$, and (ii) the received signal has Fourier transform $F(\omega) \times U(\omega)$, where $U(\omega)$ is defined as in (2-8).

2. Human speech can be modeled as the passage of a pulse train or white noise through a slowly time varying linear filter, so that the information content of speech is obtained through analysis of the filter transfer function.

The usual speech synthesizer model[67, 68] is shown in Figure 11-1. An equivalent model is shown in Figure 11-2. In Figure 11-2, the white noise generator has been replaced by a generator of pulses that occur at random times (Poisson process or shot noise) and each filter (for voiced and unvoiced components) has been divided into a filter with transfer function $U(\omega)$ and a second filter in cascade. Knowledge of the transfer functions of the second filters ($F_v(\omega)$ and $F_u(\omega)$ in Figure 11-2) implies knowledge of the information content of the sounds produced by the speech synthesizer.

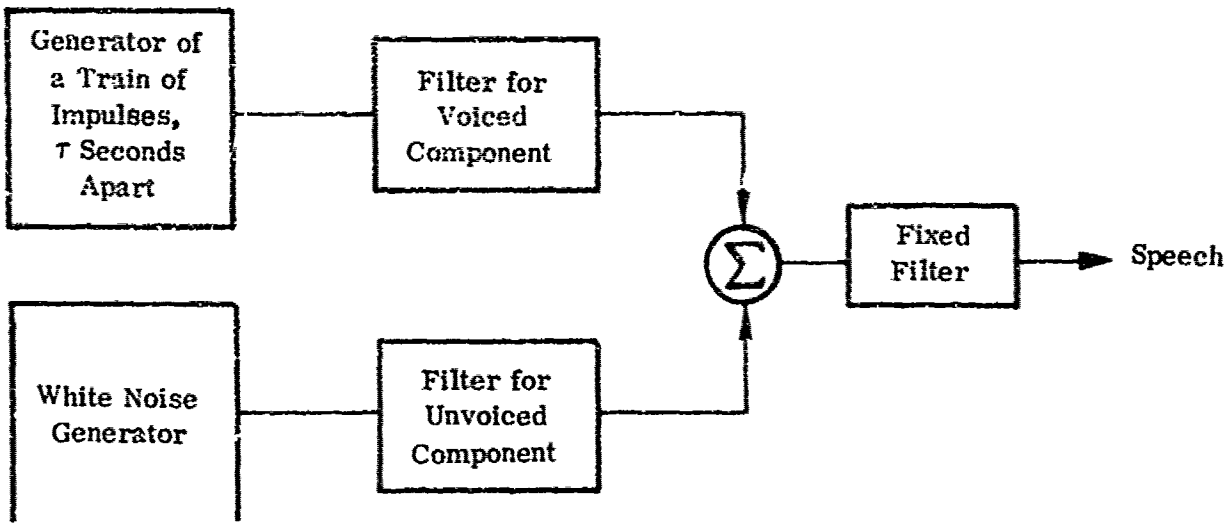

Figure 11-1. A Model for Speech Synthesis, Devised and Tested by Flanagan, et. al.[61]

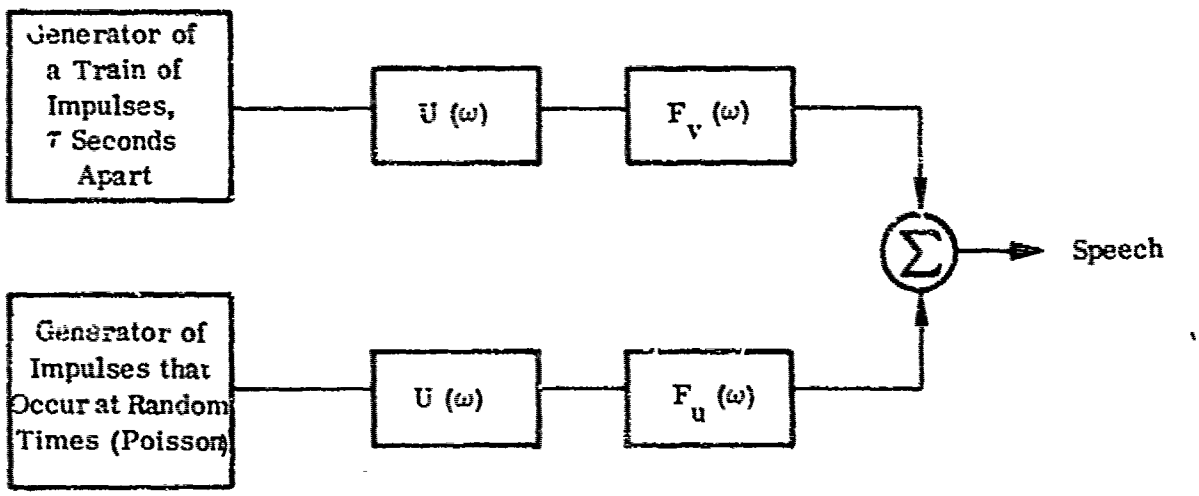

Figure 11-2. A Model for Speech Synthesis that is Equivalent to the Model in Figure 11-1.

U (ω) is given by Equation (2-8).

11. --Continued.

It was deduced in Section 3 that the ear is designed in such a way as to characterize the transfer functions of the filters $F_v(\omega)$ and $F_u(\omega)$ (Figure 11-2) in terms of their power series spectral coefficients. Furthermore, a specific method has been derived for processing the data at the output of the ear's critical bandwidth filter bank. Receiver configurations to detect a given set of coefficients (by implementing a likelihood ratio test) or to estimate the coefficients of an unspecified filter (by maximum likelihood estimation) were deduced in Section 4. A complete receiver specification has thus been obtained for both detection and estimation.

The above deductions could have been made without the added insight that has been provided by animal echolocation studies. Nevertheless, it has been observed that signals with transform $U(\omega)$ (Equation 2-8 and Figure 11-2) are actually utilized by both bats and cetaceans to characterize a linear filter (i.e., a nonplanar sonar target). This observation was, of course, the impetus for an interpretation of the auditory spectrum analyzer as a device for power series spectral characterization. More important, animal echolocation signals provide evidence that the speech synthesizer in Figure 11-2 is more than a convenient mathematical model. Animal sonar strongly suggests that the human brain interprets speech exactly as if phonemes were synthesized by the model shown in Figure 11-2.

Animals that echolocate are forced to utilize sonar signals that are commensurate with their built-in receivers. The same reasoning implies that humans are also forced to utilize communication signals that are commensurate with their built-in sound analyzers. The optimum processing methods of Section 4, together with critical bandwidth filter transfer functions, should therefore yield an extremely

11. --Continued.

simple characterization of speech. A reasonable hypothesis, then, is that if Taylor series spectral analysis is applied to speech, the basic information-carrying parameters of the speech waveform should be obtained. Access to these parameters would greatly simplify the computer understanding of speech, as well as data compression for transmission of speech.

Finally, one can apply the foregoing ideas to a very interesting topic - the analysis of animal communication signals. By determining the appropriate coefficients of cetacean communication sounds, one can compare the data rate with that of humans. The analysis may also provide a method for computer understanding of cetacean speech (if there is such a thing*), as well as that of human beings.

* Some observations concerning exchange of information between cetaceans are discussed on pages 55-58 of R. Stenuit's book.[69]

12. SUMMARY.

A particular set of signals provides an excellent match to the measured echolocation clicks of both Tursiops truncatus, the Atlantic bottlenose dolphin, and Myotis lucifugus, the little brown bat. This signal set can be derived in at least two different ways. The derivations are based upon observed properties of sonar targets, the animals' auditory systems, or the measured signals themselves.

The derivations incorporate new ideas concerning sonar target characterization, mammalian auditory processing, and modulation theory. Each new insight is, in turn, pregnant with many applications that seem far removed from the rather esoteric desire to formulate a unified theory for animal echolocation.

The first derivation is based upon the concept that sonar targets can be characterized by their transfer functions, just as in linear system theory. An implication of this concept is that proper signal and filter design can accomplish automatic clutter rejection and target recognition, on the basis of reflector shape. A separate theory of signal-filter design for signal to interference ratio maximization can thus be applied, independent of animal echolocation systems.

The second derivation is based upon the concept of a linear filtering system to determine the spectral Taylor series coefficients of any input signal. Once the system has been mathematically defined, it is hard to ignore its similarity to psychoacoustic models of the mammalian auditory processor. Furthermore, the system's operation (based on likelihood ratio testing and maximum likelihood estimation) is very simple, provided that the processed signal spectra can be written as a product $F(\cdot)\,U(\cdot)$;

12. --Continued.

F (ω) is unknown and U (ω) belongs to the set that has already been matched to bat and porpoise echolocation clicks. Obviously, if U (ω) is used as a transmitted sonar pulse, all echo spectra have the required form.

The above argument not only constitutes an alternate derivation of bat and dolphin sonar signals; it also provides insight into the workings of the human auditory system. Particularly important is the assertion that human speech is both synthesized and characterized by the Taylor series coefficients of F (ω), where the speech waveform itself can be written as the product F (ω) U (ω).

In a recent article in National Geographic, A. Novick stated that "research on these highly specialized mammals [bats] may help explain how man's brain processes information. The basic design of a brain - be it man's or bat's - is much the same. By tracking the processing of sound through a bat's brain, which is much simpler than man's, we hope to understand how sound is coded, analyzed, integrated, and acted upon."[70] The second derivation indicates that Dr. Novick's hopes have a firm foundation in mathematical modeling as well as in physiology.

Taylor series spectral analysis leads to another interesting result. Multiplication of two time functions or of two frequency functions can be described by the same type of transformation in the frequency domain, if Taylor series coefficients are used to describe the signals. For the signals used by bats and porpoises, multiplication by a function in the time domain (modulation) and multiplication by another function in the frequency domain (linear filtering) can have the same effect. This result can be applied to characterization of time varying linear systems. Such an application is undoubtedly

12. --Continued.

useful to sonars that must contend with targets such as flying insects, i.e., targets with time varying transfer functions. It is not surprising that a system which treats amplitude modulations and time invariant linear transformations in the same way should be useful for the analysis of time varying linear transformations. "Every linear instantaneous system may be characterized by a relation of the form $\underline{y}(t)$ $\underline{A}(t)$ $\underline{x}(t)$ ... . If $\underline{A}(t)$ is constant, the system is fixed."[71]

The above characterization leads to a straightforward way of equalizing a randomly time varying channel with a linear filter. Still another application is the use of matched filtering to demodulate an amplitude modulated pulse.

The signal set which seems to be basic to animal echolocation is apparently basic to many aspects of engineering. The new signals can be used as robust communication waveforms. If they have sufficient bandwidth, the signals yield correlator outputs that are not degraded by time varying, imperfect channels.

An interesting property of the new signals is that they are broadened (their mean square bandwidth is increased) when they are multiplied by any function in the frequency domain that is analytic at $\omega = 0$. In this sense, they seem to possess a minimum bandwidth property. It may therefore be reasonable to assert that the signals in Equation (2-8) constitute the most efficient probes for characterizing a linear system, when the measure of efficiency is the information that is acquired for a given mean square signal bandwidth.

The uniqueness of the derived signals has not been investigated in detail. The derivations hinge upon the existence of set of decorrelated signals such that each

12. --Continued.

signal is a normalized differentiated version of one basic time function with transform $U(\omega)$. It is difficult to establish the uniqueness of such a set. It should be emphasized, however, that decorrelation is a more stringent condition than the usual orthogonality concept. Orthogonality implies zero inner product for zero translation of one function with respect to another. Decorrelation requires very small inner product for all possible translations. At the present time, the author is pleased to have found only one solution to the problem. Although other solutions may exist, it would appear that the author's result compares nicely with the solutions that are implemented in the mammalian auditory processor and in the echolocation signals used by bats and dolphins.

Related topics that have been discussed in this report include a new model for the auditory processor, the volume of the wideband ambiguity function, and clutter suppression with a completely linear receiver.

The new model of the auditory processor was motivated by the realization that a well accepted older model cannot explain animal echolocation performance. The new model attempts to reconcile the concept of critical bandwidth spectral analysis with neural processing and behavioral observations.

An interesting result concerning ambiguity volume has been derived. Some of the signals matched to animal echolocation waveforms have wideband ambiguity volumes identical to the volume under the narrowband ambiguity function. Signals that minimize wideband ambiguity volume under realistic constraints (duration and energy kept large) have also been derived. The importance of these signals to animal echolocation theory has yet to be determined.

12. --Continued.

Clutter suppression with a square law detector at the output of a linear filter leads to the theory reviewed in Section 2.3. A different approach can be applied to a receiver that does not use square law detection. The new approach indicates that narrowband sinusoids constitute an unacceptable solution to the clutter suppression problem, unless the target is moving with respect to the clutter. A more robust solution is determined by using a basis set of wideband signals. The resulting solution is less affected by unforeseen perturbations of the environment or the sonar equipment.

The above summary indicates that most of the questions asked in Section 1.1 have indeed been answered. Special importance can be attached to the following results:

I. Sonar Systems.

1. Linear filter theory provides a straightforward method of exploiting the phenomenon that wideband echoes often are different from the transmitted signal.

2. Through proper signal design, the phenomenon can be ignored or circumvented with little degradation in matched filter response (Section 10.3).

3. Development of the theory leads directly to system implementations to achieve automatic target recognition and clutter rejection.

12. --Continued.

II. Animal Echolocation.

1. A general unified theory of animal echolocation has been presented. The theory gives rise to a restricted set of signals that seem to encompass most animal echolocation waveforms.

2. One derivation of the theory relates directly to well accepted psychoacoustic data concerning critical bandwidth.

3. The theory seems to imply the existence of a slightly different model of the auditory processor than the one that is currently in vogue. The results also stress the importance of efferent signals for neural processing of auditory data. These observations would seem to suggest some important new experiments in neurophysiology and psychoacoustics.

4. The concept of a single neuron as a correlator may lead to more efficient, cheaper wideband correlators, using printed circuits that duplicate neuronal functions.

5. The theory would seem to be a prerequisite for an understanding of speech processing in the human brain (Section 11).

12. --Continued.

III. Communication Theory, Medicine, and Other Applications.

1. Communication systems and diagnostic ultrasounders can benefit directly from the observations in Section 10.3. With proper signal design, matched filter response is minimally degraded by time varying, imperfect channels. Since the signals are wideband, high data rates are possible.

2. System theory, in particular, can benefit from the analysis presented in this report. The derived signals should be applicable to the characterization of time varying linear systems in the presence of noise. Other applications, to such areas as wideband radar, ultrasonic guidance for the blind, and seismic geophysical prospecting, should be straightforward. Further applications are left to the reader's imagination and ingenuity.

13. REFERENCES.

1. L. Ferlinghetti, A Coney Island of the Mind. San Francisco: New Directions, 1958, p. 31.

2. R. A. Altes, "Analysis and Synthesis of Echolocation Signals with Applications to Advanced Sonar Systems," ESL Progress Report PR88, 31 July 1972. Prepared under Contract No. N66001-72-C-0459 for the Naval Undersea Center, Biosystem Research Dept.

3. R. A. Altes and R. V. Jones, "Study of Animal Echolocation Signals with Applications to Advanced Sonar Technology," ESL Progress Report PR103, 1 March 1973. Prepared under Contract No. N66001-72-C-0718 for the Naval Undersea Center, Biosystem Research Dept.

4. R. O. Harger, Synthetic Aperture Radar Systems. New York: Academic Press, 1970, pp. 3 - 4, 60 - 82.

5. E. M. Kennaugh and D. L. Moffett, "Transient and Impulse Response Approximations," Proc. IEEE, Vol. 53, August 1965, pp. 893 - 901.

6. J. Rheinstein, "Scattering of Short Pulses of Electromagnetic Waves," Proc. IEEE, Vol. 53, August 1965, pp. 1069 - 1070.

7. R. R. Rojas and H. Urkowitz, "Reduced Averaging Processing in Sonar for Extended Target Detection," IEEE Trans. Aerosp. Electron. Syst., Vol. AES - 4, 1968, pp. 493 - 909.

13. --Continued.

8. E. L. Titlebaum and N. DeClaris, "A Signal Design Philosophy for High Resolution Radar," IEEE International Convention Record, Part 4, 1966.

9. R. F. Daly, "Signal Design for Efficient Detection in Dispersive Channels." IEE Trans. on Infor. Theory, Vol. IT - 16, 1970, pp. 206 - 213.

10. J. R. Mentzer, Scattering and Diffraction of Radio Waves. Oxford: Pergamon, 1955.

11. M. I. Skolnik, Introduction to Radar Systems. New York: McGraw-Hill, 1962, pp. 43.

12. W. E. Evans and B. A. Powell, "Discrimination of Different Metallic Plates by an Echolocating Delphinid," Animal Sonar Systems, Vol. 1, R. G. Busnel (ed.), Lab. de Physicl. Acous., Jouy-en-Josas, France, 1967, pp. 363 - 383.

13. A. J. F. Siegert, "Rayleigh Scattering from a Small Sphere," in Radar System Engineering. (L. N. Ridenour, ed.). New York: Dover, 1965, pp. 63 - 65.

14. R. A. Altes, "Methods of Wideband Signal Design for Radar and Sonar Systems," Ph. D. Thesis, University of Rochester, 1970. AD732494.

13. --Continued.

15. R. A. Altes, "Computer Derivation of Some Dolphin Echolocation Signals," Science, Vol. 173, 1971, pp. 912 - 914.

16. D. F. DeLong, Jr., and E. M. Hofstetter, "On the Design of Optimum Radar Waveforms for Clutter Rejection," IEEE Trans. Inform. Theory, Vol. IT-13, July 1967, pp. 454 - 463.

17. W. D. Rummler, "Clutter Suppression by Complex Weighting of Coherent Pulse Trans.," IEEE Trans. Aerosp. Electron. Syst., Vol. AEA-2, March 1966, pp. 690 - 699.

18. Ya. D. Shirman, "Optimum Detection of Radar Target in a Cloud of Passive Reflectors," Radio Engin. and Electron. Phys., Vol. 15, No. 5, 1970, pp. 799 - 806.

19. C. A. Stutt and L. J. Spafford, "A 'Best' Mismatched Filter Response for Radar Clutter Discrimination," IEEE Trans. Inform. Theory, Vol. IT-14, March 1968, pp. 280 - 287.

20. R. A. Altes, "Suppression of Radar Clutter and Multipath Effects for Wideband Signals," IEEE Trans. Inform. Theory, Vol. IT-17, May 1971, pp. 344 - 346.

21. A. Papoulis, Systems and Transforms with Applications in Optics, New York: McGraw-Hill, 1968, pp. 185 - 189.

13. --Continued.

22. D. Gabor, "Theory of Communications," J. IEE (London), Vol. 93, 1946, pp. 429 - 457.

23. A.W. Rihaczek, Principles of High - Resolution Radar. New York: McGraw-Hill, 1969.

24. J.S. Goldstein, "An Investigation of Monaural Phase Perception," Ph. D. Thesis, University of Rochester, 1965.

25. T.H. Schafer, R.S. Gales, C.A. Shewmaker, and P.O. Thompson, "The Frequency Selectivity of the Ear as Determined by Masking Experiments," J. Acous. Soc. Amer., Vol. 22, No. 4, 1950, pp. 490 - 496.

26. D.D. Greenwood, "Auditory Masking and the Critical Band," J. Acous. Soc. Amer., Vol. 33, No. 4, 1961, pp. 484 - 502.

27. H. Fletcher, Speech and Hearing in Communication. Princeton: Van Nostrand, 1953, Chapter 14.

28. E. Zwicker, "Subdivision of the Audible Frequency Range into Critical Bands (Frequenzgruppen)", J. Acous. Soc. Amer., Vol. 33, No. 2, 1961, p. 248.

29. D.M. Green, "Auditory Detection of a Noise Signal," J. Acous. Soc. Amer., Vol. 32, No. 1, 1960, pp. 121 - 131.

13. --Continued.

30. L. Kay, "Enhanced Environmental Sensing by Ultrasonic Waves," Animal Sonar Systems (R. G. Busnel, ed.). Jouy - en - Josas: Laboratoire de Physiologie Acoustique, 1966, Vol. 2, pp. 757 - 781.

31. E. Sh. Ayrapet'yants and A. I. Konstantinov, Echolocation in Nature (Echolokatsiya v Prirode). Leningrad: Nauka Publishing House, 1970, pp. 357 - 358. English Translation of Chapter 17 and conclusion: JPRS 51511.

32. H. L. Van Trees, Detection, Estimation, and Modulation Theory, Part I. New York: Wiley, 1968, pp. 96 - 116.

33. Ibid., p. 65

34. D. R. Griffin, J. H. Friend, and F. A. Webster, "Target Discrimination by the Echolocation of Bats," J. Exptl. Zool., Vol. 158, 1965, pp. 155 - 168.

35. D. R. Griffin, "Discriminative Echolocation by Bats," Animal Sonar Systems (see Ref. 30), pp. 273 - 300.

36. D. A. Cahlander, Echolocation with Wide-Band Waveforms: Bat Sonar Signals. MIT Lincoln Lab. Report 271, AD 605 322.

37. N. Suga, "Single Unit Activity in Cochlear Nucleus and Inferior Colliculus of Echo-Locating Bats," J. Physiol., Vol. 172, 1964. pp. 449 - 474.

13. --Continued.

38. A. D. Grinnell, "The Neurophysiology of Audition in Bats: Intensity and Frequency Parameters," J. Physiol., Vol. 167, 1963, pp. 38 - 66.

39. N. Suga, Private Communication, 24 September 1972.

40. R. A. Johnson, "Energy Spectra Analysis as a Processing Mechanism for Echolocation," Ph. D. Thesis, University of Rochester, 1972.

41. G. Pollak, O. W. Henson, Jr., and A. Novick, "Cochlear Microphonic Audiograms in the 'Pure Tone' Bat Chilonycteris parnellii parnellii," Science, V. 176, 7 April 1972, pp. 66 - 68.

42. J. J. G. McCue and A. Bertolini, "A Portable Receiver for Ultrasonic Waves in Air," IEEE Trans. for Sonics and Ultrasonics, Vol. SU-11, 1964, pp. 41 - 49.

43. T. H. Bullock and S. H. Ridgway, "Evoked Potentials in the Central Auditory System of Alert Porpoises to their Own and Artificial Sounds," J. Neurobiology, Vol. 3, No. 1, 1972, pp. 79 - 99.

44. R. A. Suthers, "Acoustic Orientation by Fish-catching Bats," J. Exp. Zool., Vol. 158, 1965, pp. 319 - 348.

45. C. Scott Johnson, "Relation Between Absolute Threshold and Duration-of-Tone Pulses in the Bottlenosed Porpoise," J. Acoust. Soc. Amer., Vol. 43, No. 4, 1968.

13. --Continued.

46. R. Plomp and M. A. Bouman, "Relation between Hearing Threshold and Duration for Tone Pulses," J. Acous. Soc. Amer., Vol. 31, No. 6, June, 1959, pp. 749 - 758.

47. E. G. Shower and R. Biddulph, "Differential Pitch Sensitivity of the Ear," J. Acous. Soc. Amer., Vol. 3, 275 - 287, Oct. 1931.

48. Reference 27, pp. 173 - 174.

49. R. S. Gales, Private Communication, May, 1973.

50. See References 24 and 25.

51. Reference 27, p. 106.

52. Ibid.

53. B. Katz, Nerve, Muscle, and Synapse. New York: McGraw-Hill, 1966, p. 25.

54. C. Scott Johnson, Private Correspondence, April, 1973.

55. D. M. Green, Reference 29.

56. J. A. Simmons, "Echolocation in Bats: Signal Processing of Echoes for Target Range," Science, Vol. 171, March, 1971, pp. 925 - 927.

13. --Continued.

57. R. A. Altes, "Some Invariance Properties of the Wide-band Ambiguity Function," J. Acous. Soc. Amer., Vol. 53, 1973, pp. 1154 - 1160.

58. R. A. Altes, "Methods of Wideband Signal Design for Radar and Sonar Systems," Ph. D. Thesis, University of Rochester, 1970.

59. M. Abramowitz and I. A. Stegun (eds.), Handbook of Mathematical Functions. Washington: NBS, 1970, pp. 538 - 541.

60. A. Papoulis. Probability, Random Variables, and Stochastic Processes. New York: McGraw-Hill, 1965, pp. 316 - 317.

61. E. L. Titlebaum, Private Conversation, Feb., 1971.

62. "Diagnostic Sounder - New Ultrasonic Instrument for Visualizing Internal Body Structures," Hewlett Packard Brochure, May, 1968.

63. "Low Noise Ultrasonic Probe," Nuclear Enterprises Ltd., Bulletin No. 283, March, 1969.

64. "Specifications - Ekoline 20 Diagnostic Ultrasonoscope," Smith Kline Instrument Co., Nov., 1966.

65. G. J. Rubissow and R. S. Mackay, "Ultrasonic Imaging of in Vivo Bubbles in Decompression Sickness," Ultrasonics, Oct., 1971.

13. --Continued.

66. J. Reid, "A Review of Some Basic Limitations in Ultrasonic Diagnosis," in Diagnostic Ultrasound, C.G. Grossman et. al., eds., Plenum, N.Y., 1966.

67. J. L. Flanagan, et. al., "Synthetic Voices for Computers," IEEE Spectrum, Vol. 7, No. 10, Oct., 1970, pp. 22 - 45.

68. J. E. Gunn and A. P. Sage, "Speech Data Rate Reduction," IEEE Trans. on Aerospace and Elect. Sys., Volume AES-9, No. 2, 1973, pp. 130 - 138.

69. R. Stenuit, The Dolphin, Cousin to Man. New York: Bantam, 1972, pp. 55 - 58.

70. A. Novick, "Bats Aren't All Bad," National Geographic, Vol. 143, No. 5, May, 1973, pp. 615 - 637.

71. R. Schwarz and B. Friedland, Linear Systems. New York: McGraw-Hill, 1965, p. 13.

72. L. Selin, Detection Theory. Princeton: Princeton Univ. Press, 1965, P. 34.

73. W. E. Evans and C. S. Johnson, Private Discussion, 1972.

13. --Continued.

74. G. L. Rasmussen, "Efferent Fibers of the Cochlear Nerve and Cochlear Nucleus," in Neural Mechanisms of the Auditory and Vestibular Systems, G. L. Rasmussen and W. F. Windle (eds.). Springfield: C. C. Thomas, 1960, pp. 105 - 115.

75. C. E. Cook and M. Bernfeld, Radar Signals. New York: Academic Press, 1967, pp. 160 - 164.

76. P. M. Woodward, Probability and Information Theory with Applications to Radar. Oxford: Pergamon, 1964, pp. 96 - 98.

77. Ibid., p. 120

78. H. Fletcher and W. A. Munson, "Relation Between Loudness and Masking," J. Acous. Soc. Amer., Vol. 9, No. 1, July, 1937, pp. 1 - 10.

APPENDIX

A.1 Derivation of Signals.

The theory in this report is based upon the idea that an echo from a sonar target can be expressed as a linear transformation of the transmitted signal. Targets can therefore be characterized by their transfer functions, just as linear filters are characterized in electrical engineering. The target transfer function can be parameterized by expanding the function in a Taylor series, i.e., a polynominal in frequency whose coefficients describe the target. One is then faced with the task of determining the Taylor coefficients.

In order to estimate the coefficients with a minimum of mathematical data manipulation, one should use a signal that becomes uncorrelated with itself when its Fourier transform is multiplied by ω^n, $n = 0, 1, \ldots, N$. If such a signal exists, a bank of filters can be used to decompose echoes into components whose amplitudes are the desired target coefficients.

One set of functions that become uncorrelated when they are multiplied by ω^n has the property that

$$\omega^n \, U(\omega) = C_n \, U(\omega/k^n) \quad . \tag{A-1}$$

together with the property that

A.1 --Continued.

$$| \chi_{uu} (\tau, k^n) |^2 = \left| \frac{1}{2\pi k^{n/2}} \int_0^\infty U(\omega)\ U^*(\omega/k^n)\ e^{-j\omega\tau}\, d\omega \right|^2$$

$$<< | \chi_{uu} (\tau, 1) |^2, \quad \text{for all } \tau . \qquad \text{(A-2)}$$

In Equations (A-1) and (A-2), $U(\omega)$ is the Fourier transform of the Analytic signal $u(t)$ and $| \chi_{uu} (\tau, k^n) |^2$ is the wideband ambiguity function of the signal. The ambiguity function describes the response of the filter $U^*(\omega)$ to the energy normalized signal $k^{-n/2}\ U(\omega/k^n)$.

To derive the signals that satisfy Equation (A-1), we consider a more general condition;

$$\omega^\rho\ U(\omega) = C(\rho)\ U(\omega/k^\rho) \qquad \text{(A-3)}$$

where ρ is any real number. Differentiating both sides of (A-3) with respect to ρ,

$$(\log \omega)\ e^{\rho \log \omega}\ U(\omega) = C'(\rho)\ U(\omega/k^\rho)$$

$$- C(\rho)\ \omega\ (\log k)\ e^{-\rho \log k}\ U'(\omega\, e^{-\rho \log k})$$

(A-4)

A.1 --Continued.

Setting $\rho = 0$ in (A-4) gives

$$\frac{U'(\omega)}{U(\omega)} = \frac{C'(0) - \log \omega}{C(0)\, \omega \log k} \quad . \tag{A-5}$$

By setting $\rho = 0$ in (A-3), it is evident that

$$C(0) = 1 \, . \tag{A-6}$$

Integrating both sides of (A-5) and using (A-6).

$$\log U(\omega) = \frac{C'(0) \log \omega}{\log k} - \frac{(\log \omega)^2}{2 \log k} + \text{constant}$$

$$U(\omega) = (\text{constant})\, \omega^{\nu}\, e^{-\frac{(\log \omega)^2}{2 \log k}} \quad . \tag{A-7}$$

For the special case $\rho = n$ = integer, $U(\omega)$ can be multiplied by any function $F(\omega)$ with the property that

$$F(\omega / k^n) = F(\omega) \quad . \tag{A-8}$$

A.1 --Continued.

Letting $F(\omega) = G(\log \omega)$, (A-8) becomes

$$G(\log \omega - n \log k) = G(\log \omega) \quad , \tag{A-9}$$

a condition which implies that $G(\log \omega)$ is a periodic function with period $\log k$. In other words, $G(\log \omega / \log k)$ is periodic with a period of unity;

$$G\left[(\log \omega / \log k) \pm n\right] = G(\log \omega / \log k) \quad . \tag{A-10}$$

Therefore, for ρ = integer, i.e.,

$$\omega^n U(\omega) = C_n U(\omega / k^n) \tag{A-11}$$

it follows that

$$U(\omega) \quad \omega^{\nu} e^{-\frac{(\log \omega)^2}{2 \log k}} \quad G(\log \omega / \log k) \tag{A-12}$$

where $G(\bullet)$ is any function with the property that $G(x \pm n) = G(x)$.

Any scaled version of $U(\omega)$ will also satisfy condition (A-1).

A. 2 Ambiguity Function.

The wideband ambiguity function of an Analytic signal with Fourier transform U (ω) and $E_u = 1$ is

$$| \chi_{uu} (\tau, s) |^2 = \left| \frac{1}{2\pi s^{1/2}} \int_0^\infty U(\omega)\, U^*(\omega/s)\, e^{-j\omega\tau}\, d\omega \right|^2 . \tag{A-13}$$

For the functions (A-12),

$$U(\omega/k^n) = k^{-n\nu - n^2/2}\, \omega^n\, U(\omega) \tag{A-14}$$

so that

$$\omega^n\, U(\omega) = k^{n\nu + n^2/2}\, U(\omega/k^n) \tag{A-15}$$

i.e.,

$$C_n = k^{n\nu + n^2/2} \tag{A-16}$$

in (A-1).

Using (A-14),

$$| \chi_{uu} (\tau, k^{2m}) |^2 = \left| \frac{k^{-2m\nu - 2m^2 - m}}{2\pi} \int_0^\infty \omega^{2m} | U(\omega) |^2 e^{-j\omega\tau}\, d\omega \right|^2 . \tag{A-17}$$

A. 2 --Continued.

Using (A-15) ,

$$| \omega^m U(\omega) |^2 = k^{2m\nu + m^2} | U(\omega/k^m) |^2 . \qquad \text{(A-18)}$$

Substituting (A-18) into (A-17) ,

$$| \chi_{uu}(\tau, k^{2m}) |^2 = \left| \frac{k^{-m^2-m}}{2\pi} \int_0^\infty | U(\omega/k^m) |^2 e^{-j\omega\tau} d\omega \right|^2$$

$$= \left| \frac{k^{-m^2}}{2\pi} \int_0^\infty | U(\omega) |^2 e^{-j\omega k^m \tau} d\omega \right|^2$$

$$= k^{-2m^2} | R_{uu}(k^m \tau) |^2 \qquad \text{(A-19)}$$

where $R_{uu}(\tau)$ is the signal's autocorrelation function ;

$$| R_{uu}(\tau) |^2 = \left| \int_{-\infty}^{\infty} u(t)\, u^*(t+\tau)\, dt \right|^2$$

$$\leq | R_{uu}(0) |^2 = E_u^2 = 1.$$

A. 2 --Continued.

Therefore,

$$\max_{-\infty < \tau < \infty} | \chi_{uu}(\tau, k^{2m}) |^2 = k^{-2m^2} . \qquad \text{(A-21)}$$

In Equation (A-21), $\max_{\tau} | \chi_{uu}(\tau, k^{2m}) |^2$ is the maximum output power of a filter with a scale mismatch of k^{2m}. For example, the signal could have Fourier transform $k^{-n/2} U(\omega/k^n)$, while the transfer function of the filter could be matched to a different signal with scale factor k^{n+2m}, i.e., $k^{-(n/2)-m} U(\omega/k^{n+2m})$. Equation (A-21) gives the maximum power at the output of the filter when the mismatched signal is applied to the input.

A.3 Mean Square Bandwidth.

The mean square bandwidth (MSBW) of a function is defined as the difference

$$(\text{MSBW})^2 = D_\omega^2 - \omega_o^2 ,$$

where

$$D_\omega^2 = \frac{1}{2\pi} \int_0^\infty \omega^2 \, | \, U(\omega) \, |^2 \, d\omega \; / \; E_u \qquad \text{(A-22)}$$

$$\omega_o = \frac{1}{2\pi} \int_0^\infty \omega \, | \, U(\omega) \, |^2 \, d\omega \; / \; E_u \qquad \text{(A-23)}$$

and

$$E_u = \frac{1}{2\pi} \int_0^\infty | \, U(\omega) \, |^2 \, d\omega \quad . \qquad \text{(A-24)}$$

From (A-15),

$$\omega^2 \, | \, U(\omega) \, |^2 = | \, \omega \, U(\omega) \, |^2 = k^{2\nu+1} \, | \, U(\omega/k) \, |^2 \qquad \text{(A-25)}$$

and

$$\omega \, | \, U(\omega) \, |^2 = | \, \omega^{1/2} \, U(\omega) \, |^2 = k^{\nu+1/4} \, | \, U(\omega/k^{1/2}) \, |^2 \quad .$$

(A-26)

A.3 --Continued.

In (A-26), it is assumed that the periodic function G (log ω / log k) in (A-12) has the property that G ($x \pm n/2$) = $\pm$ G (x). Using (A-25) and (A-26) to evaluate (A-22) and (A-23),

$$D_\omega^2 = k^{2\nu+1} \int_0^\infty |U(\omega/k)|^2 \, d\omega \; / \; E_u$$

$$= k^{2\nu+2} \qquad \text{(A-27)}$$

$$\omega_o = k^{\nu+1/4} \int_0^\infty |U(\omega/k^{1/2})|^2 \, d\omega \; / \; E_u$$

$$= k^{\nu+3/4} \; . \qquad \text{(A-28)}$$

Therefore,

$$(\text{MSBW})^2 = k^{2\nu+2} - k^{2\nu+3/2} = k^{2\nu+3/2}(k^{1/2} - 1) \; . \qquad \text{(A-29)}$$

For $\nu = 0$,

$$\text{MSBW} = k^{3/4}(k^{1/2} - 1)^{1/2} \; .$$

A.4 Approximate Fourier Transforms.

It is difficult to obtain exact, closed form expressions for the inverse Fourier Transforms of the functions (A-12), where, for example,

$$G(\log \omega / \log k) = e^{-j2\pi n \log \omega / \log k} . \qquad \text{(A-30)}$$

It is relatively easy, however, to obtain approximate expressions for u (t) by using the stationary phase principle.[72, 73]

First, we obtain an integral with limits $(-\infty, \infty)$ by changing variables :

$$u(t) = \frac{1}{2\pi} \int_0^\infty \omega^{\nu} e^{-(\log \omega)^2 / 2 \log k} e^{-j2\pi n \log \omega / \log k} e^{j\omega t} d\omega$$

$$= \frac{1}{2\pi} \int_{-\infty}^{\infty} e^{(\nu+1)\omega_1} e^{-\omega_1^2 / 2 \log k} e^{-j2\pi n \omega_1 / \log k} e^{jte^{\omega_1}} d\omega_1 .$$

(A-31)

According to Papoulis (ref. 73, pp. 140 - 141),

$$\frac{1}{2\pi} \int_{-\infty}^{\infty} U(\omega) e^{jt\mu(\omega)} d\omega \approx \frac{U(\omega_o)}{\sqrt{2\pi t \left| \mu''(\omega_o) \right|}} e^{j\left[t\mu(\omega_o) + \frac{\pi}{4} \operatorname{Sgn} \mu''(\omega_o)\right]} \qquad \text{(A-32)}$$

where

$$\operatorname{Sgn} \mu''(\omega_o) = \begin{cases} +1 , & \mu''(\omega_o) \geq 0 \\ -1 , & \mu''(\omega_o) < 0 \end{cases} \qquad \text{(A-33)}$$

A.4 --Continued.

and where

ω_o = the stationary point of $\mu(\omega)$, i.e., the value of ω where $\mu'(\omega_o) = 0$.

For the expression in (A-31)

$$\mu(\omega) = e^{\omega} - \frac{2\pi n \omega}{t \log k} = e^{\omega} - z\omega / t \qquad \text{(A-34)}$$

where $$z = \frac{2\pi n}{\log k} \quad .$$

Then

$$\mu'(\omega_o) = e^{\omega_o} - z / t = 0 \qquad \text{(A-35)}$$

so that

$$\omega_o = \log (z / t) \qquad \text{(A-36)}$$

and

$$\mu''(\omega_o) = e^{\omega_o} = z / t = |z / t| \operatorname{Sgn} t \, . \qquad \text{(A-37)}$$

A.4 --Continued.

From (A-37), we see that

$$\text{Sgn}\ \mu''(\omega_o) = \text{Sgn}\ t \quad \text{if} \quad z > 0. \tag{A-38}$$

Substituting (A-34) - (A-38) into (A-32), we obtain

$$u(t) \approx \frac{e^{(\nu+1)\log(2\pi n / t\log k) - [\log(2\pi n / t\log k)]^2 / 2\log k}}{\sqrt{2\pi t \mid 2\pi n / t\log k \mid}}$$

$$\cdot e^{jt\left[e^{\log\frac{2\pi n}{t\log k}} - \frac{2\pi n}{t\log k}\log\left(\frac{2\pi n}{t\log k}\right)\right]} e^{j(\pi/4)\text{Sgn}\ t}$$

$$= \left(\frac{2\pi n}{t\log k}\right)^{\nu+1} e^{-\left[\log\left(\frac{2\pi n}{\log k}\right) - \log t\right]^2 / 2\log k}$$

$$\cdot \frac{1}{2\pi}\left(\frac{\log k}{n\,\text{Sgn}\ t}\right)^{1/2} e^{j\left[\left(\frac{2\pi n}{\log k}\right)\left(1 - \log\left(\frac{2\pi n}{t\log k}\right)\right) + \frac{\pi}{4}\text{Sgn}\ t\right]}$$

$$= \frac{j(\text{Sgn}\ t)^{1/2}}{(2\pi)^{1/2}}\left(\frac{2\pi n}{\log k}\right)^{\nu+1/2} t^{-(\nu+1)} e^{-\left[\log\left(\frac{2\pi n}{\log k}\right)\right]^2 / 2\log k}$$

$$\cdot e^{-[\log t]^2 / 2\log k} \cdot t^{\log\left(\frac{2\pi n}{\log k}\right)/\log k}.$$

A.4 --Continued.

$$\cdot\ e^{j\left(\frac{2\pi n}{\log k}\right)\log t}\ e^{j\left(\frac{2\pi n}{\log k}\right)\left[1-\log\left(\frac{2\pi n}{\log k}\right)\right]}$$

$$= \left[\text{Complex constant}\right] \cdot t^{\left[\log\left(\frac{2\pi n}{\log k}\right)/\log k\right] - (\nu+1)}$$

$$\cdot\ e^{-(\log t)^2/2\log k}\ e^{j\left(\frac{2\pi n}{\log k}\right)\log t} \cdot (\text{Sgn } t)^{1/2} \qquad \text{(A-39)}$$

or

$$u(t) \approx C_1\, t^{C_2}\, e^{-(\log t)^2/2\log k}\, e^{j\left(\frac{2\pi n}{\log k}\right)\log t}\, (\text{Sgn } t)^{1/2} . \qquad \text{(A-40)}$$

It becomes apparent that (A-40) is only an approximation when one attempts to verify the functional relationship

$$\frac{d}{dt}\, u(t) = C\ u(kt) . \qquad \text{(A-41)}$$

The left hand side is

$$u'(t) = \frac{u(t)}{t}\left[C_2 - \frac{\log t}{\log k} + j\,\frac{2\pi n}{\log k}\right] \qquad \text{(A-42)}$$

A.4 --Continued.

and the right hand side is

$$u(kt) = \frac{u(t)}{t} \left[k^{C_2 - \frac{1}{2}} \right] \qquad \text{(A-43)}$$

so that

$$\frac{d}{dt} u(t) \neq \text{Const} \times u(kt) \qquad \text{(A-44)}$$

unless $t = 1$.